

Sedimentology of Neoproterozoic storm-influenced braid deltas, Varanger Peninsula, North Norway

Sten-Andreas Grundvåg^{1,2} and Julia Skorgenes¹

¹Department of Geosciences, UiT The Arctic University of Norway, PO Box 6050 Langnes, N-9037 Tromsø, Norway

²Department of Arctic Geology, The University Centre in Svalbard, Longyearbyen, Norway

E-mail corresponding author (Sten-Andreas Grundvåg): sten-andreas.grundvag@uit.no

Keywords:

- Fluvio-deltaic deposits
- Late Precambrian
- Vadsø Group
- Finnmark

Received:
23 August 2022

Accepted:
13. November 2022

Published online:
30. January 2023

The oldest part of the upper Riphean (Cryogenian) sedimentary succession of the Varanger Peninsula, North Norway, includes a series of sandstone-dominated units of fluvio-deltaic to shallow-marine origin and thinner, intercalated mudstone-rich units. The sedimentology and stratigraphic understanding of the mudstone-rich units are less complete compared to their sandstone-dominated counterparts. In this outcrop-based study, we report on the sedimentology of the mudstone-rich Klubbnasen and Andersby formations in the lower part of the Vadsø Group. Our facies analysis reveals that both units comprise offshore, storm-influenced prodelta, and fluvial-dominated to storm-affected delta-front deposits organised into two large-scale coarsening-upward cycles, each capped by >100 m-thick, cross-bedded sandstone units of braidplain affinity (belonging to the Fugleberget and Paddeby formations, respectively). An ever-dominant eastward palaeocurrent direction parallelling the Archaean crystalline basement terrane and the coinciding basin margin south of the study area, and a major regional lineament to the north, suggests structural control on sediment routing, possibly governed by differential subsidence steering the position of the palaeo-drainage system. Together, the investigated units form two vertically stacked fluvio-deltaic couplets which record the successive basin filling by eastward-prograding braid deltas. A multitude of event beds occurring in the prodelta deposits, including turbidites, wave-modified turbidites and hummocky cross-stratified tempestites, indicates that the deltas built into a shallow basin occasionally swept by storms. The shallow nature of the basin in combination with vertically extended river effluents enabled dunes to prograde far onto the slope. Here, they eventually became liquefied and collapsed, initiating sediment-gravity flows which contributed to sand deposition on the basin floor. Moreover, we describe a wide range of soft-sediment deformation structures attributed to recurrent tectonically induced seismic activity as well as gravity-driven deformation of the prodelta slope. As such, we explore sedimentary response to potential late Riphean post-rift tectonism, differential subsidence, and the interaction of fluvial and deltaic processes on a shallow, pericratonic basin on the previously rifted, Timanian margin of Baltica.

Grundvåg, S.-A. & Skorgenes, J. 2022: Sedimentology of Neoproterozoic storm-influenced braid deltas, Varanger Peninsula, North Norway. *Norwegian Journal of Geology* 102, 202217.
<https://dx.doi.org/10.17850/njg102-4-4>

© Copyright the authors.

This work is licensed under a Creative Commons Attribution 4.0 International License.

Introduction

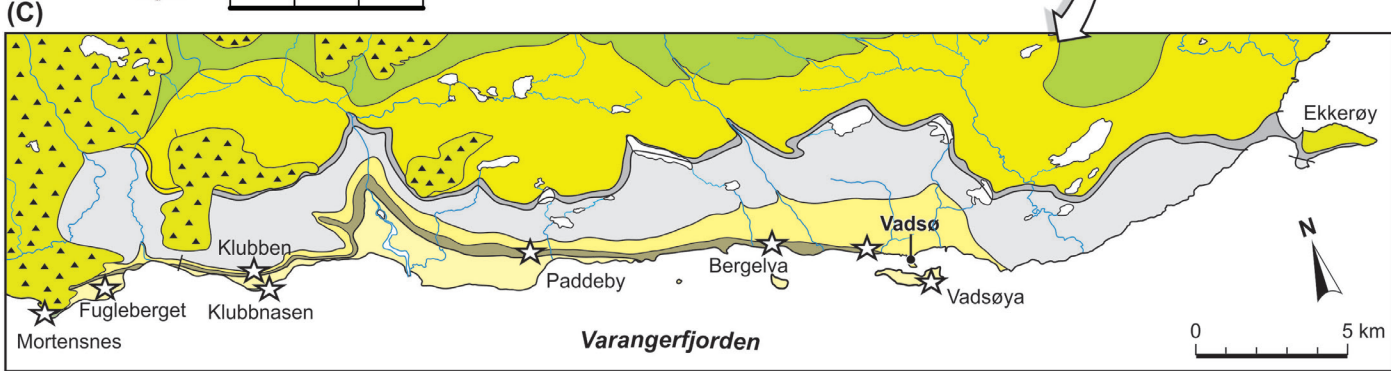
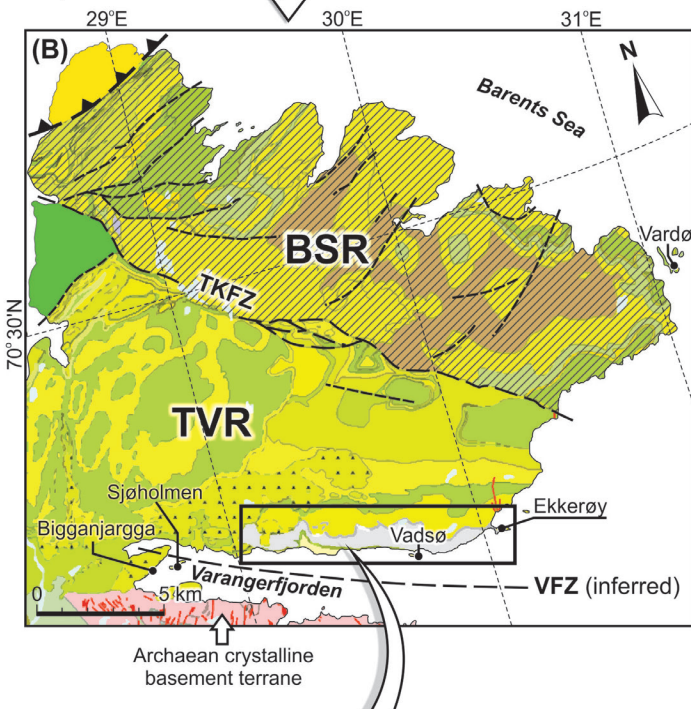
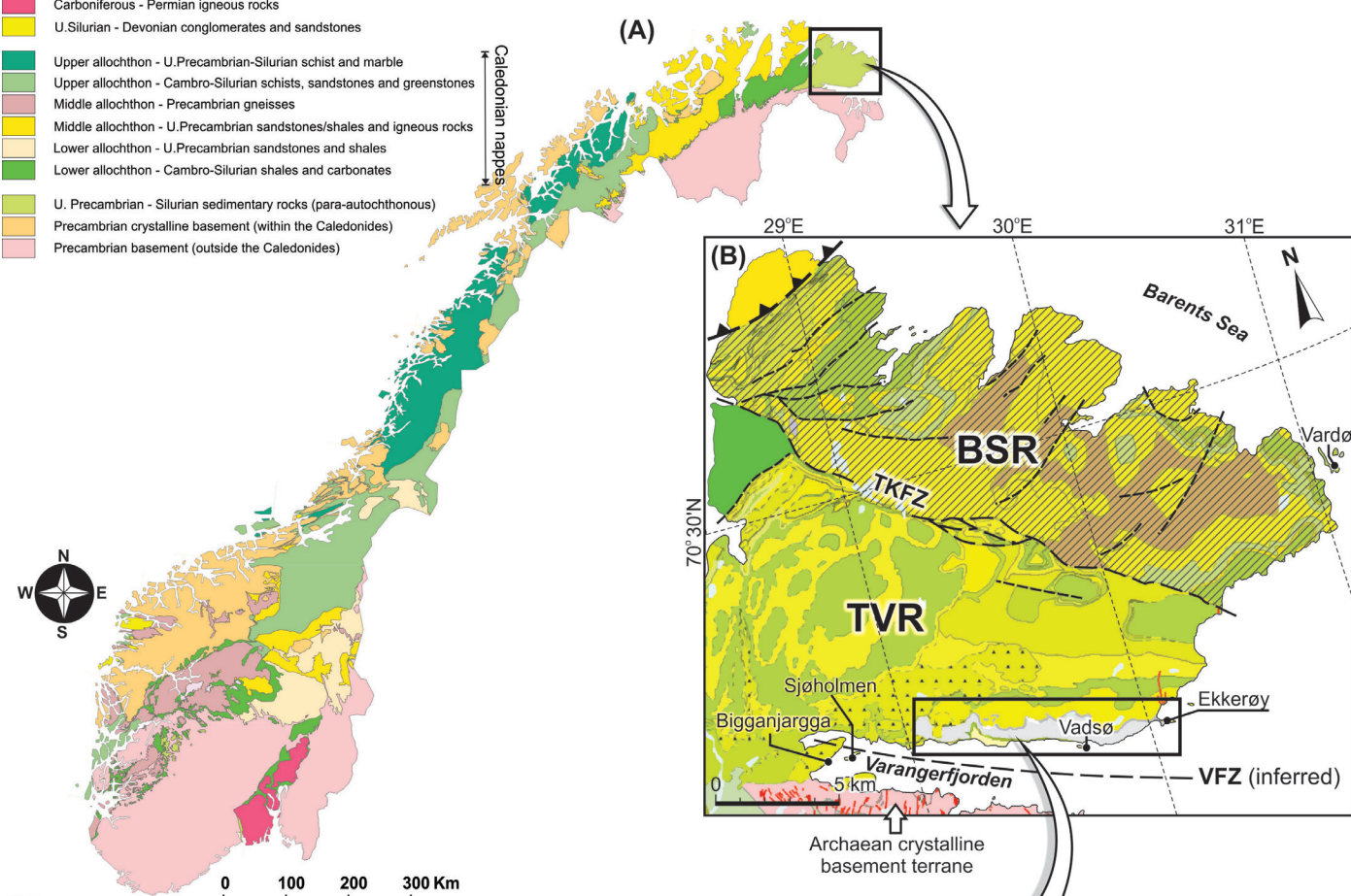
The Tanafjorden-Varangerfjorden Region (TVR) in the southwestern part of the Varanger Peninsula, eastern Finnmark, North Norway (Fig. 1), comprises a c. 4 km-thick Neoproterozoic succession consisting mostly of fluvio-deltaic to shallow-marine sandstone-dominated deposits, as well as intercalated glacial deposits, which all accumulated on a pericratonic platform on the Timanian margin of Baltica during the late Riphean (Cryogenian) (Banks et al., 1974; Johnson et al., 1978; Siedlecka, 1985; Siedlecka et al., 1995; Roberts & Siedlecka, 2002, 2012, 2022; Røe, 2003; Nystuen et al., 2008; Fig. 2). Few studies have investigated the mudstone-rich and heterolithic units that intercalate with the sandstones in the lower part of the Neoproterozoic succession of the TVR (Fig. 2B). These units, which are assigned to the Klubbnasen and Andersby formations, are the focus of the present study. Previously, these formations, which both are overlain by >100 m-thick units of cross-bedded sandstones of interpreted braided stream affinity (i.e., the Fugleberget and Paddeby formations, respectively), have been considered to be of deltaic origin (Banks et al., 1974; Hobday, 1974; Røe, 2003). Albeit, some early works suggest deposition in a wave-, and possibly tide-influenced, offshore to nearshore setting for the Klubbnasen Formation, and an interfluvial to possibly lacustrine setting for the Andersby Formation (Banks, 1971; Banks et al., 1974; Røe, 2003). The contrasting environmental interpretations demonstrate the need for improved and updated process-oriented depositional models for the two units. In addition, the stratigraphic relationship between the inferred deltaic and the overlying fluvial strata remains poorly investigated, and it is therefore unclear whether there is a genetic link between these deposits. As such, a re-evaluation of the lithostratigraphic boundaries and the relationship between the various deposits is deemed necessary.

Moreover, Røe (2003) suggested that an inferred E-W-oriented basin-bounding border fault, referred to as the Varangerfjorden Fault Zone (VFZ; Fig. 1; see also Høltedahl, 1918, who first hypothesised such a fault zone), controlled sediment routing in the basin during the late Riphean and resulted in extensive syn-tectonically-induced soft-sediment deformation of the TVR sedimentary succession (Røe, 2003). However, its presence and influence on sedimentation and deformation is only hypothetical and thus strongly debated (e.g., Røe, 2003; Roberts et al., 2011) with most authors preferring a stable pericratonic platform/passive margin interpretation for the succession (e.g., Banks et al., 1974; Johnson et al., 1978; Nystuen, 1985; Siedlecka, 1985; Siedlecka et al., 1995, 2004; Roberts & Siedlecka, 2012, 2022; Nystuen et al., 2008; Pease et al., 2008; Zhang et al., 2015). As such, a re-assessment of the distribution and styles of soft-sediment deformation structures may shed new light on the tectonic regime and development of the basin.

Although some sedimentological data are available for the Klubbnasen and Andersby formations, these units are usually treated briefly in most publications dealing with the TVR succession (Banks, 1971; Banks et al., 1974; Hobday, 1974; Røe, 2003). In this contribution we present a detailed sedimentological outcrop study of the lower part of the TVR succession, thus adding another level of resolution in comparison to previous work. The three main objectives are to: i) document the facies variability and the depositional architecture of the two inferred deltaic units (i.e., the Klubbnasen and Andersby formations), ii) elucidate their stratigraphic/genetic relationship to the overlying fluvial successions (i.e., the Fugleberget and Paddeby formations), and iii) discuss in general lateral and vertical variability in depositional processes and control mechanisms of fluvio-deltaic successions. We further present updated depositional models for these units, particularly focusing on the interaction of fluvial and deltaic processes, as well as the wide range of syn- to post-depositional deformation processes that collectively were responsible for their development. Finally, our findings are discussed with respect to basin fill history, exploring the hypothetical influence of the VFZ vs. alternative tectonic controls, as well as relative sea-level fluctuations and possible climatic forcing.

Legend

- Carboniferous - Permian igneous rocks
- U.Silurian - Devonian conglomerates and sandstones
- Upper allochthon - U.Precambrian-Silurian schist and marble
- Upper allochthon - Cambro-Silurian schists, sandstones and greenstones
- Middle allochthon - Precambrian gneisses
- Middle allochthon - U.Precambrian sandstones/shales and igneous rocks
- Lower allochthon - U.Precambrian sandstones and shales
- Lower allochthon - Cambro-Silurian shales and carbonates
- U. Precambrian - Silurian sedimentary rocks (para-autochthonous)
- Precambrian crystalline basement (within the Caledonides)
- Precambrian basement (outside the Caledonides)



Vadsø Group		
 Ekkerøya Formation	 Andersby Formation	 Vestertana Group (<i>undifferentiated</i>)
 Golneselva Formation	 Fugleberget Formation	 Tanafjord Group (<i>undifferentiated</i>)
 Paddeby Formation	 Klubbnasen Formation	 Investigated section

Figure 1. (A) Simplified geological map of Norway, showing the distribution of Precambrian basement terranes and paraautochthonous sedimentary successions, as well as Caledonian nappes. The Varanger Peninsula is marked by a black square. Map courtesy of The Geological Survey of Norway (NGU). (B) Geological map of the Varanger Peninsula showing the distribution of Neoproterozoic rocks in the southern paraautochthonous and autochthonous Tanafjorden–Varangerfjorden Region (TVR), and the northern allochthonous Barents Sea Region (BSR; not considered here). The two zones are separated by the Trollfjorden–Komagelva Fault Zone (TKFZ), which had a major influence on deposition during the Neoproterozoic. The TVR succession is bounded to the south by the inferred Varangerfjorden Fault Zone (VFZ; see Røe, 2003 for more details), which displaces Neoproterozoic sedimentary rocks against Archaean crystalline basement to the south. The map is modified from Siedlecka & Roberts (1996) and Roberts & Siedlecka (2012). (C) Geological map showing the distribution of the Vadsø Group along the northern shores of the Varangerfjorden area. Stars indicate investigated locations. Compiled and redrawn from Siedlecka (1991) and Røe (2003).

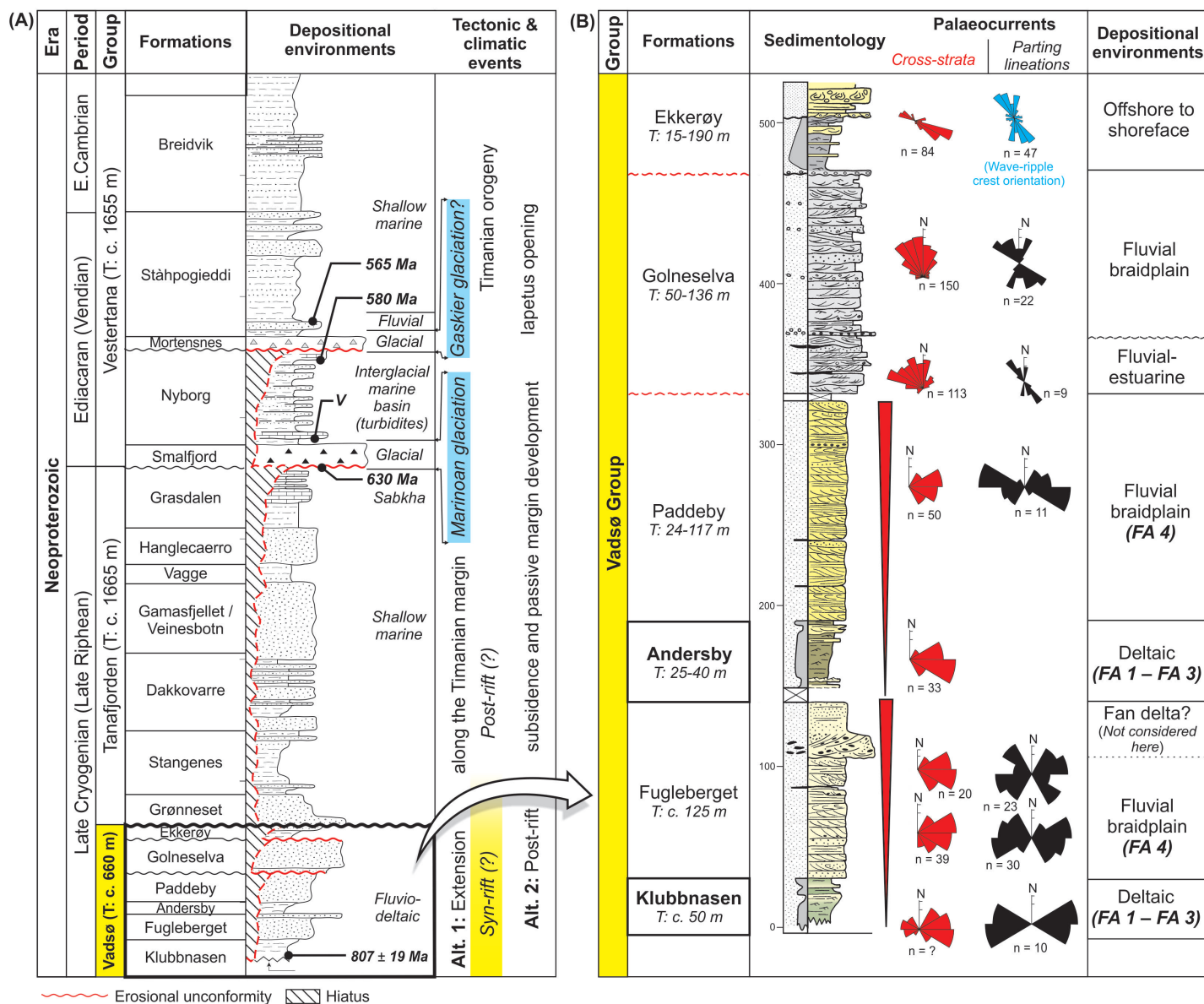


Figure 2. (A) Lithostratigraphic column of the Vadsø, Tanaffjorden and Vestertana groups. This study focuses on the lowermost part of the Vadsø Group (here excluding the Veidnesbotn Formation) which accumulated in a basin located on the northeastern, Timanian margin of Baltica (see Fig. 3). Two contrasting tectonic models have been proposed for the succession. Alternative 1: the Vadsø Group and the lower part of the Tanaffjorden Group (i.e., the Grønneset Formation) accumulated in a syn-rift setting, whereas the overlying succession represent post-rift deposits (Røe, 2003). Alternative 2: the entire succession accumulated on a pericratonic platform during post-rift passive margin development (e.g., Johnson et al., 1978; Nystuen, 1985; Siedlecka, 1985; Siedlecka et al., 1995; Roberts & Siedlecka, 2012, 2022). Redrawn and compiled from Røe (2003) and Nystuen (2008). Additional and updated age constraints from Gorokhov et al. (2001) and Jensen et al. (2018). V – Vendian. (B) Detailed lithostratigraphic overview of the Vadsø Group. This study focuses on the Klubbnasen–Fugleberget formations and the Andersby–Paddeby formations, which form two large-scale upwards-coarsening couplets (marked by red triangles) of inferred fluvio-deltaic origin. Redrawn and modified from Røe (2003). Additional paleocurrent data of the Ekkerøy Formation from Johnson (1975). The stratigraphic distribution of the facies associations (FA 1 to FA 4) documented in this study is indicated.

Geological setting

Tectonic framework

The Neoproterozoic succession of the Varanger Peninsula represents the westernmost part of the Timan-Varanger Belt, a zone comprising partly deformed and low-grade metamorphosed sedimentary rocks extending for c. 1800 km from the Varanger Peninsula in the west to the Timan Range in the

east (Siedlecka & Siedlecki, 1967; Siedlecka et al., 1995, 2004; Olovyanishnikov et al., 2000; Roberts & Siedlecka, 2002, 2022; Nystuen et al., 2008). During the middle to late Riphean, this zone formed the rifted northeastern margin of Baltica, which subsequently transformed into a passive margin prior to compressional deformation related to the Timanide orogen in the middle–late Vendian (e.g., Olovyanishnikov et al., 2000; Roberts & Siedlecka, 2002; Siedlecka et al., 2004; Nystuen et al., 2008; Pease et al., 2008; Fig. 3). Numerous papers deal with the Timanian and Caledonian orogenic histories of the Varanger Peninsula and will not be reiterated here (e.g., Gayer & Roberts, 1973; Roberts, 1996; Rice, 2014; Zhang et al., 2016; Gabrielsen et al., 2022).

In the late Mesoproterozoic, most of Earth's continental fragments, including Baltica, were assembled into the supercontinent Rodinia (e.g., Merdith et al., 2017; Fig. 3). During the assembly, several plates collided into the central plate of Laurentia, forming extensive orogenic belts along the collision zones (e.g., the Greenville and Sveconorwegian belts; Cawood et al., 2007). At this time, Baltica was apparently located on the southern hemisphere adjacent to the northeastern margin of Laurentia (Nystuen et al., 2008; Merdith et al., 2017). In the early Neoproterozoic, Rodinia eventually started to break apart after being assembled for >150 million years (Li et al., 2008). Widespread intracratonic rifting, possibly initiated by a mantle superplume, occurred during the break-up (Li et al., 2008), and gradually Baltica started to take shape with the establishment of its rifted margins during the middle to late Riphean (Siedlecka et al., 2004; Nystuen et al., 2008; Pease et al., 2008).

A major WNW–ESE-trending regional lineament, the Trollfjorden–Komagelva Fault Zone (TKFZ), divides the Varanger Peninsula into two geological provinces, the Barents Sea Region (BSR) to the northeast and the Tanafjorden–Varangerfjorden Region (TVR, the focus of this study) in the southwest (Siedlecka & Siedlecki, 1967; Johnson et al., 1978; Roberts, 1996; Røe, 2003; Fig. 1). During the late Riphean (Cryogenian), the TKFZ presumably acted as a normal fault separating the fluvial to shallow-marine pericratonic platform regime of the TVR from the shallow- to deep-marine basinal regime of the BSR in the hanging wall (Siedlecka, 1985; Røe, 2003; Siedlecka et al., 2004). The TVR succession is thinner and more condensed in comparison to the expanded BSR succession (c. 4 km vs. c. 15 km of strata, e.g., Siedlecka, 1985; Nystuen, 2008) due to differential subsidence along the TKFZ and because it sits on top of thick continental crust, whereas the latter sits on top of a thinned continental crust intruded by mafic dykes of Devonian age (e.g., Herrevold et al., 2009). The TKFZ has been reactivated multiple times and acted as a major regional dextral strike-slip displacement zone during the Caledonian deformation event (Johnson et al., 1978; Rice, 1994; Herrevold et al., 2009; Gabrielsen et al., 2022).

The proposed Varangerfjorden Fault Zone (VFZ; Røe, 2003; Fig. 1) is apparently oriented near parallel to the present-day axis of the WNW–ESE-running Varangerfjorden. The VFZ presumably acted as a north-dipping, basin-bounding border fault during the middle late Riphean rifting event on the Timanian margin, thus influencing deposition of the Vadsø Group and the lowermost Tanafjorden Group (Røe, 2003). It may also have been reactivated and rotated towards the very end of the Riphean (Røe, 2003). Although some short seismic lines in the southernmost part of Varangerfjorden could not confirm the presence of the VFZ (e.g., Roberts et al., 2011), the stratigraphic relationship and the short distance between the upper Riphean sedimentary succession on the northern shore of the Varangerfjorden and the rapidly rising Archaean crystalline (cratonic) basement on the southern shore, may indicate its presence (Holtedahl, 1918; Røe, 2003). In addition, it seems possible that the hypothetical VFZ may have exerted some structural control on the position and orientation of the so-called Varangerfjorden palaeo-valley, which was carved out during the supra-regional Vendian (Ediacaran) glaciations (Bjørlykke, 1967; Nystuen, 1985; Røe, 2003; Baarli et al., 2006).

Lithostratigraphy

The c. 4 km-thick sedimentary rock succession of the TVR is subdivided into the Vadsø and Tanafjorden groups of late Riphean (Cryogenian) age, and the Vestertana Group of Vendian (Ediacaran) to early Cambrian age (e.g., Røe, 2003; Nystuen, 2008; Fig. 2A). Only the lower part of the Vadsø Group is considered in this paper (Fig. 2B). The succession has experienced low-grade metamorphism and relatively little tectonic deformation. Several unconformities of various magnitude and extent are present, recording both tectonically-induced uplift and tilting, as well as deep erosion and palaeo-valley formation during the Ediacaran glaciations (Bjørlykke, 1967; Johnson et al., 1978; Laajoki, 2001; Røe, 2003; Baarli et al., 2006; Nystuen, 2008; Fig. 2A). In particular the unconformity between the Cryogenian and Ediacaran strata represents a significant hiatus (maybe up to a few hundred million years), where up to c. 700 m of strata was removed by glacial erosion (Føyn & Siedlecki, 1980; Nystuen, 2008).

The up to 660 m-thick sandstone-dominated Vadsø Group consists mainly of various fluvio-deltaic and shallow-marine deposits (Johnson et al., 1978; Røe, 2003; Fig. 2), which accumulated in a laterally extensive pericratonic marginal basin, in some publications referred to as the Gaiassa Basin (e.g., Rice et al., 2001; Rice, 2014; Zhang et al., 2016). According to Røe (2003), the Vadsø Group includes six formations, which may be divided into three lower-order tectono-stratigraphic units separated by regional unconformities (Fig. 2B). This study focuses specifically on the lowermost of these unconformity-bounded units which includes the Klubbnasen, Fugleberget, Andersby and Paddeby formations (Fig. 2B). We are aware that other workers also assign sandstones of the Veidnesbotn Formation, which occur in scattered outcrops on the southern shore of the Varangerfjorden, to the group (e.g., Banks et al., 1974; Hobday, 1974; Johnson et al., 1978; Siedlecka, 1985; Rice et al., 2001; Nystuen, 2008; Roberts & Siedlecka, 2022). However, we exclude this unit here as we do not possess data which can settle the dispute as to which formation the sandstones on the southern side of the Varangerfjorden belong (see discussion in Røe, 2003).

The c. 50 m-thick Klubbnasen Formation is mudstone dominated in its lower part, becoming more heterolithic and sandstone-rich upwards. An offshore to nearshore or prodelta to delta-front origin has previously been suggested for the unit (Banks et al., 1974; Hobday, 1974; Røe, 2003). A Rb–Sr isochron dating at the base of the formation yielded an age of 807 ± 19 Ma (Sturt et al., 1975; Fig. 2A). The boundary to the overlying sandstone-dominated Fugleberget Formation (up to c. 125 m thick; Fig. 2B), has previously been described as gradual (e.g., Banks et al., 1974; Hobday, 1974; Røe, 2003). The Fugleberget Formation is generally characterised by thick-bedded, cross-stratified sandstones, but also includes sandstones and intraformational conglomerates organised into large-scale (>10 m thick) foresets in its uppermost part, together recording deposition in a braided stream to fan-delta setting (Hobday, 1974; Røe, 1987; Røe & Hermansen, 2006; Fig. 3). Provenance studies and persistent east to northeast-directed palaeocurrent directions in the Fugleberget Formation are consistent with sourcing from the Archaean and Palaeoproterozoic basement terranes exposed on the craton south of the Varanger Peninsula (Zhang et al., 2015).

The c. 25–40 m-thick Andersby Formation sharply overlies the Fugleberget Formation. The unit is mudstone dominated in its lower part, becoming more sandstone-rich upwards. A deltaic or interfluvial to possibly lacustrine origin has been suggested for the unit (Banks, 1971; Banks et al., 1974; Røe, 2003). The overlying c. 120 m-thick Paddeby Formation is characterised by thick cross-bedded sandstones suggesting deposition in a braidplain setting (Banks et al., 1974; Røe, 2003). Collectively, these units form two vertically stacked, upward-coarsening stratigraphic couplets (i.e., the Klubbnasen–Fugleberget and the Andersby–Paddeby formations).

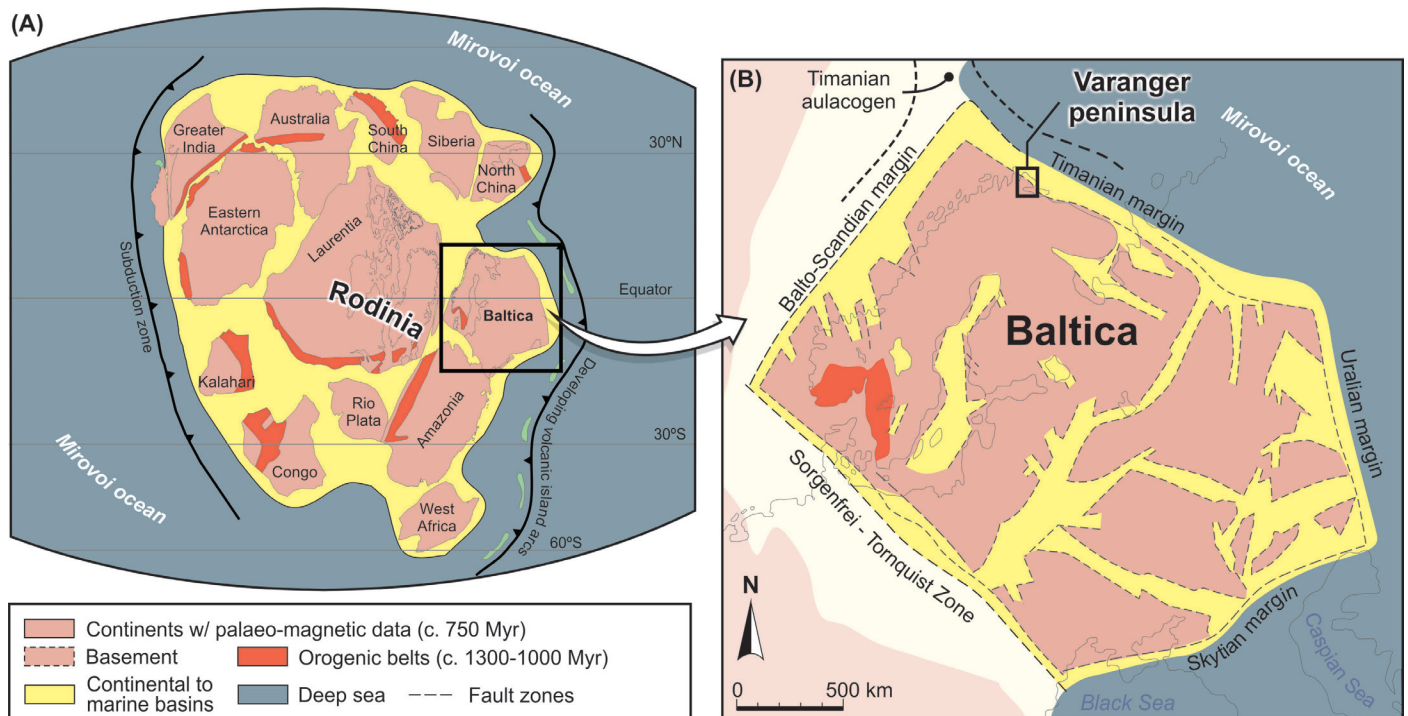


Figure 3. (A) Simplified paleo-geographic reconstruction of the paleo-continent Rodinia showing the position of Baltica. (B) Paleo-geographic reconstruction of Baltica during the Neoproterozoic, showing the position of the Varanger Peninsula at the rifted, northeastern Timanian margin of Baltica. Both figures are modified and redrawn from Nystuen (2008).

Methods

The dataset investigated in this study includes sedimentary logs measured at multiple localities along the northern coastline of the Varangerfjorden including the Bergelva, Fugleberget, Klubben, Klubbnasen, Mortensnes, Paddeby, Vadsø and Vadsøya localities (Fig. 1C). The sedimentary logs document lithology, grain size, bed thickness, bed geometry, bed boundaries and sedimentary structures.

The Klubbnasen Formation was mainly investigated at the Klubbnasen locality (Fig. 1), where the upper c. 28 m of the unit is exposed along a laterally persistent coastal section. The bedding dips by a few degrees towards the west, giving excellent access to the upper part of the unit and the boundary to the overlying sandstones of the Fugleberget Formation. A section through the uppermost part of the Klubbnasen Formation was also briefly investigated at Mortensnes (below the lighthouse). The lower part (c. 25 m) of the Klubbnasen Formation is not exposed, although Banks et al. (1974) indicates that the lower c. 5 m of the unit crops out at Sjøholmen, an island in the innermost part of the Varangerfjorden (previously referred to as Skjåholmen; Fig. 1B for location). This observation has subsequently been disputed by Røe (2003), who assigned these deposits to the uppermost part of the Veidnesbotn Formation (laterally corresponding to the Gamafjellet Formation or the lower Vagge Formation in her revised stratigraphic model, Fig. 2). Because of these uncertainties, the present study only pertains to the upper part of the Klubbnasen Formation. The Fugleberget Formation was mainly investigated at the Vadsøya locality, whereas the basal boundary and the lowermost part of the unit was documented at the Klubbnasen and Mortensnes localities. The upper conglomeratic part of the Fugleberget Formation which reportedly contains large-scale foresets (Hobday, 1974; Røe, 2003), was briefly investigated in the quarry at Vadsøya, as well as at Klubben and Fugleberget (near Mortensnes; Fig. 1C).

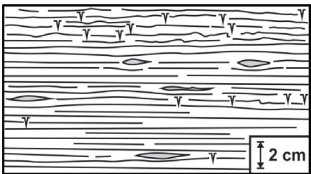
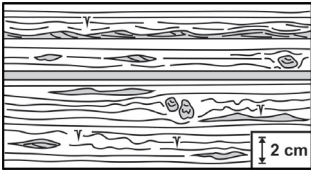
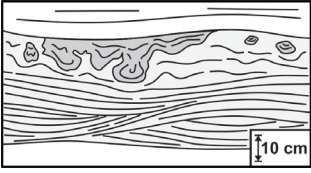
The Andersby Formation was investigated at the Bergelva and Vadsø localities (Fig. 1). At both localities, the steepness and relief of the coastal cliffs, which ranges from c. 3 to 8 m in height, occasionally limited data collection. However, the lateral extent of both outcrops enabled physical tracing of beds along the cliffs and the collection of multiple sedimentary logs, which were combined into two correlation panels to document lateral facies distribution and variations. The basal boundary of the unit was briefly investigated at Klubben, whereas the boundary to the overlying Paddeby Formation (and the lower part of this unit) were investigated at the Bergelva, Klubben and Paddeby localities (Fig. 1C).


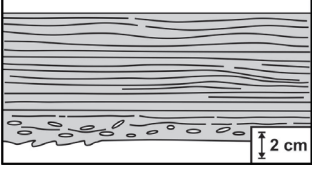
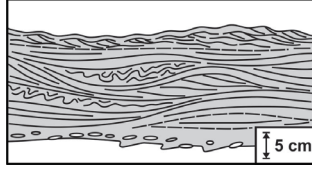
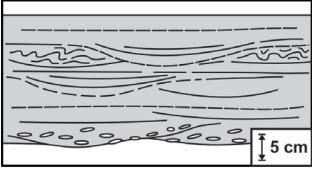
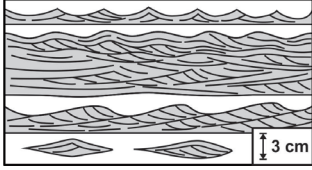
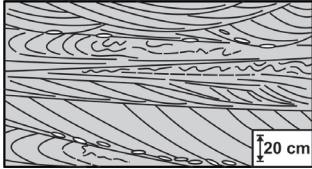
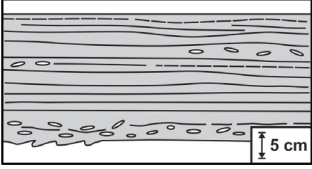
Results

Facies associations (FA)

From the facies analysis, eight lithofacies were recognised in the Klubbnasen and Andersby formations (Table 1). Additionally, two lithofacies were identified in the lower parts of the Fugleberget and Paddeby formations, which were documented to provide stratigraphic context, particularly across the formation boundaries (Table 1). The ten lithofacies were subsequently arranged into four main facies associations (FAs 1 to 4) representing offshore (FA 1), storm-influenced prodelta (FA 2), fluvial-dominated to storm-affected delta front (FA 3), and braidplain (FA 4) deposits. A description and interpretation of the four associations are presented in the following section, starting with the deposits typically occurring in the lowermost part of the logs.

Table 1. Summary of the most important lithofacies.

Lithofacies	Description	Interpretation	Facies architecture
1 Laminated mudstone to siltstone	Tabular units of laminated mudstone or siltstone with scattered cm-scale sandstone lenses, some displaying wave ripple- or combined-flow ripple cross-lamination. Sandfilled syneresis cracks occur frequently in some horizons. Thickness: 0.1 to 3 m.	Hemipelagic fallout sporadically interrupted by minor deposition of sand from weak oscillatory flows and oscillatory combined-flows. Deposition took mostly place below storm wave base (SWB). Syneresis cracks may be caused by fluctuating palaeosalinity stress or de-watering triggered by wave-induced stress or seismic shocking.	
2 Interbedded sandstone/siltstone	Interbedded very-fine grained sandstone and siltstone units. The sandstone beds are lenticular to wavy and exhibit planar lamination and combined-flow ripple cross-lamination or less commonly wave ripple cross-lamination. Ball-and-pillow structures occur locally. Thickness: 0.1 to 3 m.	Hemipelagic fallout frequently interrupted by deposition of sand from dominantly combined flows governed by storms and turbidity currents above SWB. Deformation records density contrasts and liquefaction processes.	
3 Hummocky cross-stratified siltstone to very fine-grained sandstone	Isotropic hummocky cross-stratified (HCS) and low-angle laminated sandy siltstone beds with pinch-and-swell geometries and abundant dewatering and ball-and-pillow structures. Internal truncations occur sporadically. Thickness: 0.2 to 2 m.	Erosion and deposition by storm generated, oscillatory combined-flows with relatively high aggradation rates with reworking by several storm events and/or fluctuation in the intensity of storm-produced flow. Deformation attributed to seismically-triggered liquefaction processes.	

4 Massive sandstone	Tabular, non-graded to normally graded, structureless, very-fine to medium-grained sandstone beds, occasionally with erosional bases containing frequent flute casts. Thickness: 2 to 15 cm.	Erosion by strong unidirectional turbulent currents preceded by deposition from waning flow with high aggradation rates whereby tractive transport is suppressed. Massive beds may also record liquefaction and dewatering processes following rapid deposition.	
5 Planar laminated sandstone	Planar and quasi-planar laminated (sensu Arnott, 1993) very-fine to fine-grained sandstone occasionally containing mudstone clasts. In some cases erosively based with abundant flute casts. Thickness: 2 to 30 cm.	Erosion by strong unidirectional to unidirectional dominated currents followed by deposition from high-velocity, waning unidirectional to combined flows with high aggradation rates.	
6 Hummocky cross-stratified sandstone	Isotropic to rare eastward-oriented anisotropic HCS, very fine to fine-grained sandstone beds with erosive bases exhibiting rip-up mudstone clasts and occasional flute casts. Distinct pinch-and-swell bed geometries and rippled bed tops (combined flow ripples and rare wave/interference ripples) are common. Convolute bedded horizons are common. Thickness: 5 to 40 cm.	Formed by aggradation and migration of 3D bedforms deposited by strong to intermediate oscillatory to oscillatory dominated combined flows under waning storm intensity. Deposition was generally preceded by strong, turbulent (erosive) unidirectional currents. Syn-sedimentary deformation and local liquefaction by cyclic stress created by storm waves.	
7 Swaley cross-stratified sandstone	Swaley cross-stratified (SCS, sensu Leckie & Walker, 1982) fine- to medium-grained sandstone beds with abundant mudstone clasts. Amalgamation and scours filled by low-angle stratified sandstone is common. Soft sediment deformation structures are variably present. Thickness: 5 to 30 cm.	Generated by strong and erosive, offshore-directed storm-induced currents near fair-weather base (generally overlies HCS). May record lower aggradation rates due to high sediment transport rates close to shore.	
8 Cross-laminated sandstone	Swaley cross-stratified (SCS, sensu Leckie & Walker, 1982) fine- to medium-grained sandstone beds with abundant mudstone clasts. Amalgamation and scours filled by low-angle stratified sandstone is common. Soft sediment deformation structures are variably present. Thickness: 5 to 30 cm.	Generated by strong and erosive, offshore-directed storm-induced currents near fair-weather base (generally overlies HCS). May record lower aggradation rates due to high sediment transport rates close to shore.	
9 Cross-bedded sandstone	Planar- and trough cross-bedded, fine- to medium-grained, tabular- to wedge-shaped sandstone beds. Tangential foresets and sigmoidal architectures are common. Convolute bedding, recumbent folds, as well as erosive set boundaries and troughs aligned with rip up mudstone clasts occur frequently. Set thickness: 10-50 cm, occasionally up to 1 m.	Generated by steady and uniform unidirectional currents in an intermediate flow regime. Sand deposited as bedload on the lee side of migrating two-dimensional and three-dimensional dunes. Recumbent folds may record starting liquefaction processes triggered by fast flow (i.e., upper flow regime conditions).	
10 Planar-bedded sandstone	Planar-bedded medium-grained sandstone with parting lineations on bed surfaces and occasional rip up mudstone clasts. Thickness: 0.4 to 2 m.	Formed by unidirectional currents under upper-flow regime conditions.	

Facies association 1 – Offshore deposits

Description. – Facies association 1 (FA 1) occurs in the lowermost part of both the Klubbnasen and the Andersby formations, where it typically forms up to 3 m-thick, finely laminated, mudstone packages which grade upwards into the heterolithic deposits of FA 2 (Fig. 4A). FA 1 also occurs as thin packages (<2 m thick) alternating with units of FA 2 in the upper parts of both formations. FA 1 mainly consists of parallel-laminated mudstone to siltstone (lithofacies 1, Table 1; Fig. 4B). Subordinate thin (<2 cm) interbeds of lenticular to wavy-bedded, very fine- to fine-grained sandstones are present (lithofacies 2, Table 1; Fig. 4C). The sandstones, which become more abundant upwards, typically appear structureless and normally graded, whereas planar-lamination and unidirectional ripple cross-lamination, or more rarely wave to combined flow-ripple cross-lamination occurs locally (Fig. 4C). In places, stacks of graded to non-graded, very fine- to fine-grained sandstone beds with individual bed thicknesses ranging from 0.1 to 0.4 m occur embedded within the laminated mudstone successions (best example at the Paddeby locality; Fig. 4D). The sandstone beds generally appear tabular and massive, but in many places they exhibit abundant soft-sediment deformation structures, some with an eastward vergence (Fig. 4E).

Interpretation. – Based on the predominance of laminated mudstone and siltstone, FA 1 is interpreted to have been deposited in an offshore setting mostly below storm wave base (SWB). The laminated mudstone and siltstone represent prolonged periods of suspension settling, typical of fair-weather deposition and limited sand influx to the basin (e.g., Dott Jr & Bourgeois, 1982; Brenchley et al., 1993). The local presence of sandstones exhibiting normal grading, planar-lamination, as well as local rippled tops, indicate sporadic sand influx and deposition from distally waning, high-energy events, such as low-density turbidity currents and in particular wave-modified turbidity flows (Mutti et al., 1996; Myrow et al., 2002; Lamb et al., 2008), or various combined flows generated by storms (e.g., Myrow, 1992a; Grundvåg et al., 2020; Jelby et al., 2020). The thicker graded to non-graded, massive, or soft-sediment deformed sandstone beds are interpreted as deposits from high-density turbidity currents or liquefied sediment flows/sandy debris flows (Lowe, 1982; Nemeč, 1990). The soft-sediment deformation structures indicate a combination of rapid deposition, liquefaction/water escape, and gravity-driven deformation. In summary, FA 1 is considered to represent an offshore environment where various sediment gravity flows and subordinate storm-generated flows originating from the approaching deltas infrequently brought sand onto the basin floor.

Facies association 2 – Storm-influenced prodelta deposits

Description. – Facies association 2 (FA 2) transitionally overlies and locally interfingers with fine-grained deposits of FA 1 and is characterised by up to 7 m-thick heterolithic units (Figs. 4A & 5). FA 2 consists of planar-laminated mudstone to siltstone and interbedded sandstone (lithofacies 1 to 3; Table 1; Figs. 5, 6, 7 & 8). The abundance of sandstones increases upwards, giving rise to pronounced upward-coarsening and thickening trends (Fig. 6A).

The sandstone interbeds are thin (<0.1 m) to thick bedded (0.1–0.4 m, some rare examples exceeding 0.7 m), and consist of very fine- to fine-grained sandstones with lenticular to tabular geometries (Figs. 5 & 6A, B, C). Thin lenticular beds have wavelengths at the scale of a few decimetres (Fig. 6B), whereas thicker lenticular beds have wavelengths of several metres (Fig. 6C). Most of the sandstone beds are normally graded with sharp and erosive bases and commonly exhibit load casts, or in the case of the thick beds, eastward-directed flute casts (Fig. 6B, C, D). Bed tops are generally sharp with gently undulating to rippled top surfaces. Eastward-directed combined-flow ripples (i.e., ripples with near symmetric to asymmetric geometries, rounded tops, and unidirectional-dipping cross-lamination, e.g., Harms, 1969; Yokokawa, 1995) occur frequently (lithofacies 8, Table 1), and wave/interference

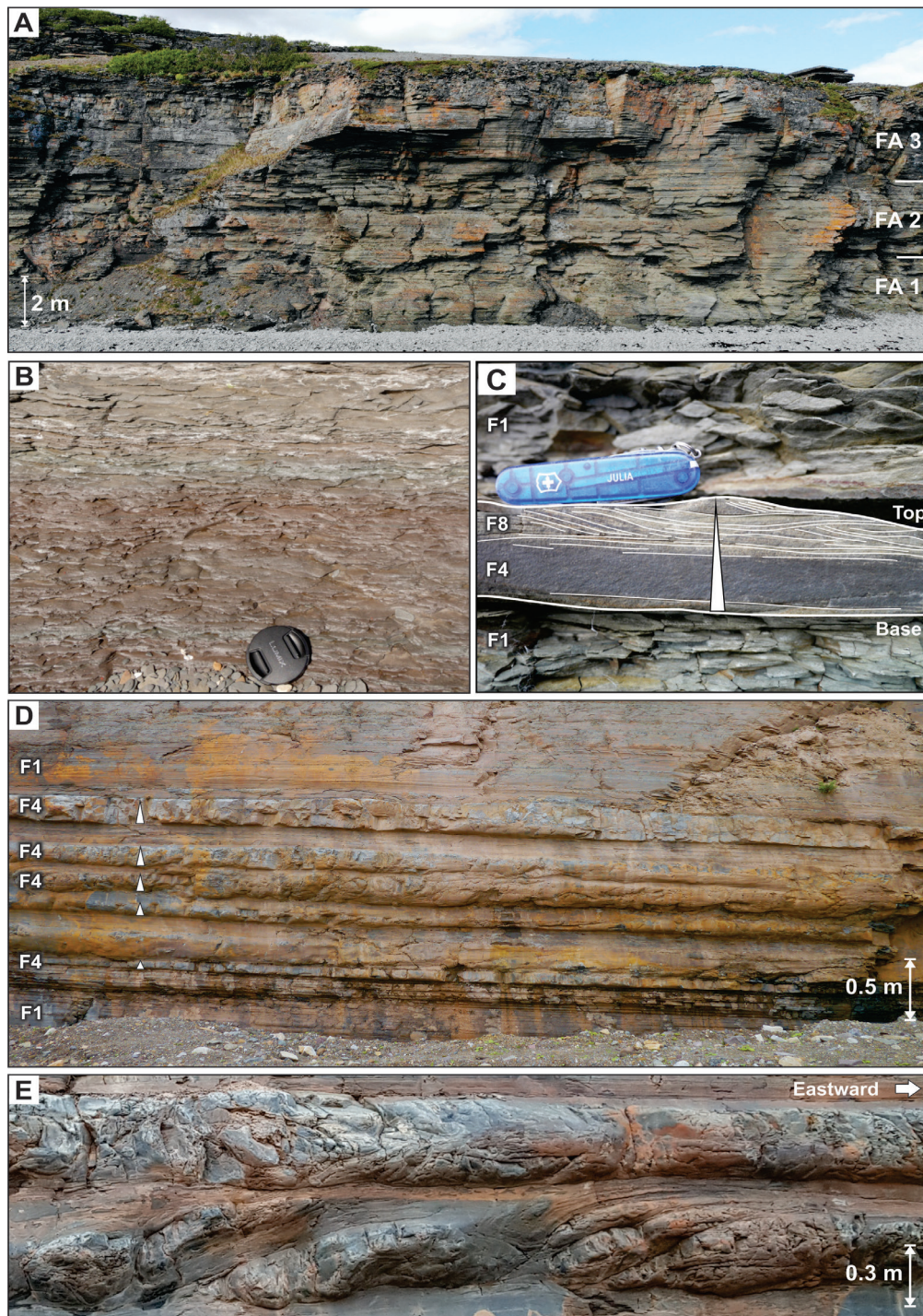


Figure 4. Representative photos of FA 1 (offshore deposits). (A) FA 1 typical forms the lower part of large-scale coarsening-upward units. Klubbnasen Formation at the Klubbnasen locality. (B) Laminated mudstone (lithofacies 1, Table 1) is the volumetrically most important facies of FA 1. Lens cap for scale (5 cm). (C) Thin, normally graded sandstone beds, typically with a lower massive division (lithofacies 4) overlain by combined-flow ripple cross-lamination (lithofacies 8) and a rippled top occur frequently in the upper parts of FA 1. Note the sigmoidal foresets and the convex-up geometries of some laminae. Pocket knife for scale (8 cm). (D) Locally, stacks of tabular, graded to non-graded turbiditic sandstone beds (lithofacies 4) embedded within mudstone (lithofacies 1) characterizes FA 1. Andersby Formation at the Paddeby locality. (E) Close-up photo of two turbidite beds. Note the pervasive soft-sediment deformation of both beds and the preferred eastward vergence of the folded strata in the lower bed. Locations are given in Fig. 1C.

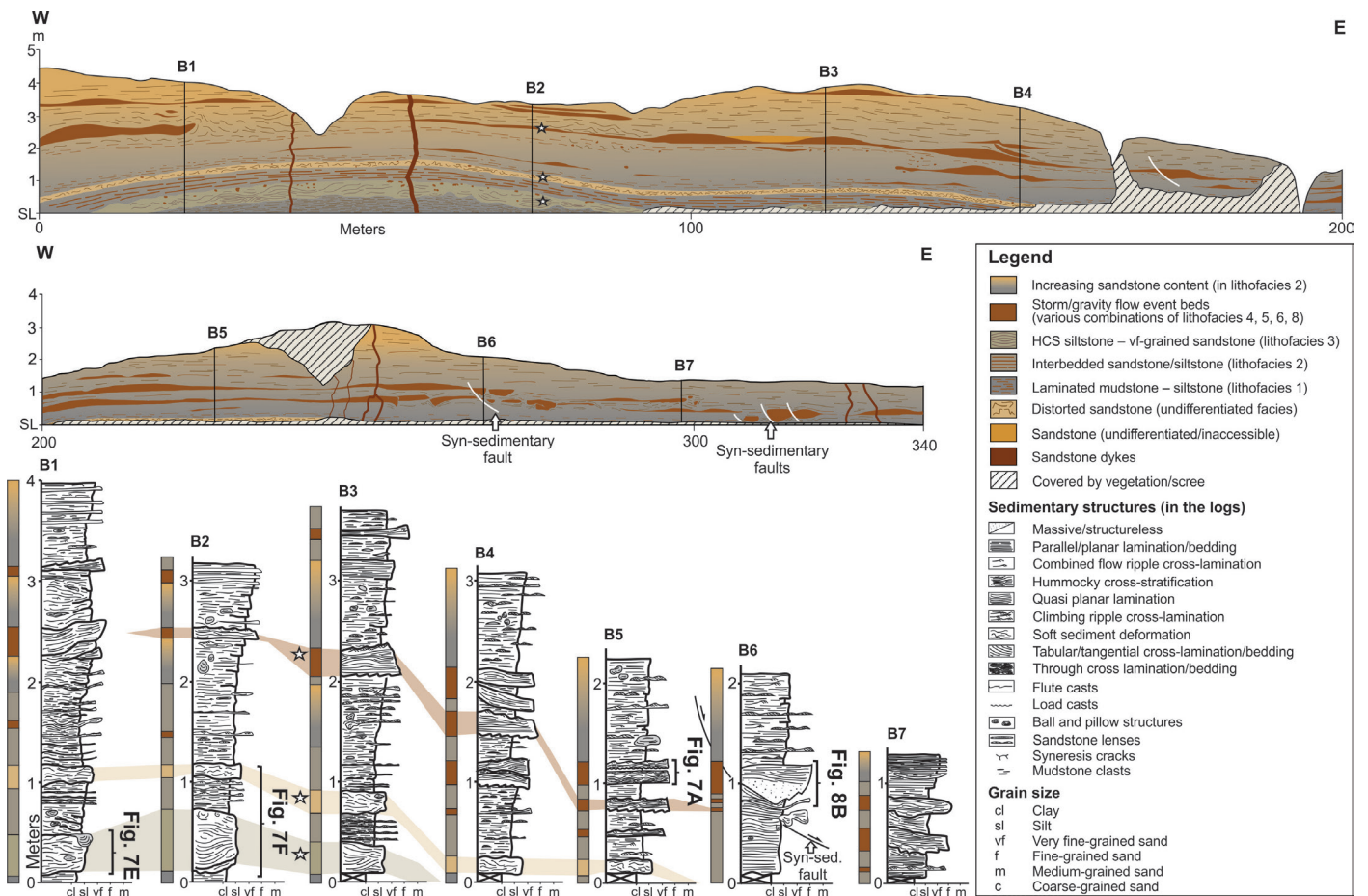


Figure 5. Panel and logs documenting the heterolithic nature and internal architecture of FA 2 (storm-influenced prodelta deposits) in the upper part of the Andersby Formation at the Bergelva locality (Fig. 1C for location). Several sandstone beds, emplaced during storms or gravity flow events, can be traced across the outcrop. The white stars in section B2 indicates the three marker beds correlated in the logs. Note the presence of syn-sedimentary faults. The legend is valid for all other figures that include logs and panels. The panel is not corrected for (some minor) post-depositional folding.

ripples are also present (lithofacies 2; Fig. 6E). Scours (some few decimetres deep and up to 1.5 m wide) filled with thin-bedded heterolithics that drape or onlap, and in some cases thicken towards the basal scour surface, occur in places (Fig. 6F). Locally, some scour fill units are slightly rotated and displaced against the scour surface (Fig. 6F) whereas others are contorted and strongly deformed (see Hobday, 1974).

The thick-bedded sandstones typically exhibit a lower structureless, graded to non-graded division (lithofacies 4, Table 1), which either passes upwards into isotropic or more rarely anisotropic hummocky-cross stratification (HCS; lithofacies 6, Table 1; Fig. 7A, B), or in places via planar to quasi-planar lamination (lithofacies 5, Table 1, Fig. 7C, D). Locally, sets of climbing, combined-flow, ripple cross-lamination occur below the rippled bed tops (lithofacies 8, Table 1, Fig. 7C, D). In places, up to c. 0.7 m-thick, siltstone to very fine-grained sandstone beds exhibiting isotropic HCS are present (lithofacies 3, Table 1; Fig. 7E). Locally, convolute bedding with a preferred eastward vergence is present within these beds, and ball-and-pillow structures forming pseudo nodules occur abundantly in their upper part (Fig. 7F).

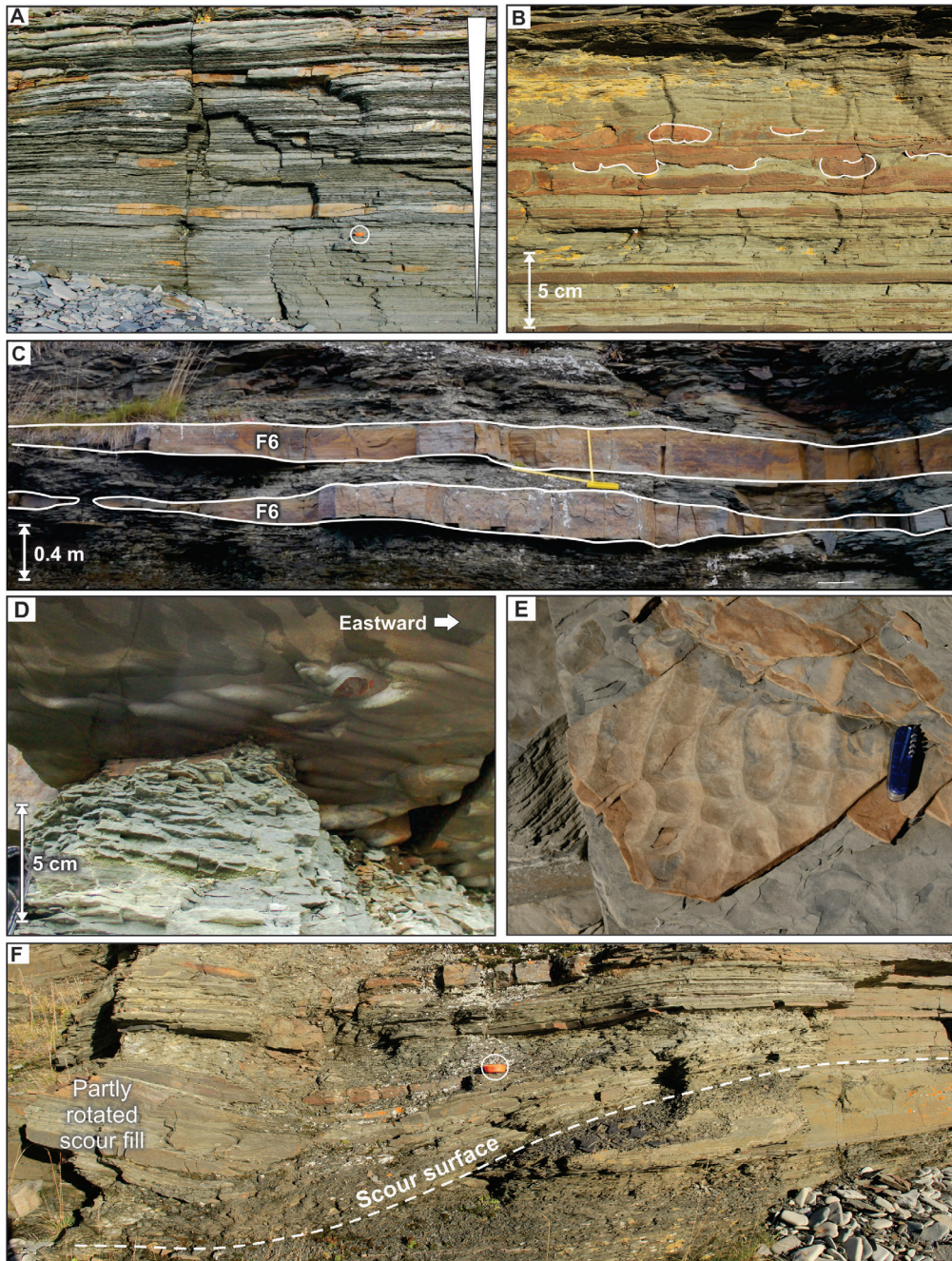


Figure 6. Representative photos of FA 2 (storm-influenced prodelta deposits). (A) FA 2 consists of lenticular to wavy bedded sandstones and interbedded mudstones forming heterolithic units which exhibit upwards coarsening trends. Klubbnasen Formation, Klubbnasen locality. Encircled cup for scale (8 cm). (B) The lower part of FA 2 typically shows a thin-bedded development with abundant delicate, ball-and-pillow structures (forming pseudo nodules). Klubbnasen Formation, Klubbnasen locality. (C) Thicker, sandstone event beds, with tabular or well-developed pinch-and-swell geometries increase in abundance upwards in FA 2. Andersby Formation, Bergelva locality. (D) Eastward-oriented flute casts occur frequently along the base of the thick sandstone event beds. (E) Wave/interference ripples on an exposed bed top surface. Pocket knife for scale (8 cm). (F) A partly rotated heterolithic scour fill in the Klubbnasen Formation, Klubbnasen locality. These may represent erosion and deposition by hyperpycnal flows in combination with gravity-driven syn-sedimentary deformation of the prodelta slope. Encircled cup for scale (8 cm).

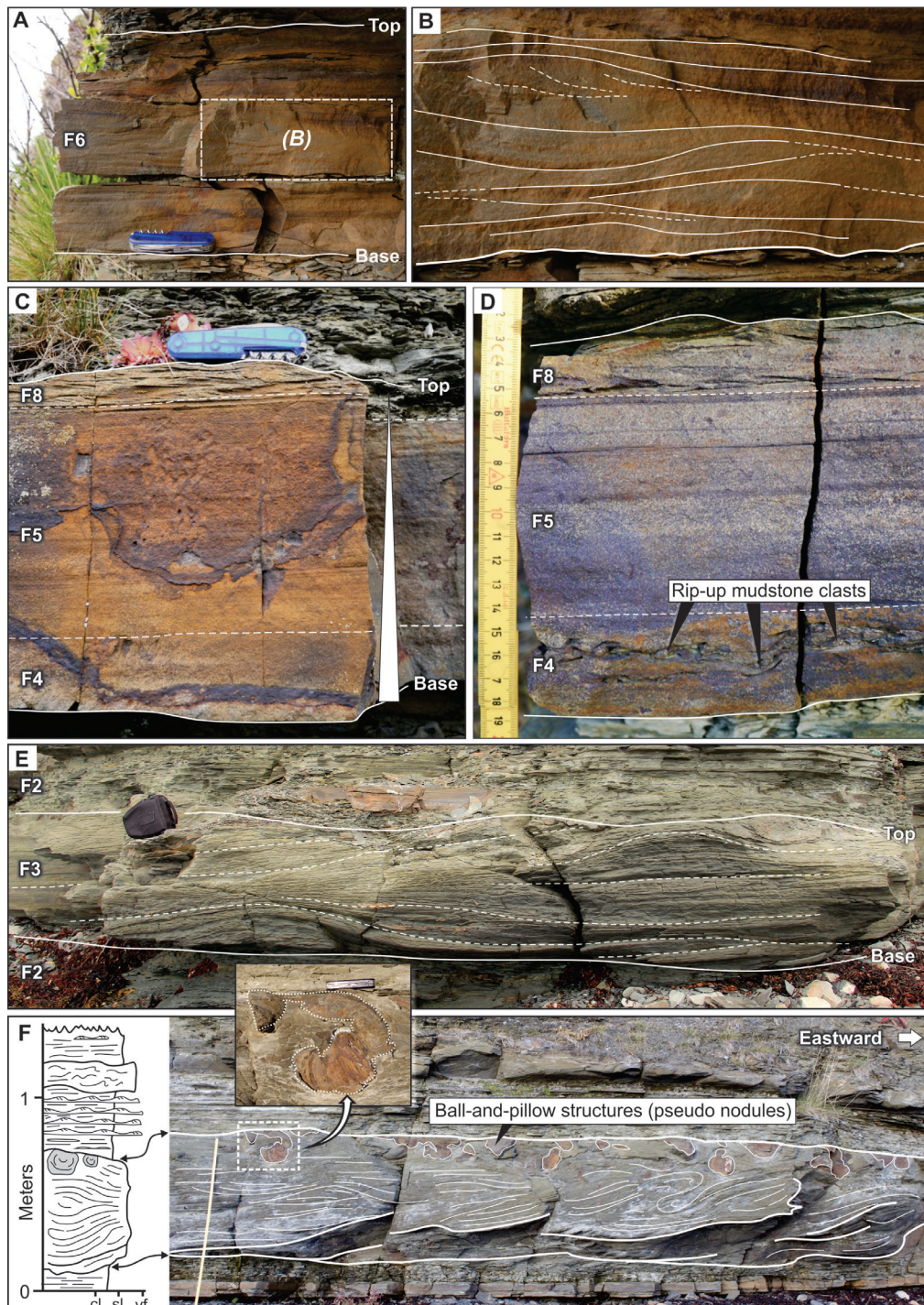


Figure 7. (A) Amalgamated sandstone beds displaying planar lamination (lithofacies 5) and isotropic hummocky cross-stratification (HCS; lithofacies 6). Pocket knife for scale (8 cm). (B) Close-up view of the isotropic HCS bed. Notice the occurrence of combined-flow ripple cross-lamination in the upper left part. (C) Close-up view of a normally graded (indicated by white triangle) event bed with a massive lower division (lithofacies 4) overlain by planar- to quasi-planar lamination (lithofacies 5) capped with combined flow ripples (lithofacies 8). This bed-scale facies sequence is typical of wave-modified turbidites. Pocket knife for scale (8 cm). (D) Rip-up mudstone clasts occur at the base of some of these event beds. (E) Sandy siltstone bed with isotropic HCS and a marked pinch-and-swell geometry. These beds resemble classical tempestites deposited by oscillatory-dominated combined flows. Camera bag for scale (25 cm). (F) Some HCS sandstone beds exhibit convolute bedding with an eastward vergence, which is traceable across the full length of the bed. Abundant ball-and-pillow structures (forming sandstone pseudo nodules) occur in the upper part of these beds. Some of these “nodules” contain internal lamination and represent partly rotated, loaded ripples (see inset photo). All photos from the Andersby Formation, Bergelva locality.

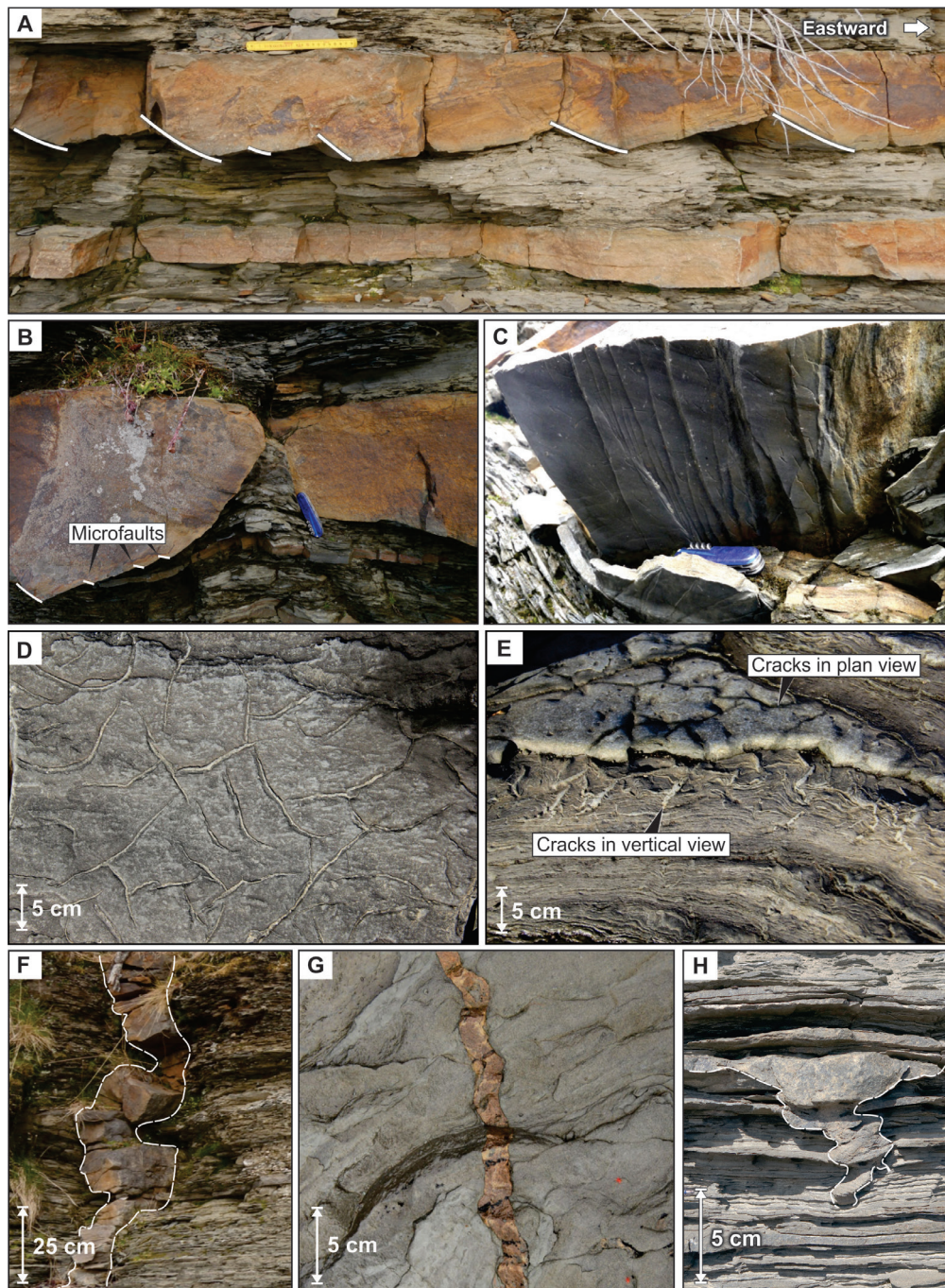


Figure 8. (A) A syn-sedimentary faulted sandstone bed (occurring in FA 2 prodelta deposits) in the Andersby Formation at the Bergelva locality. Internally, the bed repeatedly thickens toward each of the east-dipping fault planes (marked by white lines) whereas the stratification is concomitantly rotated. This deformation is attributed to gravity-driven, extensional forces acting on the prodelta slope in combination with sediment loading. Note the undeformed sandstone underlying the faulted sandstone bed. Ruler for scale (20 cm). (B) A sandstone bed fully segmented by a fault. A series of syn-sedimentary micro faults are present along the base of the bed. Pocket knife for scale (8 cm). (C) Photo showing the sole of the same bed which contains the syn-sedimentary micro faults. Pocket knife for scale (8 cm). (D) Syneresis cracks observed on a bedding surface. Note the incomplete network of polygons. (E) Syneresis cracks observed in both plan view on a sandstone bed surface extending down into the underlying mudstone unit. Note the irregular, sub-vertical geometry of the cracks in cross-section. (F) A sandstone dyke cutting through heterolithic prodelta deposits (FA 2). (G) Plan view of a dyke exposed on a sandstone bedding surface. (H) Wedge-shaped, dewatering pipe occurring in heterolithic prodelta deposits. Photos in A–C, F, and G: Andersby Formation, Bergelva locality. Photos in D, E, and H: Klubbnasen Formation, Klubbnasen locality.

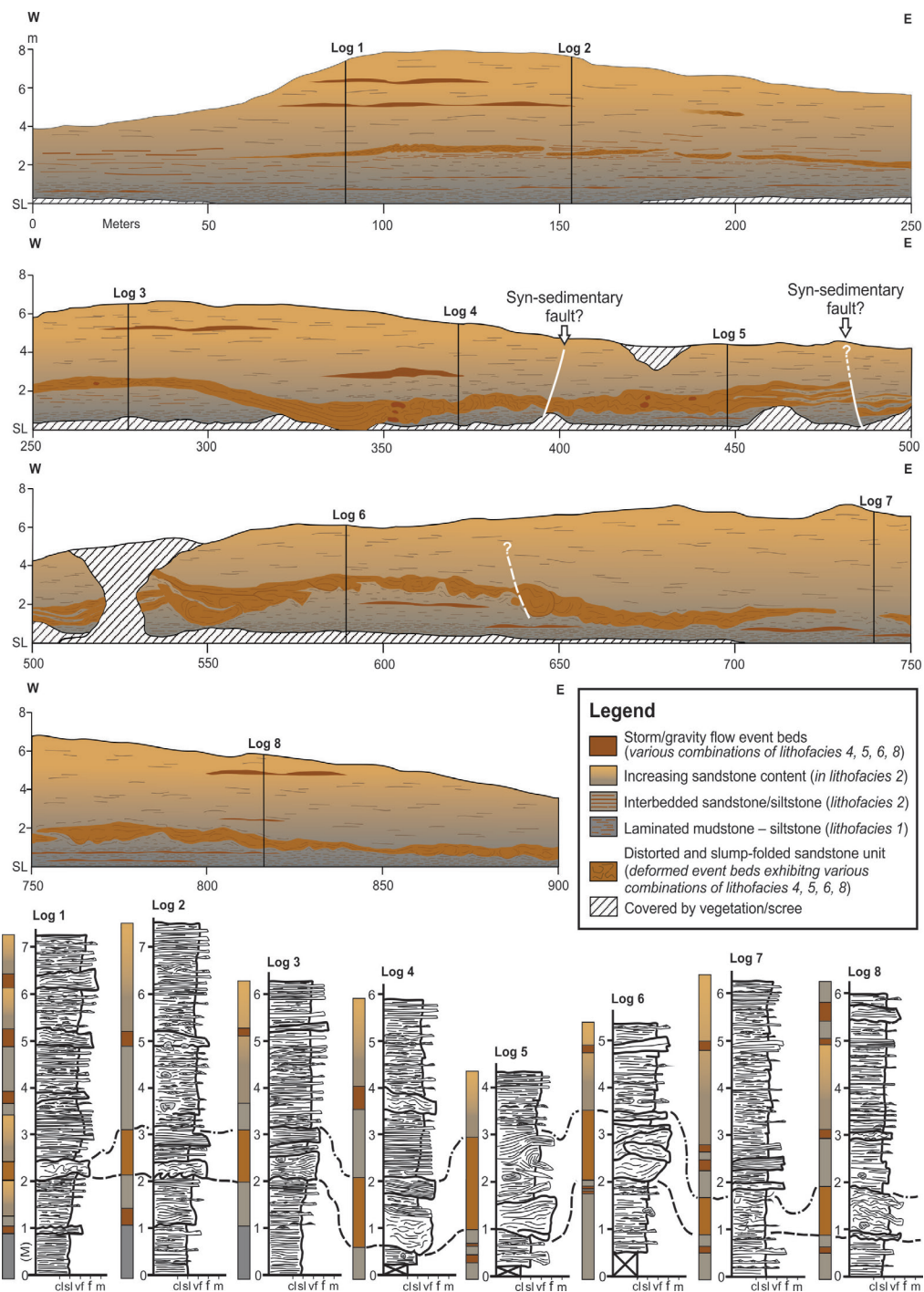


Figure 9. Panel with corresponding logs capturing the architecture of the storm-influenced prodelta succession (FA 2) of the Andersby Formation at the Vadsø locality. This outcrop displays a spectacularly distorted and slump-folded unit representing a prodelta slump deposit, which can be traced along the entire outcrop (c. 0.9 km). The top and base of the slump deposits is marked and correlated in the logs (stippled lines) See next figure for some detailed photos of the slump deposit. See Table 1 for lithofacies information and Fig. 5 for a log legend.

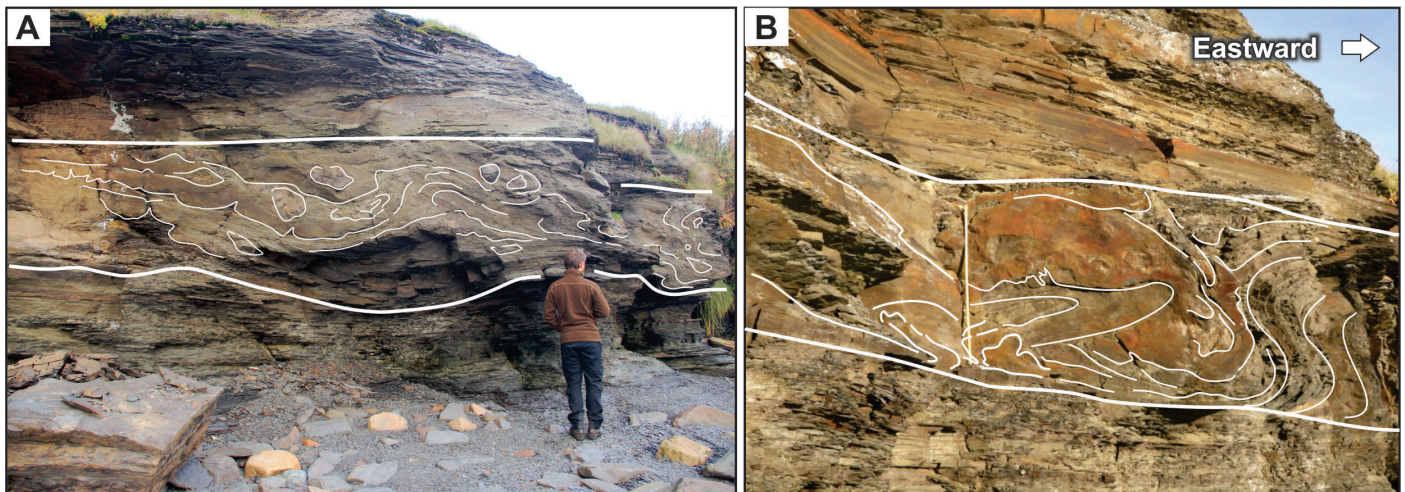


Figure 10. Representative photos of the slump deposit recorded in the Andersby Formation at the Vadsø locality. (A) The slump deposit is characterised by a chaotic, slump-folded and severely deformed fabric containing isolated sandstone blocks, variably sized ball-and-pillow structures, and flame structures with a vergence towards the east. (B) Examples of large-scale open folds and overturned folds with an almost horizontal axial plane oriented towards the east. Measuring stick for scale (1 m).

Small-scale syn-sedimentary faults with offsets in the range of some few centimetres to decimetres occur frequently in FA 2. Some sandstone beds may be dissected by a lateral series of such faults and a delicate bed thickening can be observed towards each of the faults (Fig. 8A). Other beds are completely segmented by faults, splitting the beds into several isolated and rotated sandstone blocks, each exhibiting multiple syn-sedimentary microfaults along their bases (Fig. 8B, C). Sandstone-filled, spindle-shaped, syneresis cracks (Fig. 8D, E) are abundant in FA 2, whereas sandstone dykes and small dewatering pipes occur sporadically (Fig. 8F, G, H).

In the Andersby Formation at the Vadsø locality, FA 2 comprises a 0.1–3 m-thick, eastward-thickening, laterally extensive (traceable for c. 0.9 km), chaotically deformed unit (Figs. 9 & 10). Internally, compressional and extensional features occur interchangeably, and include abundant eastward-oriented slump folds, small-scale faults, rotated sandstone blocks, and various syn-sedimentary deformation structures (SSDS). The deformation within the unit varies from weak distortion of the primary bedding to complete loss of stratification, in particulate towards the east. The overlying strata onlap and conformably drape the deformed unit (Fig. 10).

Interpretation. – The general fine-grained, yet heterolithic nature of FA 2, together with the presence of thick-bedded, HCS sandstones, indicate deposition under fluctuating energy conditions above SWB. The abundance of laminated mudstone and siltstone suggests deposition below fairweather wave base, in a generally quiescent background environment dominated by deposition from suspension fallout and prolonged periods with little sand transport into the basin. The sandstones, which become more frequent upwards, record sporadic, yet increasing, deposition from high-energy events with transport governed by various storm-generated currents and low-density turbidity currents.

The many thin-bedded sandstone beds exhibiting normal grading, sharp, erosive bases and various traction-generated structures, mostly of combined flow origin, are interpreted to record deposition from weak or distal, waning storms capable of maintaining sand in suspension and transporting it onto the shelf before final deposition (Dott Jr & Bourgeois, 1982; Myrow, 1992a).

The thick-bedded sandstones with erosive bases, flute casts, normal grading and abundant HCS, indicate that the seafloor was at times disrupted by more violent storms. Flute casts indicate initial scouring by powerful unidirectional (turbulent) flows, which preceded deposition. The returning flow following the coastal set-up during storms, may have generated strong down-welling flows capable of eroding the seafloor, and the same accounts for various storm-flood-generated, and commonly wave-supported/wave-modified, gravity flows (Myrow et al., 2002; Pattison, 2005; Lamb et al., 2008; Collins et al., 2017; Grundvåg et al., 2020; Jelby et al., 2020). The typical facies sequence recorded in the thick sandstone beds (i.e., a structureless, graded to non-graded lower division, followed by isotropic HCS or planar- to quasi-planar lamination, and combined-flow ripple cross-lamination), indicates deposition during waning oscillatory-influenced combined-flow (e.g., Arnott & Southard, 1990; Myrow & Southard, 1991). The documented sparsity of pure oscillatory-generated structures within or atop of the beds, indicates that post-depositional reworking by waves rarely occurred. Most of the investigated beds thus display features typical of event beds generated by main storm-ebb surges (e.g., Dott Jr & Bourgeois, 1982; Duke, 1991; Brenchley et al., 1993; Grundvåg et al., 2020; Jelby et al., 2020). Similar bed-scale sequences have occasionally been referred to as wave-modified turbidites and have been reported in numerous ancient offshore to nearshore, as well as prodeltaic to deltaic successions (e.g., Myrow, 1992a; Pattison, 2005; Lamb et al., 2008; Collins et al., 2017; Jelby et al., 2020).

A variety of processes may have formed the scour-and-fill features, including hyperpycnal flows deriving from nearby deltaic distributary channels, storm-generated currents coinciding with river floods, or by storm-generated, offshore-directed unidirectional-dominated combined flows (e.g., Myrow, 1992b; Pattison et al., 2007; Eide et al., 2015; Collins et al., 2017; Onyenanu et al., 2018; Grundvåg et al., 2020; Jelby et al., 2020). The displaced and rotated character of the fill and occasional bed thickening towards the scour surface indicate syn-sedimentary gravity-driven deformation. For the contorted scour fills exhibiting a chaotically deformed fabric in the Klubbnasen Formation, Hobday (1974) suggested slumping into small delta-front channels.

The wide range of deformation features observed in the chaotically deformed unit in the Andersby Formation at the Vadsø locality (Figs. 9 & 10), is attributed to liquefaction and fluidisation processes under the influence of lateral shear stress induced by slope failure. Based on the eastward thickening and the onlapping to draping nature of the strata above, the unit is interpreted to represent the deposits of a single, instantaneous slump event on a low-angle, eastward-dipping palaeo-slope. Potential triggering mechanisms for such slumps are difficult to deduce, but may include delta-front oversteepening, rapid sediment loading, hyperpycnal discharge, storm wave reworking, seismic shocking, relative sea-level change, or a combination of several of these processes (e.g., Nemeč et al., 1988; Piper & Normark, 2009; Clare et al., 2016).

Collectively, the documented facies variability, the upwards increase in sandstone, and the sporadic occurrence of scour-and-fill features are consistent with deposition in a storm-influenced prodelta setting for FA 2, where storm-generated flows and gravity-driven processes governed erosion and emplacement of tempestitic sands. The flute casts, combined flow-ripple cross-lamination, as well as the convolute bedding and slump folds in both the Klubbnasen and the Andersby formations, indicate general eastward delta progradation and an eastward-dipping palaeo-slope. This conforms to previous work, which have reported eastward-inclined foresets in the Klubbnasen Formation (Hobday, 1974) and an overall eastward thickening of the Vadsø Group (Banks et al., 1974; Røe, 2003). Thus, the rotated scour fills and the small-scale, syn-sedimentary faults and microfaults may thus be attributed to gravitational deformation and instability on a gently inclined prodelta slope in combination with concurrent sediment loading. The implications of abundant syneresis cracks, dewatering pipes and sandstone dykes are discussed further below.

Facies association 3 – Fluvial-dominated to storm-affected delta-front deposits

Description. – Facies association 3 (FA 3) typically forms up to 3 m-thick sandstone-dominated units which transitionally or sharply overlie the heterolithic deposits of FA 2 in the upper parts of the Klubbnasen and Andersby formations (Figs. 4A, 11A, 12 & 13). In just a few localities, the thickness of FA 3 may exceed 7 m (Fig. 13A). However, if traced eastward, such thick units tend to split into multiple thinner units (each <3 m thick) which interfinger with packages of FA 2 (Fig. 13B). Internally, the FA 3 units, which in places are highly amalgamated, consist of 0.1–0.4 m-thick fine- to medium-grained, tabular to wedge-shaped sandstone beds (Figs. 11B & 12). Swaley cross-stratification (SCS; lithofacies 7, Table 1; Fig. 11C), tangential cross-bedding (lithofacies 9, Table 1) and abundant convolute bedding characterise the lower part of the FA 3 units. Scours and internal truncation surfaces are present (Fig. 11D), and thin (<0.5 m thick) siltstone or lenticular- to wavy-bedded sandstone units exhibiting combined flow to current-ripple cross-lamination occur locally. The upper parts of the FA 3 units are characterised by trough- or tabular cross-bedding (lithofacies 9, Table 1) alternating with quasi-planar to low-angle inclined bedding (lithofacies 10; Table 1; Fig. 11B, E). The foreset dip azimuths of the cross-beds as well as rib-and-furrow structures on exposed surfaces indicate an overall eastward-directed palaeo-current flow direction (Fig. 11E, F). In some places, the cross-bedded sandstones are recumbently folded, in some cases overturned (Fig. 13C), and can be traced down-dip (over a distance of some few tens of metres) into severely soft-sediment deformed and slump-folded sandstones (Fig. 13A). In other places, the tabular- or trough cross-bedded sandstones (in the upper part of FA 3) transition down-dip into SCS, and more rarely, anisotropic HCS (in the lower part of FA 3). Some FA 3 units are very thin (<1 m), and in other units only the upper, cross-bedded facies assemblage occurs sharply overlying prodelta heterolithics of FA 2 (Figs. 12 & 13C).

In the Klubbnasen Formation at the Klubbnasen locality, several listric normal faults with throws of up to a few decimetres dissect up to 1.2 m of FA 3 strata before soling out (Fig. 14A). In plan-view, the faults are cusped, defining a series of small, low-angle, tilted fault blocks, each with an area <15 m². Fault-drag and minor fault-tip folding is observed in some beds dissected by the faults (Fig. 14A), whereas the sandstone beds above and below the fault blocks are barely affected by the faulting. These features have not been described in previous contributions and should not be confused with the reported post-depositional normal faults in the area which cut and offset the entire succession independent of facies associations and stratigraphic units (cf., Siedlecka et al., 1998). In places, some FA 3 units have a contorted appearance exhibiting a chaotic deformation fabric with abundant slump folds and other SSDS (Fig. 14B). The best example of such contorted FA 3 deposits is at the Mortensnes locality (near the lighthouse), where these deposits, which are in part affected by a small listric normal fault, appear to fill in the relief created by the faulting (Fig. 14B).

Interpretation. – Based on its stratigraphic position above FA 2 and the two-folded architecture with an upper part dominated by cross-bedded sandstones and a lower part exhibiting various storm-affected facies (i.e., SCS), FA 3 is interpreted to represent deposition in proximal fluvial-dominated to distal storm-affected delta-front settings. The cross-bedded sandstones are thus attributed to the offshore migration of 2D and 3D subaqueous dunes, presumably forming mouth bars or terminal distributary channel fills in the proximal fluvial-dominated delta-front reaches (e.g., Nemeč, 1992; Olariu & Bhattacharya, 2006). The ambiguous lack of structures compatible with wave activity in the proximal delta front may record the combined effects of high rates of fluvial sediment supply (with limited time for wave reworking) and the braided character of the feeder system with multiple, closely spaced, river effluents which collectively suppressed approaching waves. In contrast, bed amalgamation, internal truncations, and the lateral relationship between cross-bedded sandstones and SCS/anisotropic HCS in some units, suggest occasional storm-wave reworking of the distal delta front where storm waves

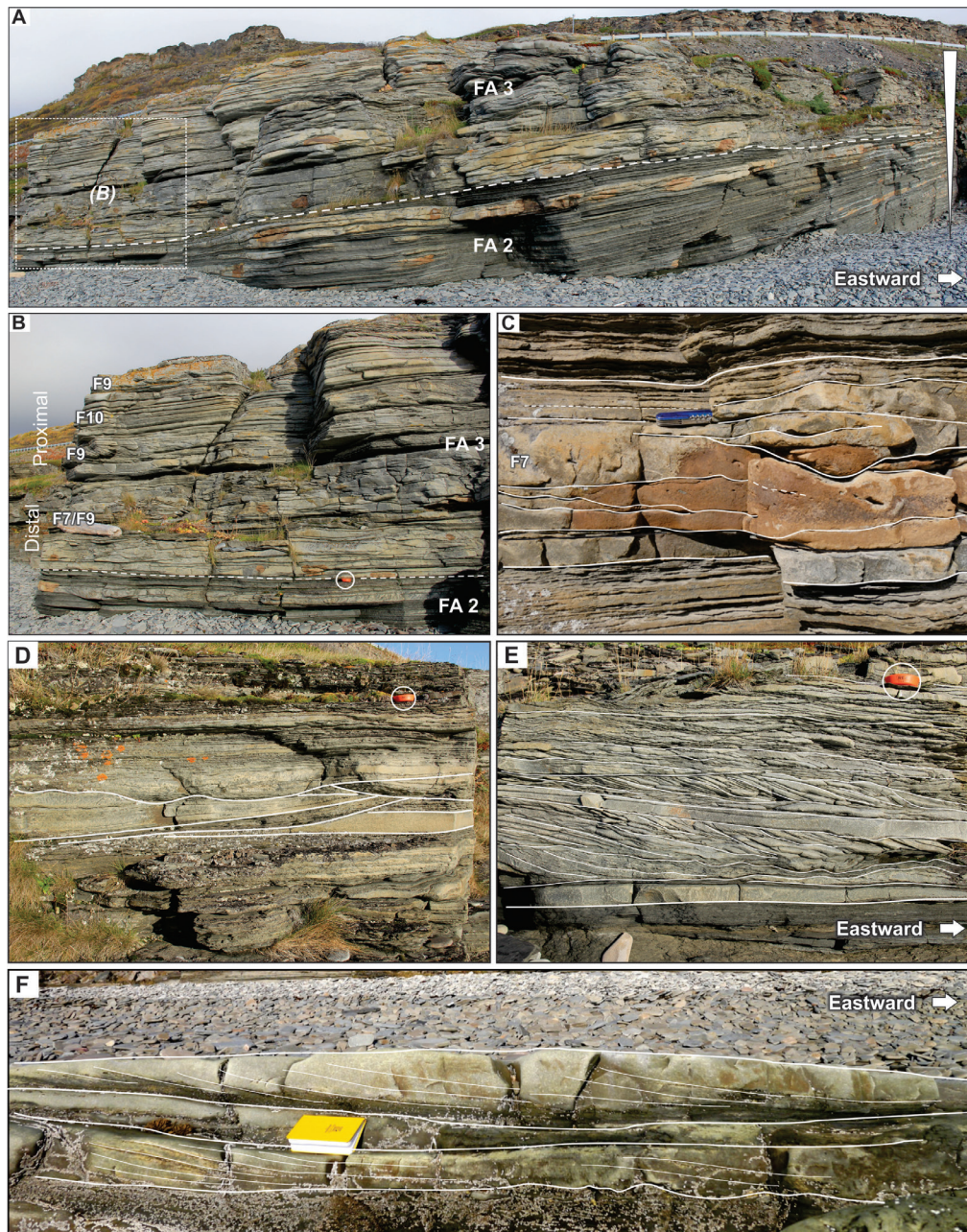


Figure 11. (A) Panorama displaying the vertical relationship between FA 2 (prodelta deposits) and FA 3 (delta front deposits) in the Klubbnasen Formation at the Klubbnasen locality. The white triangle indicates the coarsening- and thickening-upward trend typical of FA 2, thus marking a gradual transition into FA 3. (B) Photo showing the two-folded architecture of FA 3 with sub-associations representing distal (lower part) and proximal (upper part) delta front deposits. (C) Photo showing amalgamated sandstone beds exhibiting swaley cross-stratification (SCS; lithofacies 7). (D) Small scours occur locally in the lower part of FA 3, recording the passage of various turbulent flows. (E) Typical expression of the upper, proximal delta-front deposits dominated by traction-generated structures. (F) Example of a cross-bedded sandstone (lithofacies 9) in FA 3 of the Klubbnasen Formation. Note the tangential geometry of the foresets. Notebook for scale (19 cm).

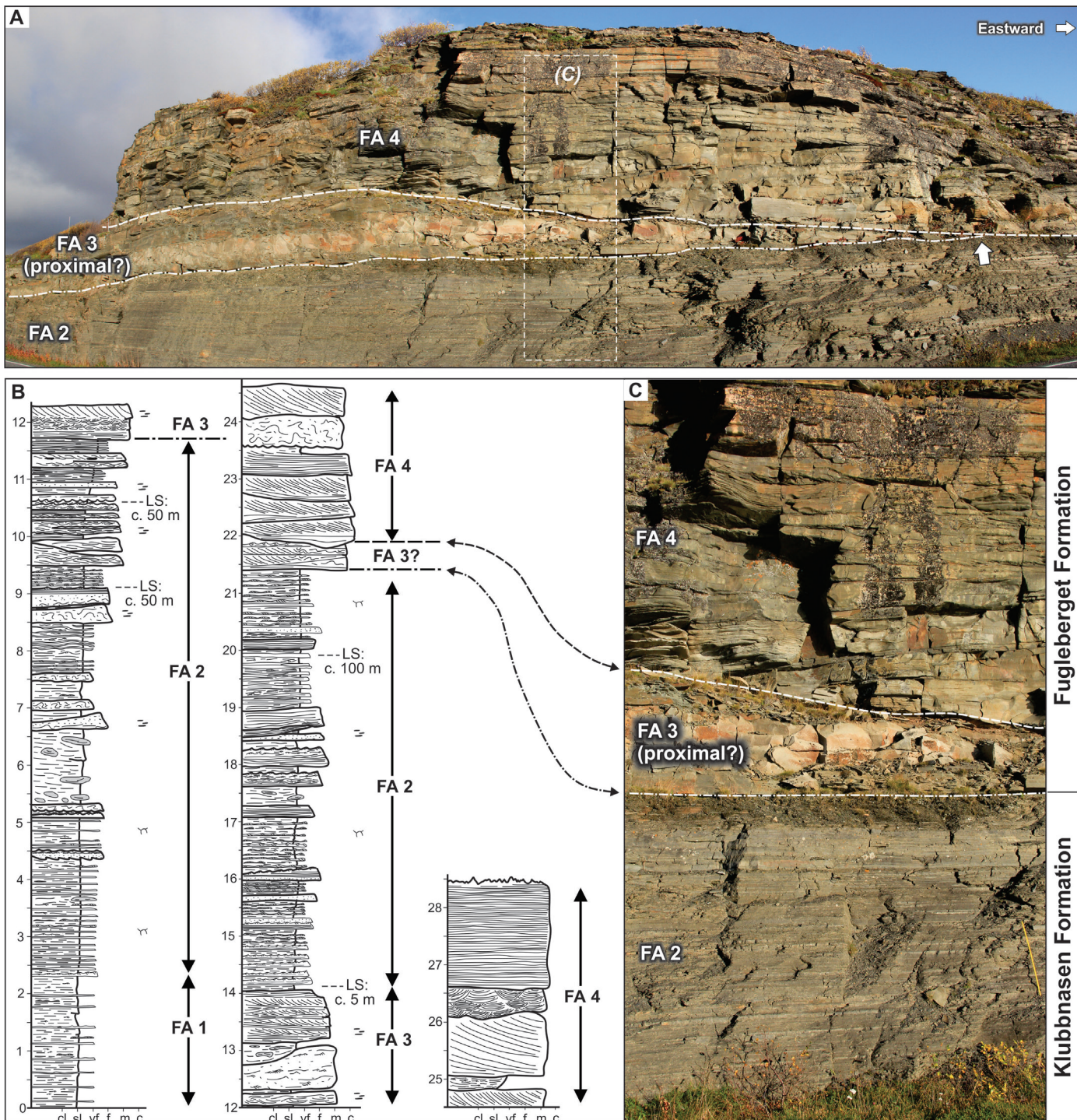


Figure 12. (A) Overview photo showing the apparent sharp boundary between the Klubbnasen and Fugleberget formations in the road-cut at the Klubbnasen locality. However, a thin, sharp based sandstone unit with slightly different characteristics than the braidplain deposits (FA 4) which dominate the Fugleberget Formation may represent an intervening, poorly developed, proximal delta front deposit (FA 3). (B) Detailed sedimentological log of the Klubbnasen Formation and transition to the lower part of the Fugleberget Formation at the Klubbnasen locality. LS: lateral step in the log. (C) Close-up photo showing the transition from prodelta heterolithics (FA 2) via the interpreted, sharp-based delta-front deposits (FA 3) of the Klubbnasen Formation to the braidplain sandstones (FA 4) of the Fugleberget Formation. Metre stick for scale.

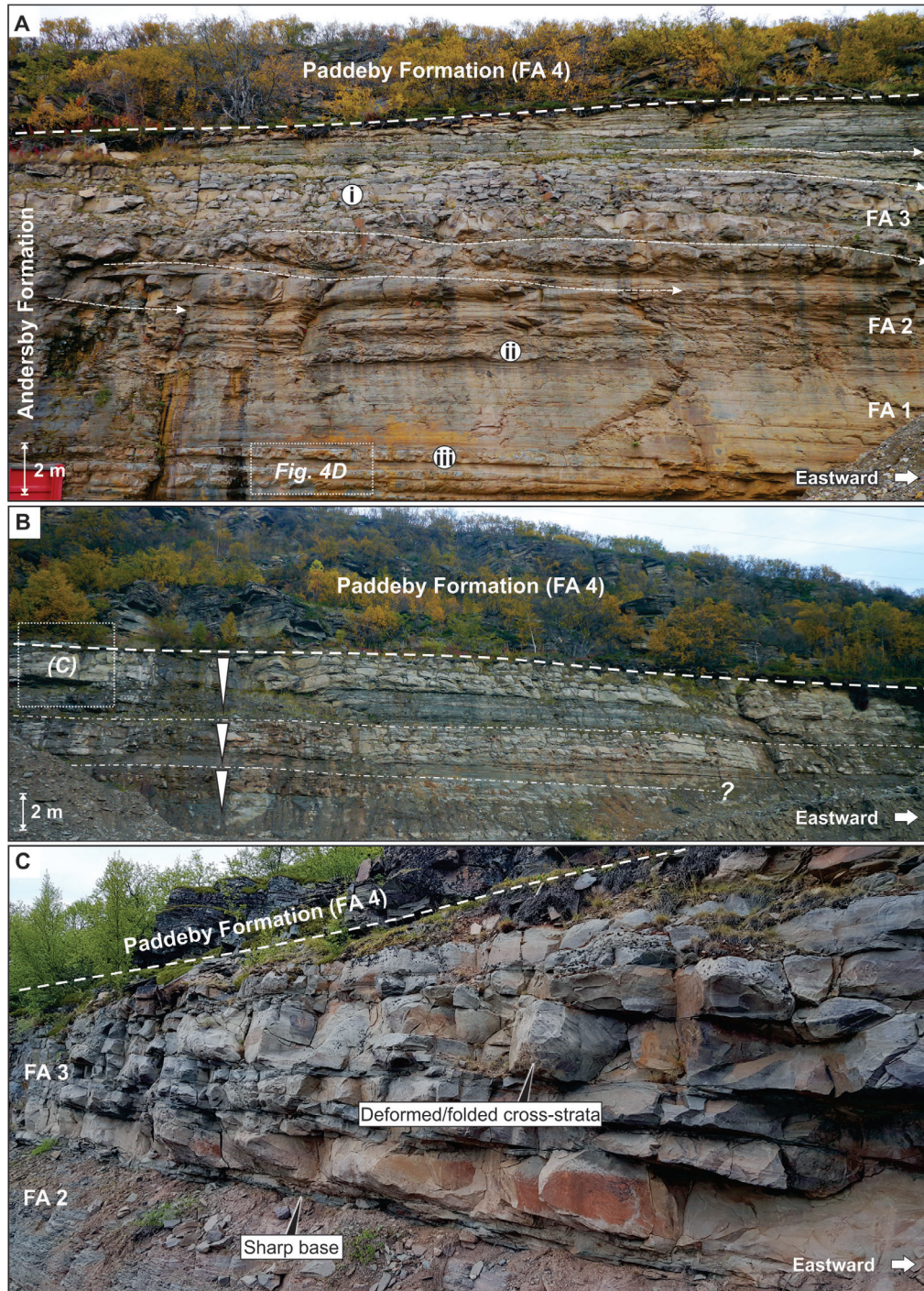


Figure 13. Photos illustrating the transition from delta-front deposits (FA 3) of the Andersby Formation to braidplain (FA 4) deposits of the Paddeby Formation at the Paddeby locality (in the local quarry). (A) Locally, the delta front deposits form up to 7 m thick, sandstone successions which internally exhibit low-angle, eastward dipping surfaces which defines shingled, basinward-thinning sandstone wedges. A proximal-distal facies transition from cross-bedded to recumbently folded sandstones in the proximal delta front (i) via slump-folded and de-watered sandstones in the distal delta front to prodelta (ii) to massive sandstones on the basin floor (iii) can be deduced from the vertical facies stacking. This indicated that dune migration onto the sloping delta front followed by dune liquefaction and collapse, eventually triggered turbidity currents which deposited sand on the basin floor. (B) When traced laterally, the thick delta-front successions tend to split into multiple delta-front units (marked by white triangles) separated by prodelta deposits. (C) Photo illustrating the sharp-based nature of some proximal delta-front deposits. Internally, these are dominated by cross-bedded to recumbently folded sandstones.

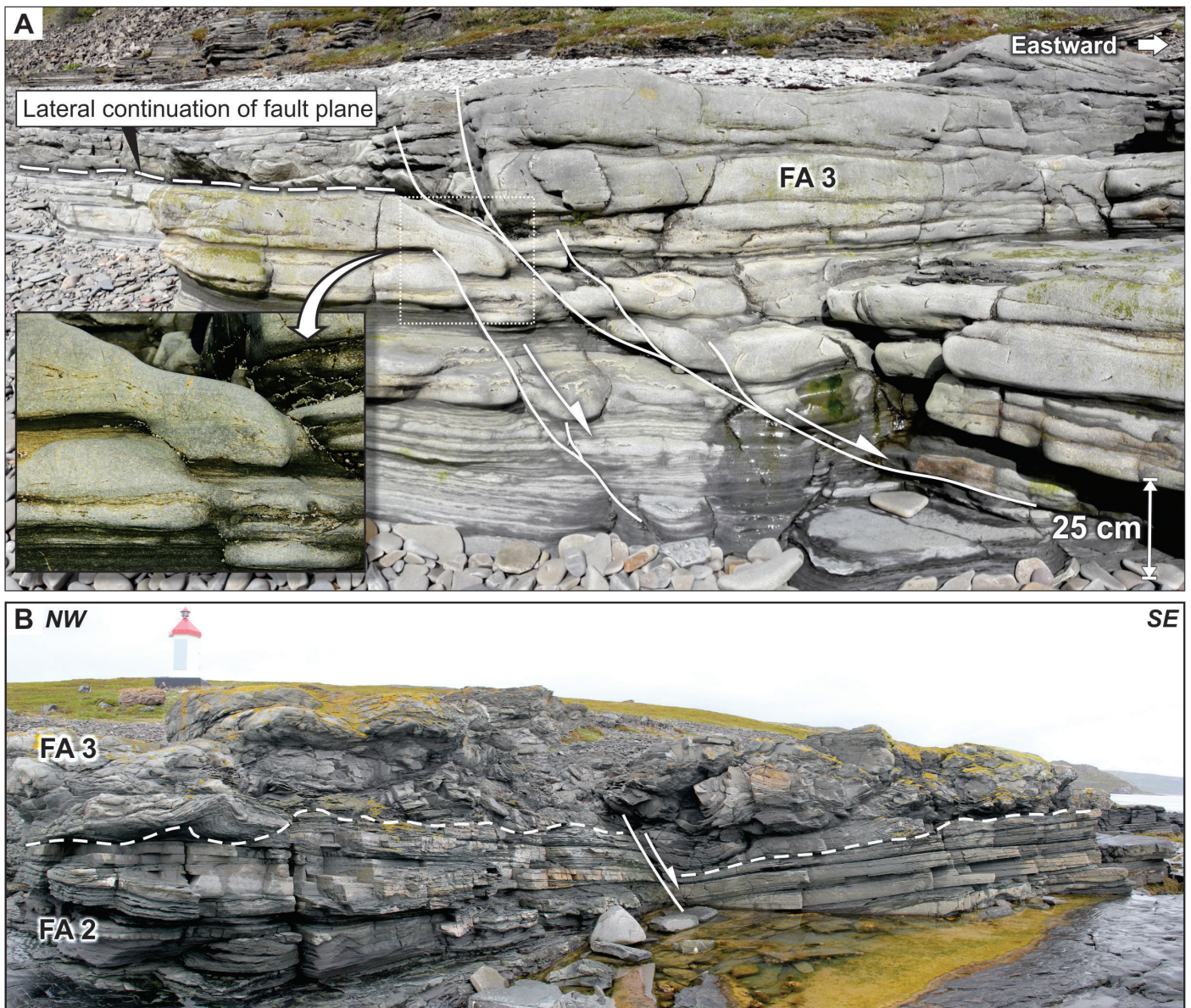


Figure 14. (A) Photo showing one of several syn-sedimentary faults penetrating the delta-front deposit (FA 3) of the Klubbnasen Formation, at the Klubbnasen locality. Note its listric geometry and the lateral continuation of the fault plane (marked by stippled line). In plan-view, these faults define a series of small (each <math><15\text{ m}^2</math>) “scoop-shaped” fault blocks attributed to syn-sedimentary, gravity-driven delta-front instability. (B) Slump-folded delta front deposits (FA 2) overlying undeformed prodelta deposits (FA 2). Klubbnasen Formation, Mortensnes locality. Notice the small normal fault with dm-scale offset. Because the fault seems to terminate in the deformed unit (FA 3) and this unit appear to thicken across the fault, we infer this to be a result of brittle syn-sedimentary deformation. Apart from apparent thickening due to fault drag, there is virtually no growth toward the fault in the underlying FA 2 unit.

generally were not suppressed by the river effluents off the proximal fluvial-dominated delta front (Mutti et al., 1996; Bowman & Johnson, 2014; Collins et al., 2017).. Liquefaction caused by cyclic stress induced by storm waves in combination with gravity-driven deformation on the distally deepening, storm-affected delta front may thus explain the proximal to distal transition from cross-bedded into slump-folded sandstones.

The anisotropic HCS sandstone beds suggest deposition by intermediate oscillatory flows with a sufficient unidirectional component that promoted bedform migration (Duke, 1991; Dumas & Arnott, 2006). The unidirectional component of these flows may have been caused by the returning downwelling flows following the coastal set-up (Duke, 1991; Myrow & Southard, 1996), or by various density-induced flows trailing down the delta front (Myrow & Southard, 1996; Jelby et al., 2020). SCS and small scours indicate that the dunes migrated into an environment repeatedly eroded by storm waves and turbulent, bottom scouring flows originating from the approaching fluvial system (e.g., Eide et al., 2015; Grundvåg et al., 2020). The interbedded units of siltstone to thin-bedded sandstone may record variations in river discharge or lateral switching of distributary channels.

Based on their restricted stratigraphic appearance with virtually unaffected deposits above and below, as well as their listric appearance and cusped plan-view geometries, the small faults appear to be of syn-sedimentary origin and are thus attributed to gravity-driven deformation during an early stage of slumping on the delta front (e.g., Bhattacharya & Davies, 2001). It is well known that slumping tends to produce scoop-shaped head scarps, listric faults, and rotated blocks like those reported here (e.g., Nemeč et al., 1988; Bhattacharya & Davies, 2001; Martínez et al., 2005). We suggest that the contorted and chaotically deformed FA 3 units are inherently linked to the slump blocks possibly representing their down-dip slump deposits. As such, some of the internal truncation surfaces in FA 3 may represent former failure surfaces at the base of healed slump scars.

Facies association 4 – Braidplain deposits

Description. – Facies association 4 (FA 4) is restricted to the Fugleberget and Paddeby formations, where it, in both cases, forms more than 100 m-thick successions dominated by cross-bedded sandstones (Figs. 2B, 12, 13 & 15). The base of FA 4 is erosive and is typically accompanied by an abrupt upwards shift in lithology and grain size from mudstone-dominated or heterolithic units (FA 1 or FA 2, respectively) into thick-bedded, predominantly cross-bedded, medium-grained sandstones (Figs. 12 & 13). The sandstone beds of FA 4 range in thickness from 0.5 to 2 m with an average thickness of c. 0.6 m (Fig. 15A, B). In general, the cross-bed dip azimuths are towards the east in both the Fugleberget and the Paddeby formations. Thin sandy siltstone interbeds (<0.2 m) are present locally. The sandstone beds are tabular to trough cross-bedded (lithofacies 9; Table 1) with foresets commonly having tangential geometries grading laterally into planar-bedded sandstones (lithofacies 10; Table 1; Fig. 15B). Convolute bedding is abundant, and a large portion of the cross-beds are recumbently overturned, particularly occurring in the tabular cross-sets (Fig. 15C). Sigmoidal cross-sets with well-developed topset-foreset-bottomset geometries are present locally, and up to 1.2 m-thick, sheet-like units of planar-bedded siltstone to medium-grained sandstones exhibiting west-to-east-oriented parting lineations are also common (Fig. 15D). Locally, current-ripple cross-lamination occurs in the bottomsets of the thickest (>1 m) tangential and sigmoidal cross-beds. Some ripple sets record migration directions opposing that of the hosting cross-bedded unit. Many of the recumbently overturned cross-beds grade upwards or down-dip into massive, structureless sandstones which contain mudstone and siltstone intra-clasts that exhibit poorly developed imbrication to the east (Fig. 15E). Scours with depths and widths ranging between a few decimetres to a few metres occur in places. Mudstone or siltstone intra-clasts are present in some places along the base of these scour surfaces.

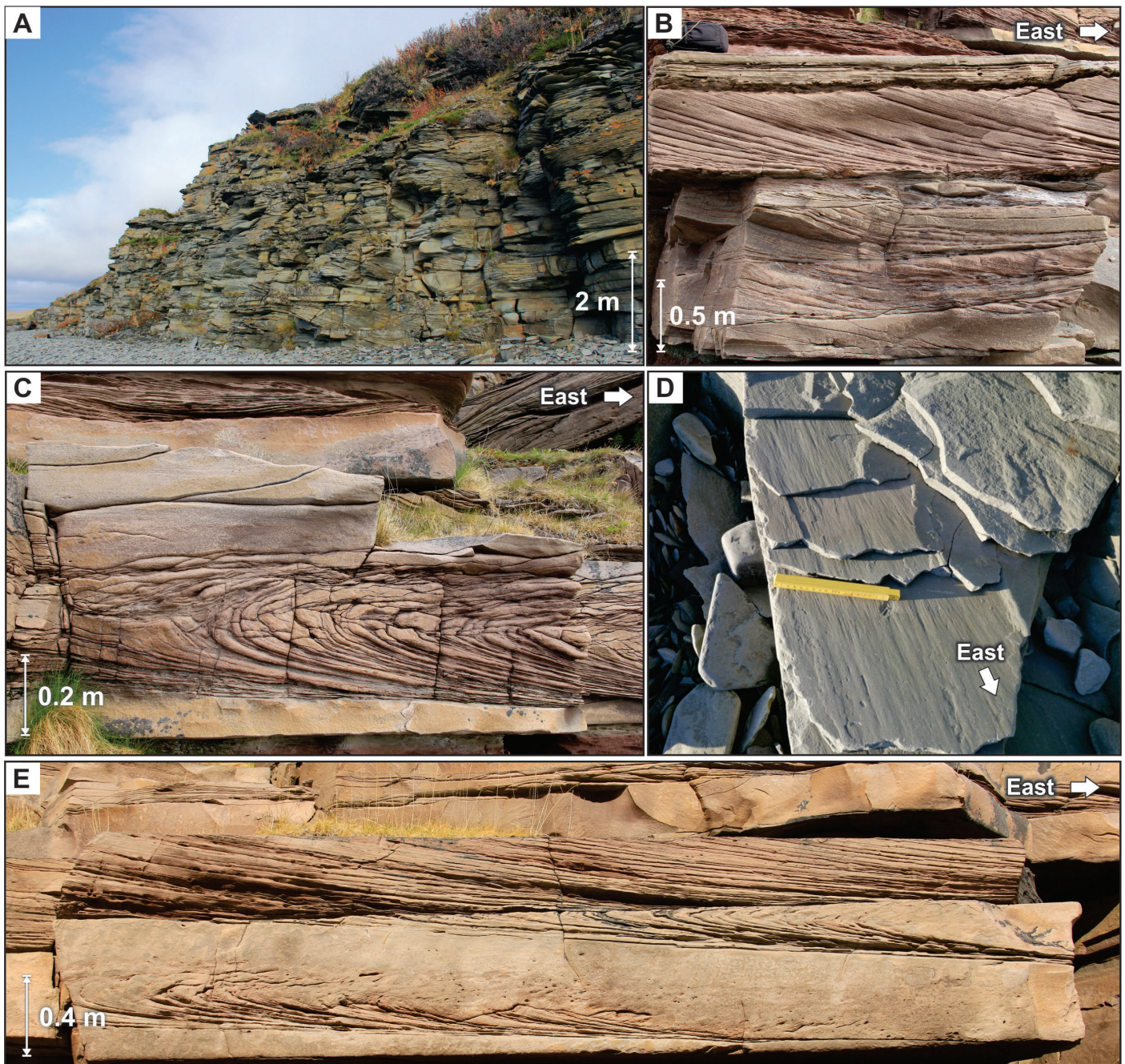


Figure 15. Representative photos of the braidplain deposits (FA 4) which dominates the Fugleberget and Paddeby formations. (A) Thick stack of cross-bedded sandstone beds. Fugleberget Formation, Klubbnasen locality. (B) Example of sandstone beds exhibiting eastward-oriented cross-beds with tangential geometries and planar bedding. Fugleberget Formation, Vadsøya locality. (C) Recumbently folded cross-bedded sandstone overlain by a massive, non-graded sandstone bed. Fugleberget Formation, Vadsøya locality. (D) East–west-oriented parting lineations occurring on the exposed surfaces of a planar-bedded sandstone. Ruler for scale (20 cm). (E) Spectacular exposures showing the down-dip relationship between cross-bedded, recumbently folded, and massive, de-watered sandstones occurring in the Fugleberget Formation at the Vadsøya locality. The deformation has previously been attributed to autokinetic processes and upper flow regime conditions. See Røe (1987) and Røe & Hermansen (1993; 2006) for more details on these facies transitions.

Interpretation. – The erosive base, the abundance of thick-bedded, cross-stratified sandstone beds, the uniform eastward dip azimuths of the cross-beds, the frequent scours of various sizes, and the general lack of wave-generated structures suggest that FA 4 is of fluvial origin. The lateral extent and aggradational stacking pattern of these units indicate deposition on extensive, sand-dominated braidplains (e.g., Nemeč, 1992; Tirsgaard & Øxnevald, 1998; Ielpi & Rainbird, 2016). This interpretation is consistent with former studies of the Fugleberget and Paddeby formations (Hobday, 1974; Røe, 1987, 2003; Røe & Hermansen, 1993). As such, the tabular and trough cross-bedded sandstones record the migration and stacking of variably-sized 2D and 3D dunes (e.g., Nemeč, 1992; Røe & Hermansen, 1993). The thick cross-beds with tangential to sigmoidal geometries together with the planar-bedded units imply deposition by medium- to high-velocity currents carrying considerable amounts of sand-grade sediments in suspension (Røe, 1987; Røe & Hermansen, 1993). The development of sigmoidal bars has commonly been attributed to flood-dominated alluvial systems (Mutti et al., 1996). The planar bedding and parting lineations thus originate from strong unidirectional currents of the upper flow regime, typically across bar tops (Hobday, 1974; Allen, 1983; Røe, 1987), or they may be attributed to deposition during ephemeral flash floods (Tirsgaard & Øxnevald, 1998). The convolute-folded and recumbently overturned cross-beds, which grade upwards or down-dip into massive sandstones, represent a remarkable continuum of soft-sediment deformation which record local liquefaction events caused by shear stress from overriding high-velocity currents operating in the dune to upper plane bed transitional flow regime. Because of their localised appearance, these features must be of an autokinetic origin (i.e., caused by the fluvial system itself; for more details, see Røe, 1987; Røe & Hermansen, 2006). The variably-sized scours indicate local erosion by strong currents and frequent channel switching (Nemeč, 1992). Similar facies successions are commonly attributed to braidplain deposits comprising different architectural elements such as channels, scour pools, mid-channel bars and various dune complexes (e.g., Nemeč, 1992; Røe & Hermansen, 1993; Røe, 1995; Hjellbakk, 1997; Ielpi & Rainbird, 2016).

Facies association stacking patterns

Description. – The Klubbnasen–Fugleberget and Andersby–Paddeby couplets are organised into two large-scale upward-coarsening units (each being c. 160–170 m thick), which both record a transition from mudstone-dominated offshore deposits (FA 1) at their base, upwards via heterolithic storm-influenced prodelta deposits (FA 2) into sandstone-rich delta-front deposits (FA 3), which is erosively capped by sandstone-dominated braidplain deposits (FA 4; e.g., Fig. 12). An eastward palaeo-current flow direction is recorded in all the facies associations (Fig. 3B; Røe, 2003). In both couplets, the marine/deltaic part (FA 1 to FA 3) is significantly thinner (c. 50 m) than the overlying fluvial part (FA 4), which has a thickness typically exceeding 100 m. Units of offshore, prodelta and delta-front deposits commonly alternate and stack into smaller coarsening-upward cycles (typically <15 m thick) superimposed on the overall coarsening-upward trend in both the Klubbnasen and the Andersby formations. These cycles are bounded by abrupt vertical facies association transitions either with offshore deposits sharply overlying prodelta deposits, or more commonly, prodelta deposits sharply overlying delta-front deposits (Figs. 12 & 13B). Moreover, the >100 m-thick succession of braidplain deposits (FA 4) of the Fugleberget Formation in the uppermost part of the first couplet are sharply overlain by offshore deposits (FA 1) of the Andersby Formation at the base of the second couplet (e.g., Fig. 2). We have not investigated either the uppermost part of the Paddeby Formation (in the top of the second couplet) or the boundary to the overlying Golneselva Formation. According to Røe (2003), the lower part of the Golneselva Formation is a sharp-based estuarine deposit which displays palaeo-current flow directions to the northwest.

The erosive bases of the sandstone-dominated braidplain deposits (FA 4) of both the Fugleberget and the Paddeby formations, correspond to regionally extensive formation boundaries (Figs. 2B, 12 & 13). In several places, the braidplain deposits sit erosively on top of offshore (FA 1) or storm-influenced prodelta (FA 2) deposits apparently without any intervening delta-front deposits (FA 3). However, albeit difficult to recognise, thinly developed (<3 m), sharp-based, cross-bedded, proximal delta-front deposits are usually present immediately beneath the braidplain deposits in several of the investigated outcrops (e.g., Fig. 13C). Because the proximal delta-front deposits are very similar to the overlying braidplain deposits, careful investigations are thus needed to distinguish them from one another and correctly establish the actual base of the braidplain successions (Figs. 12 & 13).

Interpretation. – The Klubbnasen–Fugleberget and Andersby–Paddeby couplets represent two fluvio-deltaic systems which prograded eastward under highly comparable physiographic conditions as evident from their similar lithofacies distribution and facies association stacking patterns (Fig. 16). The marked difference in thickness between the lower deltaic and the overlying fluvial parts is conspicuous (Fig. 2B). The upward-coarsening trend in the deltaic parts is thus attributed to basinward progradation and filling of a shallow, low-accommodation basin. The thickness (>100 m) and monotonous facies development (dominantly cross-bedded sandstones, lithofacies 9; Table 1) in the fluvial units implies a persistent supply of fluvial sand in combination with steady creation of accommodation space, which eventually promoted deposition of highly aggrading braidplain successions (Fig. 16A).

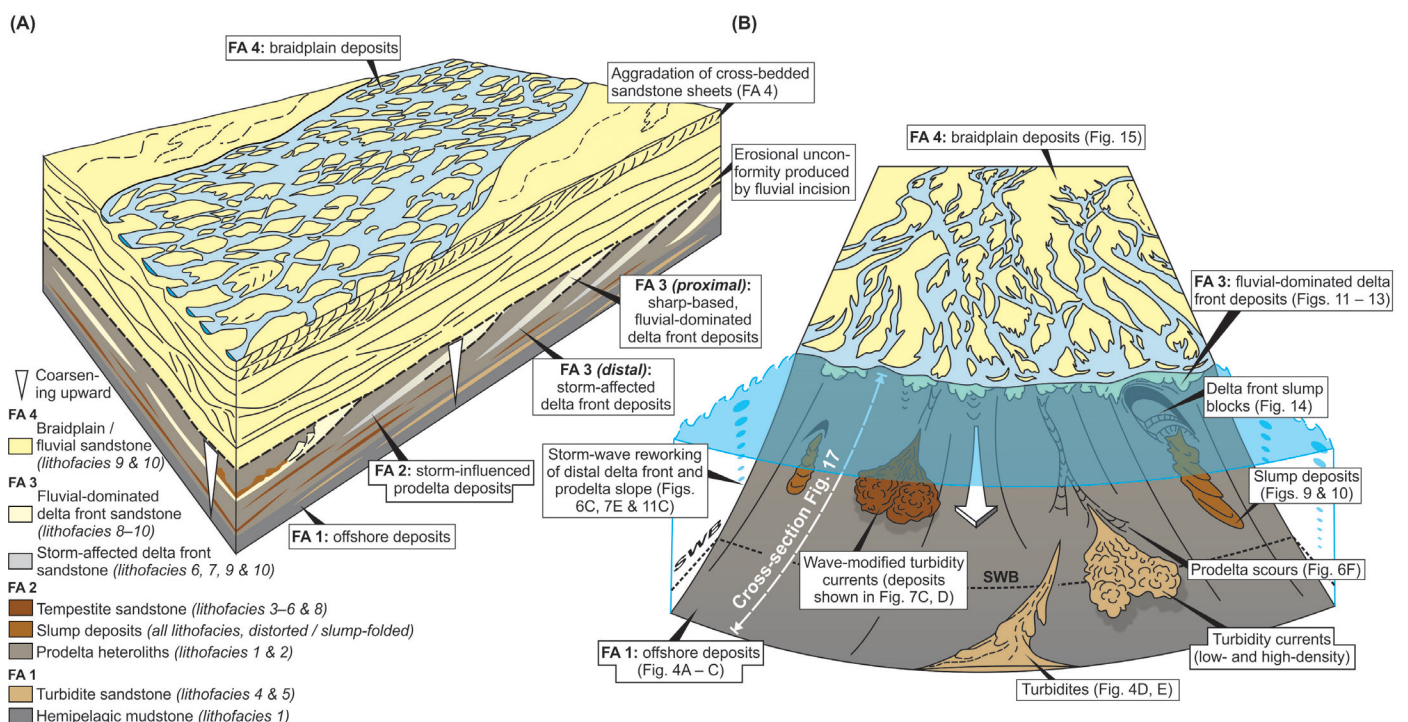


Figure 16. Conceptual depositional models summarizing facies association distribution and stratigraphic architecture of the investigated fluvio-deltaic couplets. (A) Model illustrating the character of the thick braidplain succession (FA 4) and the stratigraphic relation to its underlying deltaic deposits (FA 1 to FA 3). The basin-wide erosional unconformity at the base of the braidplain succession, produced by fluvial incision, and the sharp-based nature of the proximal fluvial-dominated delta front deposits points to progradation under low-accommodation or forced regressive conditions. (B) Model illustrating the most important depositional processes and products on the delta front to prodelta reaches of the system, including various sediment gravity flows originating from the fluvial feeder system (producing scours and depositing turbidites), storm-generated flows and storm-wave reworking (depositing wave-modified turbidites and hummocky-cross-stratified tempestites), and gravity-driven instability (producing rotated slump blocks and slump deposits, see Fig. 17 for more details). Event beds in the offshore deposits show no signs of storm-wave reworking, whereas most of the prodelta event beds appear to be modified by storm waves, suggesting that the prodelta environment was above storm wave base (SWB). The general sparsity of oscillatory-generated structures and the concomitant dominance of unidirectional, traction-generated structures in the delta front deposits, suggests that strong river effluents generally suppressed incoming fairweather waves. As such, it is not possible to infer fairweather wave base.

The presence of abrupt vertical shifts of facies associations in the deltaic Klubbnasen and Andersby formations marks minor upwards deepening events, which indicates that the eastward delta progradation periodically came to a halt. In deltaic systems elsewhere, such minor flooding surfaces are commonly attributed to autogenic delta lobe switching, which occurs at relatively short temporal scales (e.g., <10 kyr; Hampson, 2016). Because tectonics usually operate at a significantly lower frequency than autogenic processes, a tectonic origin for these surfaces seems unreasonable. The abrupt upwards deepening from braidplain (FA 4) atop the first couplet into offshore (FA 1) deposits at the base of the second (i.e., the boundary between the Fugleberget and Andersby formations; Fig. 2B) represents a marine flooding surface of regional extent (Fig. 16B). The fact that it bounds two very similar fluvio-deltaic cycles, suggests that allogenic forcing controlled its development rather than autogenic processes. Increased rates of basin subsidence or eustatic sea-level rise, possibly in combination with a sudden decrease in sediment supply, eventually drowned the Fugleberget Formation braidplain, marking the onset of the second couplet. Røe (2003) interpreted the upper conglomeratic member of the Fugleberget Formation (see Fig. 2B) to represent a retrograding fan-delta succession, possibly marking a gradual deepening of the basin prior to the regional flooding event.

The sharp and abrupt vertical shift from offshore (FA 1) or prodelta (FA 2) upwards into braidplain (FA 4) deposits across the basal boundaries of both the Fugleberget and the Paddeby formations, marks erosional unconformities that record dramatic basinward shifts in facies caused by fluvial downcutting (Figs. 12, 13 & 16A). Because the two braidplain units have been eroded into the underlying deposits in all the visited outcrops, their bases appear to represent basinwide erosional events. In many cases, such surfaces are used as a criterion for recognising subaerial unconformities formed during a fall in relative sea level (Nemec, 1992; Røe, 1995; Helland-Hansen & Hampson, 2009; Grundvåg & Olaussen, 2017). As such, the thinly developed, sharp-based, intervening delta-front deposits (FA 3; Fig. 12), which in places occur below the erosively-based braidplain deposits, may suggest progradation under forced regressive conditions (e.g., Nemec, 1992; Røe, 1995; Helland-Hansen & Hampson, 2009; Grundvåg & Olaussen, 2017). However, similar stratigraphic expressions may also emerge from progradation of low-accommodation, shallow-water deltas and associated river channel cannibalism of its own delta-front deposits during basinward extension of the channel (e.g., Fielding et al., 2005).

Our preferred interpretation, that the erosive bases of the Fugleberget and Paddeby formations represent basin-extensive subaerial unconformities, deviates from earlier works where the two formation boundaries are reported to be gradational (e.g., Hobday, 1974; Banks et al., 1974). Potential allogenic factors that controlled the stratigraphic architecture of the two couplets are discussed later.

Soft-sediment deformation and other indicators of syn-tectonic sedimentation

The Klubbnasen–Fugleberget and the Andersby–Paddeby stratigraphic couplets include a wide range of soft-sediment deformation structures (SSDS), which vary morphologically in size and style of deformation. SSDS are present in all stratigraphic intervals, occur in all the described facies associations, and may involve solitary beds as well as entire bed stacks. Albeit the bulk of these SSDS, if considered separately, may be attributed to processes occurring during or soon after deposition in all the interpreted environments, the wide range of structures, as well as the abundance and distribution, may suggest a common, allogenic forcing factor controlling their development. Røe (2003) argued for active tectonism during deposition of the lower Vadsø Group, and attributed the abundance of SSDS to seismic shocking, a view largely supported herein as discussed later. Therefore, the most important SSDS which may result from tectonic activity are described and interpreted below.

Load structures

Description. – In both the Klubbnasen and the Andersby formations, load and accompanying flame structures, as well as ball-and-pillow structures are abundant, particularly in the upper sandstone-bearing parts of FA 1 and more commonly in the heterolithic deposits of FA 2 (Figs. 5, 6B, 7F & 9). The load structures vary in sizes from a couple of centimetres to several decimetres in diameter and record a morphological continuum from simple, pendulous load casts to detached ball-and-pillow structures forming pseudo-nodules fully encapsulated in siltstone or mudstone (Figs. 6B & 7F). The load structures typically consist of very fine- to fine-grained sandstone, and in some cases they exhibit folded, albeit well preserved internal laminae. Locally, load-casted ripples are present, appearing as rotated ripple sets partly embedded in the underlying fine-grained deposits (Fig. 7F). Although most load structures are randomly distributed, they are particularly abundant in some horizons where they form stratabound ball-and-pillow structures. In many cases, these laterally extensive horizons are associated with other SSDS such as slump folds and convolute bedding (Fig. 7F).

Interpretation. – Load structures are commonly formed in water-saturated sediments as a response to either unstable density inversion between two contrasting layers (e.g., sand and silt) or from lateral variation in load (by the migration of ripples; e.g., Owen, 2003). In general, contrasts in sediment density alone are not enough to create load structures (Berra & Felletti, 2011). This is evident by the presence of many beds that do not exhibit load structures at their bases. Loading is commonly initiated by a drastic reduction in shear strength or in response to liquefaction and fluidisation processes. Several trigger mechanisms such as storm waves, earthquake or rapid sediment loading may lead to liquefaction of the upper denser layer and gravitational readjustment leading to the development of load structures (Molina et al., 1998; Alfaro et al., 2002). The abundance of load structures in FA 2 (storm-influenced prodelta), may indicate that the combination of storm waves and rapid sediment loading played an important role in the present case. However, the occurrence of stratabound ball-and-pillow structures associated with convolute bedding and slump folds may also indicate earthquake activity.

Syneresis cracks

Description. – Syneresis cracks are very abundant in the heterolithic deposits of FA 2 (with some rare occurrences in FA 3) in both the Klubbnasen and the Andersby formations (Fig. 8D, E). Here, the syneresis cracks occur on the bedding planes of thin-bedded, storm-deposited sandstones as sandstone-filled cracks with simple spindle- to more complex polygonal-shaped geometries (Fig. 8D). The width of the individual cracks is typically in the range of 0.2 to 1 cm. In cross-section, the cracks are wedge-shaped and commonly extend down into the underlying mudstone cross-cutting multiple laminae and layers (Fig. 8E).

Interpretation. – Syneresis cracks are commonly attributed to fluctuation in palaeo-salinity stress within the water column close to the water-sediment interface in shallow subaqueous settings (e.g., Astin & Rogers, 1991; Bhattacharya & MacEachern, 2009). Changes in salinity may cause deflocculation or intra-crystalline de-watering of muddy to silty sediments resulting in shrinkage and thus the formation of cracks. However, syneresis cracks may also be attributed to de-watering and grain-reorientation processes related to seismic shocking. Cracks of seismic origin are formed within the strata and typically involve multiple layers (Pratt, 1998; McMahon et al., 2017). Syneresis cracks are reported in several other Precambrian successions around the world and are believed to be related to the absence of sediment-binding bacteria, making the sediments prone to deformation (Pratt, 1998).

Sandstone dykes and various pipe structures

Description. – In the Andersby Formation, dominantly at the Bergelva locality, several distinctive vertically to steeply inclined sandstone dykes with a massive internal appearance penetrate several metres of the succession, independent of lithology and facies association (Figs. 5 & 8F, G). They are typically 3 to 30 centimetres wide with sharp contacts to the surrounding deposits (Fig. 8F). One dyke, which penetrates an exposed sandstone bedding-plane, was investigated in plan-view, and exhibits sharp outer contacts and an undulating morphology (Fig. 8G). Several of the dykes seemingly thin and pinch-out in both upward and downward directions. Bifurcation is observed in places. In addition, sub-vertically- to vertically oriented circular sandstone columns occur locally within FA 2 and FA 3 in both the Klubbnasen and the Andersby formations. These columns, here referred to as pipes, extend for some centimetres to several decimetres, and typically penetrate one or several beds, independent of lithology. Some of the pipes extend upwards from a source bed, which typically appear massive and structureless in the area near the basal part of the pipe. Smaller (<0.1 m wide) wedge-shaped varieties also exist in FA 2, typically extending downward (a few centimetres to decimetres, only penetrating some very few layers) from a massive, structureless sandstone bed into the underlying sediments where the pipe soles out (Fig. 8H).

Interpretation. – Sandstone dykes and associated pipes are dewatering structures (or clastic intrusions) formed by liquefaction and injection of unconsolidated sand into surrounding sediments sometime after deposition (i.e., post-depositional remobilisation; Owen, 1987). Although sandstone dykes may occur in many types of basins (e.g., along passive margins and within sag basins), they are commonly reported from tectonically active basins where they reportedly may dissect a wide range of deposits from deep marine to terrestrial, with seismic shocking being one of the most cited triggering mechanisms for the liquefaction and injection to take place (e.g., Owen, 1987; Owen & Moretti, 2011). The vertically extensive dykes observed in the Andersby Formation probably developed when water-saturated sand, emplaced by turbidity currents or storm-generated combined flows, was buried beneath low-permeability sediments (i.e., mud and silt) which promoted overpressure. Subsequently, when being subjected to seismic shocking, the sandy sediments were fluidised and injected upwards through cracks formed by hydraulic fracturing of the overlying semi-consolidated sediments, eventually leading to the formation of vertical to sub-vertical dykes and pipes (Owen & Moretti, 2011; Wheatley & Chan, 2018). The rift-related stress regime in the basin probably influenced the formation and orientation of the dykes. The fact that these dykes and pipes penetrate multiple layers across several metres, strongly advocate a tectonic origin (e.g., Owen, 1987; Owen & Moretti, 2011). The smaller scale de-watering wedges in FA 2 (storm-influenced prodelta deposits) may be attributed to localised excess pore pressure build-up and liquefaction triggered by depositional events such as rapid deposition of sand and the passage of storm waves (Martel & Gibling, 1993).

Recumbently folded cross-beds and convolute bedding

Description. – Abundant recumbently overturned cross-bedding characterises the thick-bedded sandstones of FA 4 (Fig. 15C). Within a single bed, a down-dip continuum from undisturbed via recumbently folded cross-beds into the massive sandstones is common (Fig. 15E; see previous work on the Fugleberget Formation and other similar facies successions on the Varanger Peninsula by Røe, 1987; Røe & Hermansen, 1993; Hjellbakk, 1997). In addition, convolute and contorted bedding of various scale (few cm to metre scale), lateral extent, and complexity, in some cases affecting multiple vertically stacked beds, are present in FA 4. Slump-folded units occur locally in FA 2 and FA 3 (Figs. 9, 10 & 14B).

Interpretation. – Recumbently overturned cross-bedding and associated massive sandstone are a common feature in many ancient fluvial successions, and have been attributed to drag and shearing underneath strong, sediment-laden, unidirectional currents in combination with liquefaction processes (Allen & Banks, 1972; Jones & Rust, 1983; Røe, 1987; Hjellbakk, 1997). Previous models have also suggested a link between the development of such features and earthquake-induced seismic shocks (e.g., Allen & Banks, 1972), as well as foreset failure promoted by liquefaction during changing water level (in the river) and nearby bank collapse (e.g., Jones & Rust, 1983). In the present case, the abundant and recurrent appearance of these features in FA 4 and their limited lateral and stratigraphic extent (typically only affecting the upper half of a bed), suggest an autokinetic, depositional mechanism governing their development. Several possible models are discussed by Røe (1987), Hjellbakk (1997), and Røe & Hermansen (2006), and include repetitive liquefaction deformation caused by intermittent changes in flow conditions, as well as the occurrence of short-lived, mass-flows rapidly dumping sediments during river floods. However, the complex varieties of convolute and distorted cross-bedding, particularly in cases where multiple beds are affected, record post-depositional deformation which may be attributed to de-watering of loosely packed sand induced by seismic shocking. The locally occurring slump-folded units in the prodelta and delta-front deposits, which we attribute to gravity-driven deformation and slope failure (see above descriptions and interpretations of FA 2 and FA 3), cannot be used as indicators of palaeo-seismic activity.

Discussion

Processes and facies tracts in storm-influenced braid deltas

Judging from the facies association stacking patterns in the two couplets, it appears that the sandy braidplains (FA 4; Fig. 16) of both systems fed deltas which successively prograded into a sheltered, low energy basin, as shown by the abundance of finely laminated mudstone deposits of FA 1 in the lower part of both couplets (Figs. 4, 5 & 6). Based on the limited accumulative thickness of these fine-grained sediments and their overlying prodelta (FA 2) to delta front (FA 3) deposits (altogether <50 m), as well as the sharp-based nature of the latter, a relatively shallow basin of limited accommodation can be inferred, at least when compared with the deep basin of the BSR to the north of the TKFZ (e.g., Røe, 1995). This is consistent with some of the previous models, which indicate deposition in a pericratonic marginal basin for the entire TVR succession (Banks et al., 1974; Hobday, 1974; Nystuen, 1985; Siedlecka, 1985; Roberts & Siedlecka, 2012, 2022).

The upwards increase of sandstone beds in the marine/deltaic part (FA 1 to FA 3) of both couplets indicate that the shallow basin recurrently experienced a progressive increase in the influx of sand-grade sediments as the deltas successively approached and crossed the study area (Fig. 16). Various sediment gravity flows initiated at the delta front in combination with periodic storm activity that resulted in the deposition of turbidites (both low- and high-density types), wave-modified turbidites, and classical HCS tempestites (*sensu* Jelby et al., 2020) in the prodelta to offshore regions of both systems (see FA 2; Figs. 6, 7 & 16B).

It is well known from many other sedimentary basins that heavy and intense rainfalls commonly accompany storms, thus promoting erosion and increased fluvial run-off, which eventually transport large amounts of sediment from the hinterland into the basin where storm-waves concurrently rework the fluvially-derived sediments (e.g., Mutti et al., 1996; Mulder et al., 2003; Bhattacharya & MacEachern, 2009). Such coupled storm-floods are particularly described from fluvial systems in tectonically active basins which are characterised by small to medium-sized catchments, relatively short- and high-gradient transfer zones, and poorly developed alluvial plains (e.g., Mutti et al., 1996;

Mulder et al., 2003; Collins et al., 2017). More importantly, the severe climate and general lack of binding vegetation during the Neoproterozoic gave rise to a highly erodible drainage basin, and in combination with the sandy braidplains in the present case, conditions were ideal for generating catastrophic flash floods during seasonal rain storms (e.g., Hjellbakk, 1993; Fig. 17A). Similar pre-vegetation sandy braidplains influenced by seasonal floods are commonly portrayed in Precambrian successions elsewhere (e.g., Tirsgaard & Øxnevald, 1998; Ielpi & Rainbird, 2016). When entering a body of standing water, flash floods tend to go hyperpycnal and transfer large volumes of sediments into the receiving basin (Mulder et al., 2003; Katz et al., 2015; Fig. 17A). If these flows interact with storm waves and/or get enhanced by downwelling currents following the coastal set-up, they may as well bypass the nearshore energy fence and transfer sand-grade sediments across the shelf, potentially contributing to deep-water deposition (e.g., Mulder et al., 2003; Pattison, 2005). As such, the variably sized scours in the prodelta (FA 2) and distal delta-front (lower part of FA 3) deposits of the Klubbnasen and Andersby formations, which we attribute to the passage of highly erosive hyperpycnal flows, the corresponding lack of related hyperpycnites (*sensu* Mulder et al., 2003) in the offshore deposits (FA 1) may indicate frequent sediment bypass and deposition farther to the east (outside the outcrop belt) where the basin is inferred to have deepened (Fig. 17A). It is thus intriguing that recent provenance studies indicate a link between the fluvial braidplain sandstones of the Fugleberget Formation and deep-water turbidite sandstones of the Kongsfjorden Formation, each located on either side of the TKFZ (Zhang et al., 2015). Based on this relationship we further suggest that the erosional unconformities at the bases of the two braidplain units documented here (FA 4; Figs. 12, 13 & 16A) acted as major sediment bypass surfaces.

Delta-front collapse is evidently one of the most important triggering mechanisms for turbidity currents (e.g., Nemeč et al., 1988; Piper & Normark, 2009). High rates of sedimentation leading to oversteepening, delta lip failure following hyperpycnal discharge events, wave-induced stress associated with storm events, or seismic shocking may all promote the collapse of a delta front (e.g., Nemeč et al., 1988; Nemeč, 1990; Pattison et al., 2007; Clare et al., 2016; Collins et al., 2017; Jelby et al., 2020). The presence of multiple syn-sedimentary faults and slump-folded units in the delta-front deposits (FA 3) in the Klubbnasen Formation record unstable conditions with periodic gravity-induced remobilisation of the mouth-bar deposits (Figs. 14 & 16B). Some of the thicker event beds and particularly the slump deposits recorded in the prodelta deposits of FA 2 (Figs. 9 & 10), probably originated from such up-dip delta-front collapses (Fig. 17B).

Many shallow-water (sandy) braid deltas are characterized by a vertically expanded river effluent (caused by the limited depth of the receiving basin) which forces dunes to prograde far down the sloping delta front (Cole et al., 2021; Fig. 17C). Contemporaneously, as dunes migrate down-slope, the shear force imposed by the strong, over-riding river effluent may promote liquefaction and collapse of the water-saturated sandy bedforms. Given the right slope angle, such liquefied sediments may transform into downwelling turbidity currents (i.e., the liquefied sediment flow of Nemeč, 1990; Fig. 17C). In many shallow-water deltas, where the slope tends to be of low gradient, storm waves can be an equally important process in generating or enhancing turbulence and thus maintaining and driving turbulent suspensions in a basinward direction (Myrow et al., 2002).

The abundance of tabular- and trough cross-bedding and planar-bedding within the sandstones of FA 3 in both the Klubbnasen and the Andersby formations (Figs. 11, 12 & 13) indicates that the delta front of both systems was dominated by fluvial processes, especially in their proximal reaches where dunes aggraded and stacked into sand-rich mouth bars (Figs. 16B & 17C). In the distal reaches of the delta front (i.e., represented by the lower part of FA 3), however, where the river effluents diminished, storm waves may at times have reworked and remobilised older deposits, resulting in the formation of SCS and anisotropic HCS tempestites (Figs. 11B, C & 17C). The preservation of these storm-generated features, and their limited lateral and vertical extent, indicates rapid burial and suggests that high sedimentation rates accompanied storms, thus testifying to coupled storm-flood processes.

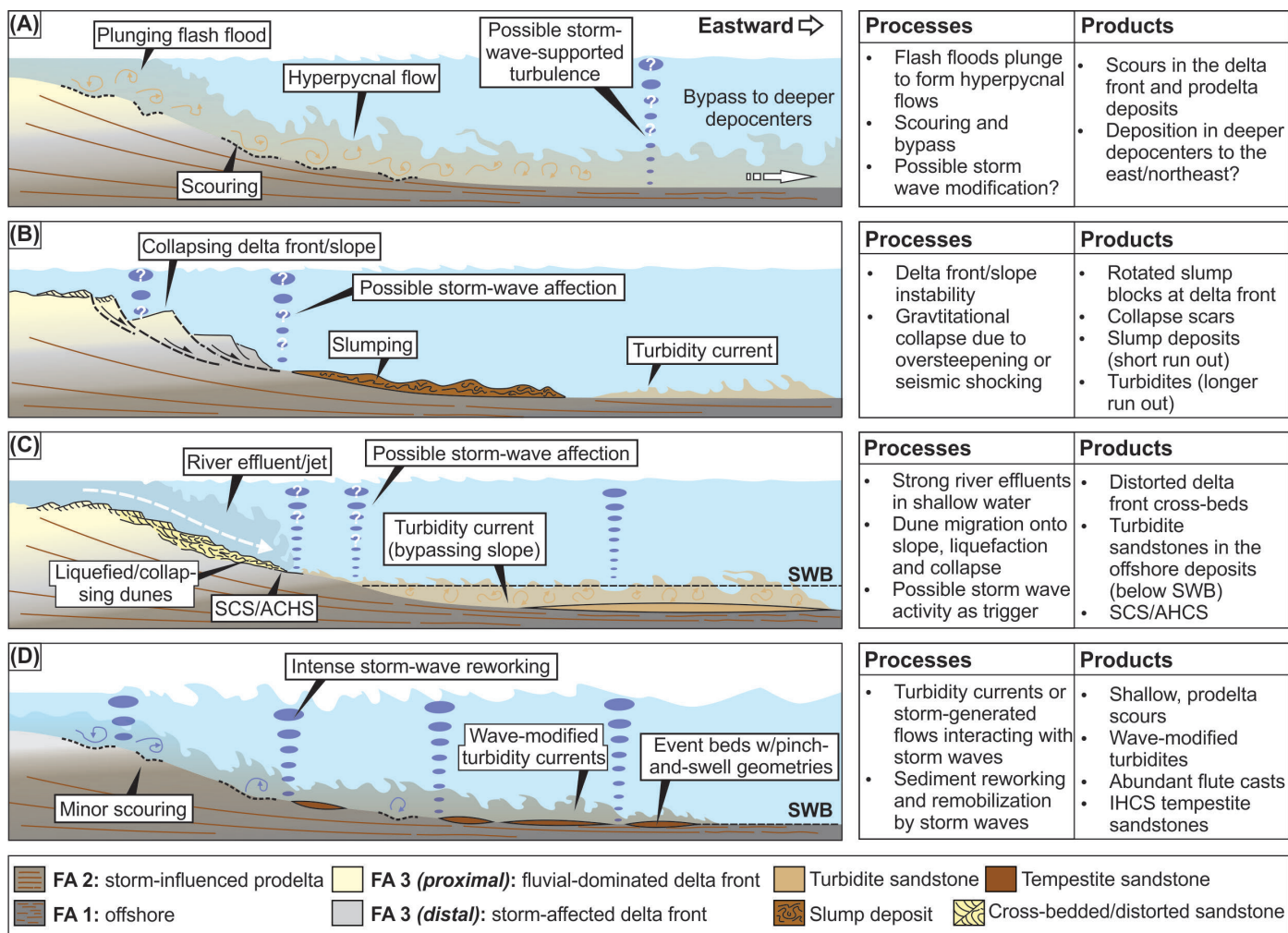


Figure 17. Conceptual model illustrating different modes of sediment transport and deposition on the delta front to prodelta slope. (A) Flash floods, generated during coupled storm-floods, may have played an important role given the pre-vegetated setting and the sandy, braided nature of the feeder system. When these dense flows entered the basin, they plunged to form powerful and highly erosive, turbulent hyperpycnal flows, which scoured into the prodelta slope and possibly transported sediments farther east into deeper depocenters. (B) Gravitational collapse of the delta front due to oversteepening and sediment loading, or seismic shocking (either induced by tectonics or by storm-waves), resulted in slump deposition on the prodelta slope (see Fig. 9). Because of the low-gradient slope these mass flows generally had short runouts and rarely made it far into the basin. Delta front slumping may also have triggered turbidity currents, which contributed to sand deposition in deeper parts of the basin. (C) The shallow water of the basin resulted in a vertically extended river effluent which promoted dune migration onto the gradually steepening delta front. Dune liquefaction and collapse, possibly under the affection of storm waves (as evident by the occasional presence of SCS/AHCS in the distal delta front deposits), may ultimately have triggered liquefied flows and turbidity currents which deposited sand in front of the deltas. (D) In shallow parts of the basin where the storm wave base (SWB) coincided with the basin floor, or during intense storms, which lowered the SWB, various down-trailing sediment gravity flows or storm-generated combined flows interacted with the storm waves, depositing wave-modified turbidites (sensu Myrow et al., 2002). Intense storm wave reworking and oscillatory-dominated combined flows resulted in the deposition of IHCS tempestites. AHCS – anisotropic hummocky cross-stratification, IHCS – isotropic hummocky cross-stratification, SCS – swaley cross-stratification

We further attribute the proximal to distal facies transition in FA 3, from cross-bedded sandstones via folded and overturned cross-beds into convolute bedded and slump-folded sandstones, to a natural down-slope deformation continuum recording dune migration, liquefaction and ultimately collapse (Figs. 13A & 17C). As such, the local occurrence of turbidite sandstones in FA 1 may originate from collapsing dunes which triggered turbidity currents that managed to bypass the prodelta and deposit their sandy load in front of the accreting deltas in deeper parts of the basin (below SWB; Figs. 4D, 13A, 16B & 17C). Although we have not yet been able to trace any of the FA 1 turbidite sandstones up-dip into cross-bedded delta-front sandstones via the deformed variety, the vertical relationship documented in the Andersby Formation at the Paddeby location is convincing (Figs. 4D & 13A).

Origin of the prodelta event beds

Previous work has favoured a turbidite interpretation for the many sandstone event beds in the Klubbnasen and Andersby formations (e.g., Banks et al., 1974; Hobday, 1974). However, our investigations show that the sandstones occurring in the prodelta deposits (FA 2) of the two units (Figs. 5, 6, 7 & 9), display a diversity of sedimentary structures and architectures consistent with interaction of unidirectional-, oscillatory- and combined-flows. Only some few beds display features consistent with deposition by pure oscillatory flow or by turbidity currents completely unaffected by wave action. Instead, most of the FA 2 sandstone beds exhibit erosive bases with frequent flute marks, normal grading, various combined-flow generated structures, and pinch-and-swell geometries (Figs. 5, 6 & 7), all features consistent with deposits of wave-modified turbidity currents (Myrow et al., 2002; Pattison, 2005; Lamb et al., 2008; Basilici et al., 2012; Fig. 17D). Such wave-supported, turbulent flows, which form when storm waves interact with turbidity currents or other downwelling storm-generated flows, are known to transport sand and silt across low-gradient slopes (e.g., Swift, 1985; Bhattacharya & MacEachern, 2009; Macquaker et al., 2010; Fig. 17D). The erosional bases with quite common down-slope (i.e., eastward) oriented flute marks, are thus indicative of initially, powerful, and turbulent, unidirectional, near-bottom flows preceding deposition (Fig. 17D). In prodelta settings, turbulent currents may originate from a multitude of processes, including turbidity currents triggered by slope failure, downwelling flows following the coastal set-up, storm resuspension of sediments near shelf-slope conduits, as well as from hyperpycnal flows related to river floods (Piper & Normark, 2009; Basilici et al., 2012; Eide et al., 2015; Collins et al., 2017; Jelby et al., 2020). The presence of HCS sandstone beds with combined flow ripple cross-lamination and occasional wave/interference rippled tops, indicate that oscillatory-dominated combined flows and storm-wave reworking also played an important role (Basilici et al., 2012; Jelby et al., 2020). However, the observed variety in bed architectures with a mixture of wave-modified turbidites and classical HCS tempestites (e.g., see the bed in Fig. 7E) may also record variable flow mechanisms such as wave unsteadiness (Jelby et al., 2020), temporal evolution of the initial turbidity flow (Lamb et al., 2008), as well as proximity to the fluvial feeder system (Grundvåg et al., 2020).

Implications of the soft-sediment deformation structures

If regarded separately, a large portion of the SSDS, independent of facies associations, are attributable to autokinetic and gravity-driven deformation processes, especially considering the sloping nature of the delta to prodelta parts of the investigated couplets and given the periodic input of storm- or gravity-emplaced sand onto underlying, water-saturated mud. However, in view of the proximity (<40 km) to the TKFZ to the northeast, which is considered to have been an active normal fault during the late Riphean (e.g., Johnson et al., 1978; Siedlecka, 1985; Siedlecka et al., 2004; Herrevold et al., 2009; Gabrielsen et al., 2022), and the hypothetical basin-bounding VFZ to the south (Figs. 1B & 18A), recurrent tectonically-induced seismic shocking offers a feasible explanation for the variability, complexity and abundance of SSDS (e.g., Røe, 2003). SSDS produced by tectonically induced seismic shocking typically show great variability, large lateral extents, may involve multiple layers, and occur repeatedly in a stratigraphic succession (Mohindra & Bagati, 1996; Hildebrandt & Egenhoff, 2007; Owen & Moretti, 2011). Thus, the morphological variability and distribution of SSDS documented in this study is very similar to seismically induced deformation reported in tectonically active basins elsewhere (e.g., Mohindra & Bagati, 1996; Rossetti, 1999). Of particular interest is the abundance of syneresis cracks (Fig. 8D, E) which have been attributed to an allokinetic triggering mechanism such as strong ground motion resulting in intra-stratal fracturing in many other basins (e.g., Pratt, 1998; McMahan et al., 2017). Clastic dykes and associated de-watering structures, similar to those reported here, are other features commonly attributed to tectonically induced soft-sediment deformation (e.g., Neef, 1991; Rossetti, 1999).

From a critical point of view though, it may be questioned whether the recurrency of tectonically triggered seismic events, which traditionally is thought to operate at a frequency of hundreds of thousands of years, can result in an abundance of SSDS at multiple stratigraphic levels in prograding delta systems, which typically operate at significantly shorter time spans (some few thousand to tens of thousands of years, e.g., Helland-Hansen & Hampson, 2009). Interestingly, however, is the growing body of literature which demonstrate that faults can generate earthquakes relatively often and at quasi-periodic intervals of some few thousand to tens of thousands of years (e.g., Cowan et al., 1996; Williams et al., 2017).

Røe (2003) attributed the abundance of SSDS in the Vadsø Group to seismic activity induced by syn-rift faulting along the VFZ. Johnson (1977) in his evaluation of SSDS in the Grønneset Formation in the lowermost part of the overlying Tanafjorden Group (Fig. 2A), considered storm wave processes as a potential triggering mechanism, but established tectonically induced seismic shocking to be the most likely cause, although he found it confusing given the inferred tectonically stable pericratonic platform setting. However, many studies demonstrate that tectonically induced sediment deformation and liquefaction may occur several tens to a few hundreds of kilometres away from earthquake epicentres (e.g., Obermeier, 2009). As such, it cannot be ruled out that seismic shocking, generated solely by activity along the TKFZ, may have resulted in widespread deformation of the TVR sediments on the pericratonic footwall, especially given the scale and long-lived history of this major fault zone. Even though the variability and abundance of SSDS points to tectonically induced soft-sediment deformation, this is not sufficient evidence to indubitably verify the existence of the much-disputed VFZ.

Tectonic forcing and basin development

According to Røe (2003), the Vadsø Group, including the two couplets investigated here, and the lowermost Tanafjorden Group, record late Riphean syn-rift sedimentation, whereas the overlying units record post-rift deposition (Figs. 2A & 18B). However, most authors favour a stable pericratonic platform setting for the entire TVR succession with deposition occurring after the main rifting event (e.g., Johnson et al., 1978; Nystuen, 1985; Siedlecka, 1985; Rice, 1994, 2014; Siedlecka et al., 1995; 2004; Olovyanishnikov et al., 2000; Rice et al., 2001; Roberts & Siedlecka, 2002, 2022; Nystuen et al., 2008; Fig. 18B). In the following discussion, we attempt to evaluate the architecture of the two fluvio-deltaic couplets with respect to these contrasting tectonic models.

Some of the most important evidence in support of the VFZ includes abundant soft-sediment deformation and changing palaeo-currents, as well as the revised stratigraphic relationship between the TVR succession and the Archaean basement on the southern side of the Varangerfjorden (for more details, see Røe, 2003). As already discussed, we disregard the abundance of SSDS as unequivocal evidence for the existence of the VFZ. Yet, the strikingly similar facies association stacking patterns and the progradational to aggradational architecture of the two fluvio-deltaic couplets, as well as the sharp nature of the flooding surface separating them (Figs. 2B & 16), may be suggestive of tectonically controlled sedimentation. In rift basins, sedimentary response to recurrent fault activity tends to produce distinct cyclicity whereby progradational sequences evolve during tectonic quiescence when sedimentation outpaces subsidence rates, and sharp, basin-wide flooding surfaces develop during pulses of rapid tectonic subsidence (e.g., Gawthorpe et al., 1994; Leeder, 1999; Gawthorpe & Leeder, 2000; Martins-Neto & Catuneanu, 2010; Henstra et al., 2016; Marín et al., 2018). A series of tectonically controlled fluvio-deltaic cycles of similar age (late Riphean) and near identical facies assemblage as those reported here, occurs in the Båsnæringen Formation in the BSR north of the TKFZ (Siedlecka & Edwards, 1980; Hjellbakk, 1993; Røe, 1995; Fig. 18B). There, the fluvio-deltaic succession overlies a several kilometres thick slope to basin-floor turbidite succession, testifying to the

drastic increase of fault-controlled accommodation space in the hangingwall of the TKFZ (e.g., Siedlecka & Edwards, 1980; Pickering, 1981; Siedlecka et al., 1989; Fig. 18B). In the present case though, it seems unreasonable that the stratigraphic development was only controlled by the TKFZ, especially given the (pericratonic) footwall position of the TVR during the late Riphean, albeit some influence cannot be precluded (Fig. 18B).

The consistent east-directed palaeocurrents recorded in the Klubbnasen–Fugleberget and the Andersby–Paddeby couplets (Fig. 2B; Banks et al., 1974; Johnson et al., 1978; Røe, 2003) are somewhat puzzling because it implies margin-parallel rather than transverse sediment routing, which usually is the case on passive margins, unless sediment fairways are steered by faults or structurally induced topography (Leeder, 1999). Accordingly, sediment dispersal along the axis of a rift basin, as suggested by Røe (2003), seems justifiable. Moreover, Røe (2003) attributed the changing palaeocurrents, from eastward in the Klubbnasen–Fugleberget and Andersby–Paddeby couplets, to northwest in the overlying Golneselva Formation (Fig. 2B), to fault-controlled tilting of the basin axis.

Although this observation may lend support to the existence of the VFZ, a crucial point opposing its presence is the complete lack of coarse-grained clastics in the preserved part of the basin fill. Along most basin-bounding border faults juxtaposing crystalline basement against syn-rift sedimentary strata, coarse-grained clastics typically accumulate in the hangingwall (Gawthorpe et al., 1994; Gawthorpe & Leeder, 2000; Henstra et al., 2016; Marín et al., 2018). On the speculative side though, there is a possibility of such facies being present in the subsurface beneath the TVR. Alternatively, sediment contribution from footwall degradation was insignificant or of a very localised character (Fig. 18B).

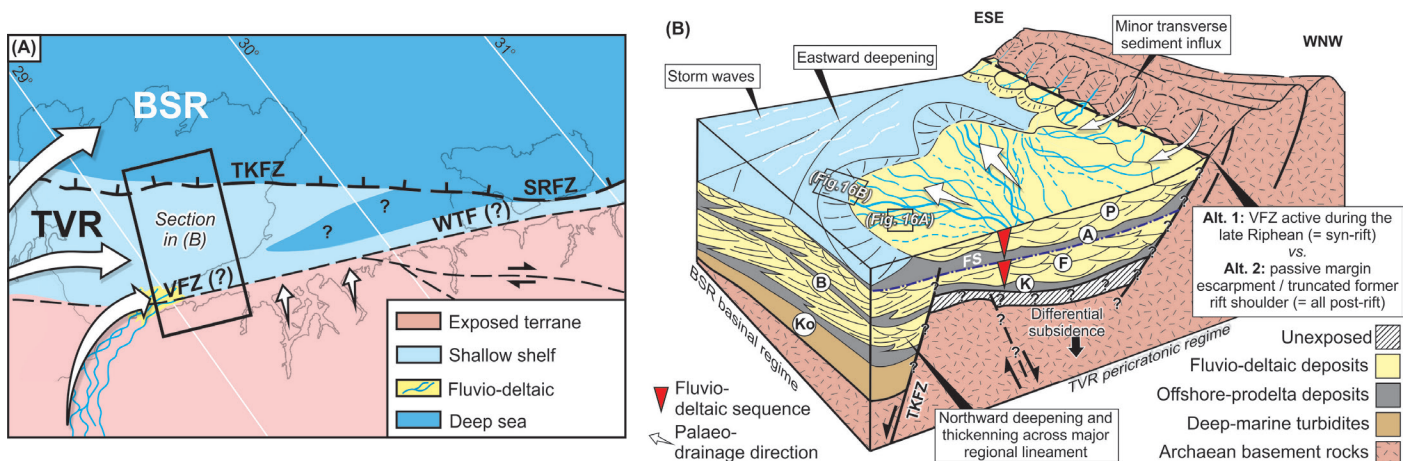


Figure 18. (A) Palaeogeographic reconstruction of the rifted Timanian margin of Baltica. Here, the investigated braid deltas prograded eastward onto the shallow, pericratonic platform of the Tanafjorden–Varangerfjorden Region (TVR), paralleling the Trolfjorden–Komagelva Fault Zone (TKFZ) and its eastward continuation, the Sredni–Rybachy Fault Zone (SRFZ). This regional lineament was an active normal fault during the late Riphean, separating the TVR from the basinal Barents Sea Region (BSR). In addition, the palaeo-current direction is parallel to the Archaean basement terrane to the south, the northern border of which coincides with the position of the proposed Varangerfjorden Fault Zone (VFZ), and the West Timan Fault (WTF) east of the study area. (B) Conceptual model for the stratigraphic architecture of the lower Vadsø Group. The two stacked fluvio-deltaic couplets (marked by red triangles) built into a shallow, occasionally storm-swept, eastward-deepening basin dominated by margin parallel drainage. Two alternatives, one implying syn-rift, fault-controlled sedimentation, and the second implying post-rift, subsidence-controlled deposition, may both explain the stratigraphic architecture and the eastward-dominated palaeo-current direction. See text for details. Abbreviations: Ko – Kongsfjorden Formation, B – Båsnæringen Formation, K – Klubbnasen Formation, F – Fugleberget Formation, A – Andersby Formation, P – Paddeby Formation.

It is conceivable to explain the observed stratigraphic architecture of the TVR succession, including the recurrent unconformities (e.g., at the base of FA 4; Fig. 2B), without invoking direct fault-controlled sedimentation. Because the TVR strata have an accumulative thickness of >2 km and are gently folded into a low-angle syncline, it has been suggested that the development of the pericratonic platform was largely controlled by post-rift subsidence and flexure-related processes (e.g., Siedlecka & Siedlecki, 1967; Johnson et al., 1978; Nystuen, 1985; Siedlecka, 1985; Roberts et al., 2011; Fig. 18B). Abrupt and repeated intercalations of fluvial and shallow-marine strata, and the presence of basin-wide unconformities, such as those occurring in the TVR succession (Bjørlykke, 1967; Siedlecka & Siedlecki, 1967; Banks et al., 1974; Johnson et al., 1978; Nystuen, 1985; Siedlecka, 1985; Roberts & Siedlecka, 2002; Røe, 2003; Fig. 2), are typical for pericratonic platforms, which are characterized by shallow bathymetry, low-gradients, and slow to moderate subsidence rates (e.g., Runkel et al., 2007; Grundvåg et al., 2020). In these settings, even minor eustatic sea-level change, or climatically driven fluctuations in sediment supply, may result in rapid shoreline translation and relocation. Therefore, these basins tend to foster well-preserved regressive–transgressive cycles (Leeder, 1999; Runkel et al., 2007; Grundvåg et al., 2020). In addition, uplift-induced erosional unconformities, like those we record at the base of the braidplain units (FA 4, e.g., Figs. 2B, 12, 13 & 16A), occur widely on many rifted margins where they signify the transition from syn-rift to post-rift (i.e., breakup unconformities, e.g., Soares et al., 2012; Alves & Cunha, 2018).

The development of pericratonic basins is characterised by an early rift phase (in the present case during the middle to late Riphean) followed by long-term thermal subsidence and concomitant construction of a passive-margin sedimentary prism (e.g., Leeder, 1999). The weight of an accreting sedimentary prism augments thermal subsidence via load-induced flexure. This eventually forces the landward edge of subsidence to migrate farther onto the craton where an uplifting forebulge may develop, concomitantly altering sediment routing along the basin margin by providing a local sediment source (Leeder, 1999).

Contrary to active faulting, the possible growth of such an east–west-oriented forebulge on the cratonward side of the TVR platform offers a viable alternative interpretation of the east-directed margin-parallel palaeocurrents and the reported abrupt reversal to northwest-dominated sediment dispersal in the Vadsø Group (Banks et al., 1974; Johnson et al., 1978; Røe, 2003; Fig. 2B). The same accounts for differential subsidence, which is known to influence sediment fairways, fluvial style (e.g., meandering vs. braided), and channel stacking patterns (Bridge & Mackey, 1993; Ryseth, 2000). In addition, vertical and sideway movements along deeply buried basement structures can give a flexural (down warping) response in the overlying sedimentary basin (Wetzel et al., 2003), and minor fault re-adjustment can generate localised, elongated, fault-parallel depocentres and concomitantly alter sedimentation patterns in the associated basin (e.g., Ryseth, 2000; Carr et al., 2003).

Judging from the many contradicting observations in the literature, the lack of subsurface data, as well as incompleteness of the sedimentary record, a combined faulted and sedimentary contact between the oldest TVR strata and the Archaean basement cannot be ruled out. In addition, the rapid rise of the Archaean basement terrane on the southern shore of the Varangerfjorden and the consistent E–W orientation of its northern boundary is remarkable, and strongly hint at some structural control of the palaeo-basin margin. In many ways it has the characteristics of a denudated *passive margin escarpment*, which are rift and breakup-related geomorphic features that separate interior hinterlands from low-lying coastal plains (e.g., Gilchrist & Summerfield, 1990), the latter represented by the TVR succession in the present case (Fig. 18). This major terrane boundary, coinciding with the VFZ, may thus represent the westward extension of the West Timan Fault (WTF), a major middle Riphean border fault which separates uplifted and denuded Archaean basement (representing the former rift shoulder) from Neoproterozoic sedimentary rocks in the coastal areas of northern Russia (Olovyanshnikov et al., 2000; Roberts & Siedlecka, 2002; Røe, 2003; Fig. 18A).

Previous studies have invoked an eastward-plunging basin axis and a coeval closure of the TVR basin some 200–250 km farther to the west, possibly against an inferred basement high (i.e., the Finnmark Ridge of Gayer & Roberts, 1973; see also Rice, 2014; Zhang et al., 2016). There are several alternatives to explain such a basin architecture, including the hypothetical presence of: i) an eastward-dipping, relay-ramp-like structure which may have developed between the TKFZ and the VFZ/WTF during the middle to late Riphean rifting event, ii) a separate, down-to-the east (strike parallel) tilted basement fault block bounded by the TKFZ and the VFZ/WTF, or iii) an underlying array of faults stepping down to the east (a possibility given the many NW–SE/N–S-oriented lineaments in the basement (e.g., Karpuz et al., 1995; Gabrielsen et al., 2002).

Based on the east-directed sediment flux, the eastward basin deepening, and the concomitant stratal thickening (e.g., Banks et al., 1974; Røe, 2003), we prefer the first option. The basin was thus predominantly fed by fluvio-deltaic systems which drained extensive hinterland catchments and entered the basin from the west via a relay ramp, which may explain the lack of coarse-grained clastics in the study area (Fig. 18B). The eastward sediment dispersal was maintained by differential subsidence governed by post-rift thermal subsidence, sediment loading, and flexuring caused by movements along deeply buried structures. Because the palaeo-currents are oriented near parallel to the TKFZ, we also speculate that this major fault zone exerted some influence on the regional subsidence pattern and consequently the sediment fairway on the pericratonic footwall (Fig. 18). Finally, although there is little compelling evidence of direct fault-controlled sedimentation in the Klubbnasen–Fugleberget and Andersby–Paddeby couplets, which would otherwise have vigorously supported the existence of the VFZ, this study presents several sedimentological indices of syn-tectonic sedimentation as well as underlying structural control on sediment routing which collectively governed the ensuing stratigraphic architecture.

Conclusions

- The lower part of the Neoproterozoic Vadsø Group contains two fluvio-deltaic couplets comprising the Klubbnasen–Fugleberget and the Andersby–Paddeby formations, both of late Riphean (Cryogenian) age. Four facies associations have been recognised in each couplet. Their lower, deltaic part includes offshore (FA 1), storm-influenced prodelta (FA 2), and fluvial-dominated to storm-affected delta-front (FA 3) deposits organised into large-scale (several tens of metres thick) coarsening-upward cycles, each erosively capped by >100 m-thick units of braidplain affinity (FA 4). Collectively, these deposits record the successive and repeated eastward migration of shallow-water braid deltas.

- A wide range of sandstone event beds documented in the prodelta deposits, including turbidites (both low- and high-density types), wave-modified turbidites, and hummocky cross-stratified tempestites, indicates that turbulent, unidirectional flows, combined flows, and oscillatory-dominated flows (i.e., storm wave) interacted during delta progradation. The event bed variability is attributed to the temporal and spatial evolution of these transport agents, as well as coupled storm-flood processes (i.e., flash floods interacting with storm waves) which affected the pre-vegetation drainage basin and coastal regions simultaneously. Proximity to the advancing braidplain feeder system also influenced event bed deposition through gradually increasing sediment flux, delta-front instability, and frequent flood-generated flows. In addition, the shallow water in the basin and the vertically expanded river effluent enabled dunes to migrate onto the prodelta slope where they became liquefied and occasionally collapsed and triggered turbidity currents which transported sand onto the basin floor in front of the deltas.

- The variability and abundance of soft-sediment deformation structures, including load structures, convolute bedding, syneresis cracks and sandstone dykes, in virtually all the facies associations independent of stratigraphic levels, indicates that syn-sedimentary tectonically-induced seismic activity was an important process triggering extensive fluidisation and deformation. However, these features cannot be used uncritically as evidence for the previously proposed Varangerfjorden Fault Zone. Based on the proximity to the Trollfjorden–Komagelv Fault Zone (<40 km), which is considered to have been active during the late Riphean, as well as its scale and long-lived nature, we speculate that seismic activity along this major lineament contributed to the observed soft-sediment deformation. In addition, cyclic stress induced by storm waves, sudden loading from storm- or gravity-emplaced sand, gravitational instability on the prodelta slope, and over-steepening of the delta front played variable roles in the development of many deformation structures.
- The near identical architecture and vertical stacking of the two fluvio-deltaic couplets, may advocate syn-tectonic, fault-controlled sedimentation in a rift basin. However, fluctuating rates of subsidence, eustasy, and sediment supply in basins of shallow bathymetry and low gradients may result in similar stratigraphic expressions. Thus, given the regional tectonic framework of a passive, yet formerly rifted margin, post-rift deposition on a shallow pericratonic platform controlled by differential subsidence and eustasy, seems more likely.
- Differential subsidence due to post-rift thermal sag, sediment load-induced flexuring, and movements along deeply buried basement structures which possibly gave a down-warping response in the overlying basin, resulted in a persistent eastward, margin-parallel sediment dispersal during deposition of the two fluvio-deltaic couplets. As such, this study presents several sedimentological indices of syn-tectonic sedimentation as well as underlying structural control on sediment routing during the Cryogenian post-rift development of this part of the Timanian margin of Baltica.

Acknowledgements. This research is funded by ARCEX partners and the Research Council of Norway (grant number 228107). Egil Edvardsen is thanked for valuable field assistance. Journal referees Johan Petter Nystuen and Tore Grane Klausen are both thanked for invaluable feedback and in-depth comments which improved and clarified our paper.

References

- Alfaro, P., Delgado, J., Estévez, A., Molina, J., Moretti, M. & Soria, J. 2002: Liquefaction and fluidization structures in Messinian storm deposits (Bajo Segura Basin, Betic Cordillera, southern Spain). *International Journal of Earth Sciences* 91, 505–513. <https://doi.org/10.1007/s00531-001-0241-z>
- Allen, J.R.L. 1983: Studies in fluvial sedimentation: bars, bar-complexes and sandstone sheets (low-sinuosity braided streams) in the Brownstones (L. Devonian), Welsh Borders. *Sedimentary Geology* 33, 237–293. [https://doi.org/10.1016/0037-0738\(83\)90076-3](https://doi.org/10.1016/0037-0738(83)90076-3)
- Allen, J.R.L. & Banks, N.L. 1972: An interpretation and analysis of recumbent-folded deformed cross-bedding. *Sedimentology* 19, 257–283. <https://doi.org/10.1111/j.1365-3091.1972.tb00024.x>
- Alves, T.M. & Cunha, T.A. 2018: A phase of transient subsidence, sediment bypass and deposition of regressive–transgressive cycles during the breakup of Iberia and Newfoundland. *Earth and Planetary Science Letters* 484, 168–183. <https://doi.org/10.1016/j.epsl.2017.11.054>

Arnott, R.W. & Southard, J. 1990: Exploratory flow-duct experiments on combined-flow bed configurations, and some implications for interpreting storm-event stratification. *Journal of Sedimentary Research* 60, 211–219. <https://doi.org/10.1306/212F9156-2B24-11D7-8648000102C1865D>

Astin, T.R. & Rogers, D.A. 1991: "Subaqueous shrinkage cracks" in the Devonian of Scotland reinterpreted. *Journal of Sedimentary Research* 61, 850–859. <https://doi.org/10.1306/D42677E4-2B26-11D7-8648000102C1865D>

Baarli, B.G., Levine, R. & Johnson, M.E. 2006: The Late Neoproterozoic Smalfjord Formation of the Varanger Peninsula in northern Norway: a shallow fjord deposit. *Norwegian Journal of Geology* 86, 133-150.

Banks, N.L. 1971: *Sedimentological studies in the late Precambrian and Lower Cambrian rocks of East Finnmark - Volume I*. PhD thesis, University of Oxford, 277 pp.

Banks, N.L., Hobday, D.K., Reading, H.G. & Taylor, P.N. 1974: Stratigraphy of the Late Precambrian 'Older Sandstone Series' of the Varangerfjord area, Finnmark. *Norges geologiske undersøkelse* 303, 1–15.

Basilici, G., De Luca, P.H.V. & Poiré, D.G. 2012: Hummocky cross-stratification-like structures and combined-flow ripples in the Punta Negra Formation (Lower-Middle Devonian, Argentine Precordillera): a turbiditic deep-water or storm-dominated prodelta inner-shelf system? *Sedimentary Geology* 267, 73–92. <https://doi.org/10.1016/j.sedgeo.2012.05.012>

Berra, F. & Felletti, F. 2011: Syndepositional tectonics recorded by soft-sediment deformation and liquefaction structures (continental Lower Permian sediments, Southern Alps, Northern Italy): stratigraphic significance. *Sedimentary Geology* 235, 249–263. <https://doi.org/10.1016/j.sedgeo.2010.08.006>

Bhattacharya, J.P. & Davies, R.K. 2001: Growth faults at the prodelta to delta-front transition, Cretaceous Ferron sandstone, Utah. *Marine Petroleum Geology* 18, 525–534. [https://doi.org/10.1016/S0264-8172\(01\)00015-0](https://doi.org/10.1016/S0264-8172(01)00015-0)

Bhattacharya, J.P. & Maceachern, J.A. 2009: Hyperpycnal rivers and prodeltaic shelves in the Cretaceous seaway of North America. *Journal of Sedimentary Research* 79, 184–209. <https://doi.org/10.2110/jsr.2009.026>

Bjørlykke, K. 1967: The Eocambrian "Reusch Moraine" at Bigganjårgga and the geology around Varangerfjord, northern Norway. *Norges geologiske undersøkelse* 251, 18–44.

Bowman, A.P. & Johnson, H.D. 2014: Storm-dominated shelf-edge delta successions in a high accommodation setting: The palaeo-Orinoco Delta (Mayaro Formation), Columbus Basin, South-East Trinidad. *Sedimentology* 61, 792–835. <https://doi.org/10.1111/sed.12080>

Brenchley, P.J., Pickerill, R.K. & Stromberg, S.G. 1993: The role of wave reworking on the architecture of storm sandstone facies, Bell Island Group (Lower Ordovician), eastern Newfoundland. *Sedimentology* 40, 359–382. <https://doi.org/10.1111/j.1365-3091.1993.tb01341.x>

Bridge, J.S. & Mackey, S.D. 1993: A revised alluvial stratigraphy model. In Puigdefabregas, C. & Marzo, M. (eds.): *Alluvial Sedimentation*. International Association of Sedimentologists Special Publication 17, 319-336.

- Carr, I.D., Gawthorpe, R.L., Jackson, C.A.L., Sharp, I.R. & Sadek, A. 2003: Sedimentology and Sequence Stratigraphy of Early Syn-Rift Tidal Sediments: The Nukhul Formation, Suez Rift, Egypt. *Journal of Sedimentary Research* 73, 407–420. <https://doi.org/10.1306/111402730407>
- Cawood, P.A., Nemchin, A.A., Strachan, R., Prave, T. & Krabbendam, M. 2007: Sedimentary basin and detrital zircon record along East Laurentia and Baltica during assembly and breakup of Rodinia. *Journal of the Geological Society* 164, 257–275. <https://doi.org/10.1144/0016-76492006-115>
- Clare, M.A., Hughes-Clarke, J.E., Talling, P.J., Cartigny, M.J.B. & Pratomo, D.G. 2016: Preconditioning and triggering of offshore slope failures and turbidity currents revealed by most detailed monitoring yet at a fjord-head delta. *Earth Planetary Science Letters* 450, 208–220. <https://doi.org/10.1016/j.epsl.2016.06.021>
- Cole, G, Jerrett, R. & Watkinson, M.P. 2021: A stratigraphic example of the architecture and evolution of shallow water mouth bars. *Sedimentology* 68, 1227–1254. <https://doi.org/10.1111/sed.12825>
- Collins, D.S., Johnson, H.D., Allison, P.A., Guilpain, P. & Damit, A.R. 2017: Coupled ‘storm-flood’-depositional model: Application to the Miocene–Modern Baram Delta Province, north-west Borneo. *Sedimentology* 64, 1203–1235. <https://doi.org/10.1111/sed.12316>
- Cowan, H., Nicaol, A. & Tonkin, P. 1996: A comparison of historical and palaeoseismicity in a newly formed fault zone and a mature fault zone, North Canterbury, New Zealand. *Journal of Geophysical Research* 101, 6021–6036. <https://doi.org/10.1029/95JB01588>
- Dott Jr, R.H. & Bourgeois, J. 1982: Hummocky stratification: significance of its variable bedding sequences. *Geological Society of America Bulletin* 93, 663–680. [https://doi.org/10.1130/0016-7606\(1982\)93<663:HSSOIV>2.0.CO;2](https://doi.org/10.1130/0016-7606(1982)93<663:HSSOIV>2.0.CO;2)
- Duke, W.L. 1991: Shelf sandstones and hummocky cross-stratification: New insights on a stormy debate. *Geology* 19, 625–628. [https://doi.org/10.1130/0091-7613\(1991\)019<0625:SSAHCS>2.3.CO;2](https://doi.org/10.1130/0091-7613(1991)019<0625:SSAHCS>2.3.CO;2)
- Dumas, S. & Arnott, R.-W.C. 2006: Origin of hummocky and swaley cross-stratification—The controlling influence of unidirectional current strength and aggradation rate. *Geology* 34, 1073–1076. <https://doi.org/10.1130/G22930A.1>
- Eide, C.H., Howell, J.A. & Buckley, S. 2015: Sedimentology and reservoir properties of tabular and erosive offshore transition deposits in wave-dominated, shallow-marine strata: Book Cliffs, USA. *Petroleum Geoscience* 21, 55–73. <https://doi.org/10.1144/petgeo2014-015>
- Fielding, C.R., Trueman, J.D. & Alexander, J., 2005: Sharp-based, flood-dominated mouth bar sands from the Burdekin River Delta of northeastern Australia: extending the spectrum of mouth-bar facies, geometry, and stacking patterns. *Journal of Sedimentary Research* 75, 55–66. <https://doi.org/10.2110/jsr.2005.006>
- Føyn, S. & Siedlicki, S. 1980: Glacial stadials and interstadials of the Late Precambrian Smalfjord Tillite on Laksefjordvidda, Finnmark, North Norway. *Norges geologiske Undersøkelse* 358, 31–45.
- Gabrielsen, R.H., Braathen, A, Dehls, J. & Roberts, D. 2002: Tectonic lineaments of Norway. *Norwegian Journal of Geology* 82, 153–174.

Gabrielsen, R.H., Roberts, D., Gjelsvik, T., Sygnabere, T.O., Hassaan, M. & Faleide, J.I. 2022: Double-folding and thrust-front geometries associated with the Timanian and Caledonian orogenies in the Varanger Peninsula, Finnmark, North Norway. *Journal of the Geological Society* 179.

<https://doi.org/10.1144/jgs2021-153>

Gawthorpe, R.L. & Leeder, M.R. 2000: Tectono-sedimentary evolution of active extensional basins. *Basin Research* 12, 195–218. <https://doi.org/10.1111/j.1365-2117.2000.00121.x>

Gawthorpe, R.L., Fraser, A.J. & Collier, R.E.L. 1994: Sequence stratigraphy in active extensional basins: implications for the interpretation of ancient basin-fills. *Marine Petroleum Geology* 11, 642–658.

[https://doi.org/10.1016/0264-8172\(94\)90021-3](https://doi.org/10.1016/0264-8172(94)90021-3)

Gayer, R.A. & Roberts, J.D. 1973: Stratigraphic review of the Finnmark Caledonides, with possible tectonic implications. *Proceedings of the Geologists' Association* 84, 405–441.

[https://doi.org/10.1016/S0016-7878\(73\)80023-9](https://doi.org/10.1016/S0016-7878(73)80023-9)

Gilchrist, A.R. & Summerfield, M.A. 1990: Differential denudation and flexural isostasy in the formation of rifted-margin upwarps. *Nature* 346, 739–742. <https://doi.org/10.1038/346739a0>

Gorokhov, I.M., Siedleka, A., Roberts, D., Melnikov, N.N. & Turchenko, T.L. 2001: Rb–Sr dating of diagenetic illite in Neoproterozoic shales, Varanger Peninsula, northern Norway. *Geological Magazine* 138, 541–562. <https://doi.org/10.1017/S001675680100574X>

Grundvåg, S.-A. & Olausson, S. 2017: Sedimentology of the Lower Cretaceous at Kikutodden and Keilhauffjellet, Southern Spitsbergen: implications for the onshore-offshore link. *Polar Research* 36, 1302124. <https://doi.org/10.1080/17518369.2017.1302124>

Grundvåg, S.A., Jelby, M.E., Olausson, S. & Śliwińska, K. 2020: The role of shelf morphology on storm-bed variability and stratigraphic architecture, Lower Cretaceous, Svalbard. *Sedimentology* 68, 196–237. <https://doi.org/10.1111/sed.12791>

Hampson, G.J. 2016: Towards a sequence stratigraphic solution set for autogenic processes and allogenic controls: Upper Cretaceous strata, Book Cliffs, Utah, USA. *Journal of the Geological Society* 173, 817–836. <https://doi.org/10.1144/jgs2015-136>

Harms, J.C., 1969: Hydraulic significance of some sand ripples. *Geological Society of America Bulletin* 80, 363–396. [https://doi.org/10.1130/0016-7606\(1969\)80\[363:HSOSSR\]2.0.CO;2](https://doi.org/10.1130/0016-7606(1969)80[363:HSOSSR]2.0.CO;2)

Helland-Hansen, W. & Hampson, G.J. 2009: Trajectory analysis: concepts and applications. *Basin Research* 21, 454–483. <https://doi.org/10.1111/j.1365-2117.2009.00425.x>

Henstra, G.A., Grundvåg, S.-A., Johannessen, E.P., Kristensen, T.B., Midtkandal, I., Nystuen, J.P., Rotevatn, A., Surlyk, F., Sæther, T. & Windelstad, J. 2016: Depositional processes and stratigraphic architecture within a coarse-grained rift-margin turbidite system: The Wollaston Forland Group, east Greenland. *Marine Petroleum Geology* 76, 187–209. <https://doi.org/10.1016/j.marpetgeo.2016.05.018>

Herrevold, T., Gabrielsen, R.H. & Roberts, D. 2009: Structural geology of the southeastern part of the Trollfjorden-Komagelva fault zone, Varanger Peninsula, Finnmark, north Norway. *Norwegian Journal of Geology* 89, 305–325.

Hildebrandt, C. & Egenhoff, S. 2007: Shallow-marine massive sandstone sheets as indicators of palaeoseismic liquefaction—An example from the Ordovician shelf of Central Bolivia. *Sedimentary Geology* 202, 581–595. <https://doi.org/10.1016/j.sedgeo.2007.04.009>

Hjellbakk, A. 1993: A 'flash-flood'dominated braid delta in the upper Proterozoic Næringselva Member, Varanger Peninsula, northern Norway. *Norwegian Journal of Geology* 73, 63–80.

Hjellbakk, A. 1997: Facies and fluvial architecture of a high-energy braided river: the Upper Proterozoic Segloddan Member, Varanger Peninsula, northern Norway. *Sedimentary Geology* 114, 131–161. [https://doi.org/10.1016/S0037-0738\(97\)00075-4](https://doi.org/10.1016/S0037-0738(97)00075-4)

Hobday, D.K. 1974: Interaction between fluvial and marine processes in the lower part of the Late Precambrian Vadsø Group. *Norges geologiske undersøkelse* 303, 39–56.

Holtedahl, O. 1918: Bidrag til Finmarkens Geologi. *Norges Geologiske Undersøkelse* 84, 314 p.

Ielpi, A. & Rainbird, R.H. 2016: Reappraisal of Precambrian sheet-braided rivers: evidence for 1.9 Ga deep-channelled drainage. *Sedimentology* 63, 1550–1581. <https://doi.org/10.1111/sed.12273>

Jelby, M.E., Grundvåg, S. A., Helland-Hansen, W., Olaussen, S. & Stemmerik, L. 2020: Tempestite facies variability and storm-depositional processes across a wide ramp: Towards a polygenetic model for hummocky cross-stratification. *Sedimentology* 67, 742–781. <https://doi.org/10.1111/sed.12671>

Jensen, S., Höglström, A.E.S., Høyberget, M., Meinhold, G., McIlroy, D., Ebbestad, J.O.R., Taylor, W.L., Agić, H. & Palacios, T. 2018: New occurrences of Palaeopascichnus from the Stáhpogieddi Formation, Arctic Norway, and their bearing on the age of the Varanger Ice Age. *Canadian Journal of Earth Sciences* 55, 1253–1261. <https://doi.org/10.1139/cjes-2018-0035>

Johnson, H.D. 1975: Tide-and wave-dominated inshore and shoreline sequences from the late Precambrian, Finnmark, North Norway. *Sedimentology* 22, 45–74. <https://doi.org/10.1111/j.1365-3091.1975.tb00283.x>

Johnson, H.D. 1977: Sedimentation and waterescape structures in some Late Precambrian shallow marine sandstones from Finnmark, North Norway. *Sedimentology* 24, 389–411. <https://doi.org/10.1111/j.1365-3091.1977.tb00129.x>

Johnson, H.D., Levell, B.K. & Siedlecki, S. 1978: Late Precambrian sedimentary rocks in East Finnmark, north Norway and their relationship to the Trollfjord-Komagelvfelt fault. *Journal of the Geological Society* 135, 517–533. <https://doi.org/10.1144/gsjgs.135.5.0517>

Jones, B.G. & Rust, B.R. 1983: Massive sandstone facies in the Hawkesbury Sandstone, a Triassic fluvial deposit near Sydney, Australia. *Journal of Sedimentary Research* 53, 1249–1259. <https://doi.org/10.1306/212F8355-2B24-11D7-8648000102C1865D>

Katz, T., Ginat, H., Eyal, G., Steiner, Z., Braun, Y., Shalev, S. & Goodman-Tchernov, B.N. 2015: Desert flash floods form hyperpycnal flows in the coral-rich Gulf of Aqaba, Red Sea. *Earth and Planetary Science Letters* 417, 87–98. <https://doi.org/10.1016/j.epsl.2015.02.025>

Karpuz, M.R., Roberts, D., Moralev, V.M. & Terekhov, E. 1995: Regional lineaments of eastern Finnmark, Norway, and the western Kola Peninsula, Russia. *Norges geologiske undersøkelse, Special Publication* 7, 121-135.

Laajoki, K. 2001: Additional observations on the late Proterozoic Varangerfjorden unconformity, Finnmark, northern Norway. *Bulletin of the Geological Survey of Finland* 73, 17–34.

<https://doi.org/10.17741/bgsf/73.1-2.002>

Lamb, M.P., Myrow, P.M., Lukens, C., Houck, K. & Strauss, J. 2008: Deposits from wave-influenced turbidity currents: Pennsylvanian Minturn Formation, Colorado, USA. *Journal of Sedimentary Research* 78, 480–498. <https://doi.org/10.2110/jsr.2008.052>

Leeder, M. 1999: *Sedimentology and sedimentary basins: from turbulence to tectonics*. Wiley-Blackwell, 784 pp.

Li, Z.X., Bogdanova, S.V., Collins, A.S., Davidson, A., De Waele, B., Ernst, R.E., Fitzsimons, I.C.W., Fuck, R.A., Gladkochub, D.P. & Jacobs, J. 2008: Assembly, configuration, and break-up history of Rodinia: a synthesis. *Precambrian Research* 160, 179–210. <https://doi.org/10.1016/j.precamres.2007.04.021>

Lowe, D.R. 1982: Sediment gravity flows; II, Depositional models with special reference to the deposits of high-density turbidity currents. *Journal of Sedimentary Petrology* 52, 279–297.

<https://doi.org/10.1306/212F7F31-2B24-11D7-8648000102C1865D>

MacQuaker, J.H.S., Bentley, S.J. & Bohacs, K.M. 2010: Wave-enhanced sediment-gravity flows and mud dispersal across continental shelves: Reappraising sediment transport processes operating in ancient mudstone successions. *Geology* 38, 947–950. <https://doi.org/10.1130/G31093.1>

Marín, D., Escalona, A., Grundvåg, S.-A., Nøhr-Hansen, H. & Kairanov, B. 2018: Effects of adjacent fault systems on drainage patterns and evolution of uplifted rift shoulders: The Lower Cretaceous in the Loppa High, southwestern Barents Sea. *Marine and Petroleum Geology* 94, 212–229.

Martel, A.T. & Gibling, M.R. 1993: Clastic dykes of the Devonian-Carboniferous Horton Bluff Formation, Nova Scotia; storm-related structures in shallow lakes. *Sedimentary Geology* 87, 103–119.

[https://doi.org/10.1016/0037-0738\(93\)90038-7](https://doi.org/10.1016/0037-0738(93)90038-7)

Martínez, J.F., Cartwright, J. & Hall, B. 2005: 3D seismic interpretation of slump complexes: examples from the continental margin of Israel. *Basin Research* 17, 83–108.

<https://doi.org/10.1111/j.1365-2117.2005.00255.x>

Martins-Neto, M.A. & Catuneanu, O. 2010: Rift sequence stratigraphy. *Marine Petroleum Geology* 27, 247–253. <https://doi.org/10.1016/j.marpetgeo.2009.08.001>

McMahon, S., van Smeerdijk Hood, A. & McIlroy, D. 2017: The origin and occurrence of subaqueous sedimentary cracks. *Geological Society, London, Special Publications* 448, 285–309.

<https://doi.org/10.1144/SP448.15>

Merdith, A.S., Collins, A.S., Williams, S.E., Pisarevsky, S., Foden, J.D., Archibald, D.B., Blades, M.L., Alessio, B.L., Armistead, S. & Plavsa, D. 2017: A full-plate global reconstruction of the Neoproterozoic. *Gondwana Research* 50, 84–134. <https://doi.org/10.1016/j.gr.2017.04.001>

Mohindra, R. & Bagati, T.N. 1996: Seismically induced soft-sediment deformation structures (seismites) around Sumdo in the lower Spiti valley (Tethys Himalaya). *Sedimentary Geology* 101, 69–83.

[https://doi.org/10.1016/0037-0738\(95\)00022-4](https://doi.org/10.1016/0037-0738(95)00022-4)

- Molina, J.M., Alfaro, P., Moretti, M. & Soria, J.M. 1998: Soft-sediment deformation structures induced by cyclic stress of storm waves in tempestites (Miocene, Guadalquivir Basin, Spain). *Terra Nova* 10, 145–150. <https://doi.org/10.1046/j.1365-3121.1998.00183.x>
- Mulder, T., Syvitski, J.P.M., Migeon, S., Faugeres, J.-C. & Savoye, B. 2003: Marine hyperpycnal flows: initiation, behavior and related deposits. A review. *Marine Petroleum Geology* 20, 861–882. <https://doi.org/10.1016/j.marpetgeo.2003.01.003>
- Mutti, E., Davoli, G., Tinterri, R. & Zavala, C. 1996: The importance of ancient fluvio-deltaic systems dominated by catastrophic flooding in tectonically active basins. *Memorie di Scienze Geologiche* 48, 233–291.
- Myrow, P.M. 1992a: Bypass-zone tempestite facies model and proximity trends for an ancient muddy shoreline and shelf. *Journal of Sedimentary Research* 62, 99–115. <https://doi.org/10.1306/D426789D-2B26-11D7-8648000102C1865D>
- Myrow, P.M. 1992b: Pot and gutter casts from the Chapel Island Formation, southeast Newfoundland. *Journal of Sedimentary Research* 62, 992–1007. <https://doi.org/10.2110/jsr.62.992>
- Myrow, P.M. & Southard, J.B. 1991: Combined-flow model for vertical stratification sequences in shallow marine storm-deposited beds. *Journal of Sedimentary Research* 61, 202–210. <https://doi.org/10.1306/D42676D1-2B26-11D7-8648000102C1865D>
- Myrow, P.M., Fischer, W. & Goodge, J.W. 2002: Wave-modified turbidites: Combined-flow shoreline and shelf deposits, Cambrian, Antarctica. *Journal of Sedimentary Research* 72, 641–656. <https://doi.org/10.1306/022102720641>
- Myrow, P.M. & Southard, J.B. 1996: Tempestite deposition. *Journal of Sedimentary Research* 66, 875–887. <https://doi.org/10.1306/D426842D-2B26-11D7-8648000102C1865D>
- Neef, G. 1991: A clastic dike-sill assemblage in late Miocene (c. 6 Ma) strata, Annedale, Northern Wairarapa, New Zealand. *New Zealand Journal of Geology and Geophysics* 34, 87–91. <https://doi.org/10.1080/00288306.1991.9514442>
- Nemec, W. 1990: Aspects of sediment movement on steep delta slopes. In Colella, A. & Prior, D.B. (eds.): *Coarse-Grained Deltas*, International Association of Sedimentologists Special Publication 10, pp. 29–73. <https://doi.org/10.1002/9781444303858.ch3>
- Nemec, W. 1992: Depositional controls on plant growth and peat accumulation in a braidplain delta environment: Helvetiafiellet Formation (Barremian-Aptian), Svalbard. In McCabe, P.J. & Parrish, J.T. (eds.): *Controls on the distribution and quality of Cretaceous coals*, Geological Society of America, pp. 209–226. <https://doi.org/10.1130/SPE267-p209>
- Nemec, W., Steel, R.J., Gjelberg, J., Collinson, J.D., Prestholm, E. & Øxnevad, I. E. 1988: Anatomy of collapsed and re-established delta front in Lower Cretaceous of eastern Spitsbergen: gravitational sliding and sedimentation processes. *American Association of Petroleum Geologists Bulletin* 72, 454–476. <https://doi.org/10.1306/703C8EB6-1707-11D7-8645000102C1865D>
- Nystuen, J.P. 1985: Facies and preservation of glaciogenic sequences from the Varanger Ice Age in Scandinavia and other parts of the North Atlantic region. *Palaeogeography, Palaeoclimatology, Palaeoecology* 51, 209–229. [https://doi.org/10.1016/0031-0182\(85\)90086-0](https://doi.org/10.1016/0031-0182(85)90086-0)

Nystuen, J.P. 2008: Break-up of the Precambrian continent. In: Ramberg I.B., Bryhni, I., Nøttvedt, A. & Ranges K. (eds.): *The Making of a Land - Geology of Norway*. Trondheim, Norges geologiske undersøkelse, pp. 120–133.

Nystuen, J.P., Andresen, A., Kumpulainen, R.A. & Siedlecka, A. 2008: Neoproterozoic basin evolution in Fennoscandia, East Greenland and Svalbard. *Episodes* 31, 35–43.

<https://doi.org/10.18814/epiugs/2008/v31i1/006>

Obermeier, S.F., 2009: Using liquefaction-induced and other soft-sediment features for paleoseismic analysis. *International Geophysics* 95, 497–564. [https://doi.org/10.1016/S0074-6142\(09\)95007-0](https://doi.org/10.1016/S0074-6142(09)95007-0)

Olariu, C. & Bhattacharya, J.P. 2006: Terminal distributary channels and delta front architecture of river-dominated delta systems. *Journal of Sedimentary Research* 76, 212–233.

<https://doi.org/10.2110/jsr.2006.026>

Olovyanishnikov, V.G., Roberts, D. & Siedlecka, A. 2000: Tectonics and sedimentation of the Meso- to Neoproterozoic Timan–Varanger Belt along the northeastern margin of Baltica. *Polarforschung* 68, 267–274.

Onyenanu, G.S.I., Jacquemyn, C.E.M.M., Graham, G.H., Hampson, G.J., Fitch, P.J.R. & Jackson, M.D. 2018: Geometry, distribution and fill of erosional scours in a heterolithic, distal lower shoreface sandstone reservoir analogue: Grassy Member, Blackhawk Formation, Book Cliffs, Utah, USA. *Sedimentology* 65, 1731–1760. <https://doi.org/10.1111/sed.12444>

Owen, G. 1987: Deformation processes in unconsolidated sands. *Geological Society, London, Special Publications* 29, 11–24. <https://doi.org/10.1144/GSL.SP.1987.029.01.02>

Owen, G. 2003: Load structures: gravity-driven sediment mobilization in the shallow subsurface. *Geological Society, London, Special Publications* 216, 21–34.

<https://doi.org/10.1144/GSL.SP.2003.216.01.03>

Owen, G. & Moretti, M. 2011: Identifying triggers for liquefaction-induced soft-sediment deformation in sands. *Sedimentary Geology* 235, 141–147. <https://doi.org/10.1016/j.sedgeo.2010.10.003>

Pattison, S. 2005: Storm-influenced prodelta turbidite complex in the lower Kenilworth Member at Hatch Mesa, Book Cliffs, Utah, U.S.A.: Implications for shallow marine facies models. *Journal of Sedimentary Research* 75, 420–439. <https://doi.org/10.2110/jsr.2005.033>

Pattison, S.A.J., Ainsworth, R.B. & Hoffman, T.A. 2007: Evidence of across-shelf transport of fine-grained sediments: turbidite-filled shelf channels in the Campanian Aberdeen Member, Book Cliffs, Utah, USA. *Sedimentology* 54, 1033–1064. <https://doi.org/10.1111/j.1365-3091.2007.00871.x>

Pease, V., Daly, J.S., Elming, S.Å., Kumpulainen, R., Moczydlowska, M., Puchkov, V., Roberts, D., Saintot, A. & Stephenson, R. 2008: Baltica in the Cryogenian, 850–630 Ma. *Precambrian Research* 160, 46–65. <https://doi.org/10.1016/j.precamres.2007.04.015>

Pickering, K.T. 1981: The Kongsfjord Formation - a Late Precambrian submarine fan in northeast Finnmark, North Norway. *Norges geologiske undersøkelse* 367, 295–306.

Piper, D.J.W. & Normark, W.R. 2009: Processes that initiate turbidity currents and their influence on turbidites: a marine geology perspective. *Journal of Sedimentary Research* 79, 347–362.

<https://doi.org/10.2110/jsr.2009.046>

Pratt, B.R. 1998: Syneresis cracks: subaqueous shrinkage in argillaceous sediments caused by earthquake-induced dewatering. *Sedimentary Geology* 117, 1–10.

[https://doi.org/10.1016/S0037-0738\(98\)00023-2](https://doi.org/10.1016/S0037-0738(98)00023-2)

Rice, A.H.N. 1994: Stratigraphic overlap of the late Proterozoic Vadsø and Barents Sea Groups and correlation across the Trollfjorden-Komagelva Fault, Finnmark, North Norway. *Norwegian Journal of Geology* 74, 48–57.

Rice, A.H.N. 2014: Restoration of the external Caledonides, Finnmark, North Norway. Geological Society, London, *Special Publication* 390, 271–299. <https://doi.org/10.1144/SP390.18>

Rice, A.H.N., Hofmann, C. & Pettersen A. 2001: A new sedimentary succession from the southern margin of the Neoproterozoic Gaissa basin, South Varangerfjord, North Norway. *Norwegian Journal of Geology* 81, 41–48.

Roberts, D. 1996: Caledonian and Baikalian tectonic structures on Varanger Peninsula, Finnmark, Norway, and coastal areas of Kola Peninsula, NW Russia. *Norges geologiske undersøkelse* 431, 59–66.

Roberts, D. & Siedlecka, A. 2002: Timanian orogenic deformation along the northeastern margin of Baltica, Northwest Russia and Northeast Norway, and Avalonian–Cadomian connections. *Tectonophysics* 352, 169–184. [https://doi.org/10.1016/S0040-1951\(02\)00195-6](https://doi.org/10.1016/S0040-1951(02)00195-6)

Roberts, D. & Siedlecka, A. 2012: Provenance and sediment routing of Neoproterozoic formations on the Varanger, Nordkinn, Rybachi and Sredni peninsulas, North Norway and Northwest Russia: a review. *Norwegian Geological Survey Bulletin* 452, 1–19.

Roberts, D. & Siedlecka, A. 2022: Revised stratigraphy and correlation of the Neoproterozoic successions of Varanger Peninsula, East Finnmark, northern Norway, and the Rybachi-Sredni peninsulas and Kildin Island in Northwest Russia. *Norwegian Geological Survey Bulletin* 457, 1–21.

Roberts, D., Chand, S. & Rise, L. 2011: A half-graben of inferred Late Palaeozoic age in outer Varangerfjorden, Finnmark: evidence from seismic-reflection profiles and multibeam bathymetry. *Norwegian Journal of Geology* 91, 191–200.

Rossetti, D.D.F. 1999: Soft-sediment deformation structures in late Albian to Cenomanian deposits, São Luís Basin, northern Brazil: evidence for palaeoseismicity. *Sedimentology* 46, 1065–1081.

<https://doi.org/10.1046/j.1365-3091.1999.00265.x>

Runkel, A.C., Miller, J.F., McKay, R.M., Palmer, A.R. & Taylor, J.F. 2007: High-resolution sequence stratigraphy of lower Paleozoic sheet sandstones in central North America: The role of special conditions of cratonic interiors in development of stratal architecture. *Geological Society of America Bulletin* 119, 860–881. <https://doi.org/10.1130/B26117.1>

Ryseth, A. 2000: Differential subsidence in the Ness Formation (Bajocian), Oseberg Area, Northern North Sea: Facies variation, accommodation space development and sequence stratigraphy in a deltaic distributary system. *Norwegian Journal of Geology* 80, 9–26.

<https://doi.org/10.1080/002919600750042645>

Røe, S.-L. 1987: Cross-strata and bedforms of probable transitional dune to upper-stage plane-bed origin from a Late Precambrian fluvial sandstone, northern Norway. *Sedimentology* 34, 89–101.

<https://doi.org/10.1111/j.1365-3091.1987.tb00562.x>

Røe, S.-L. 1995: Stacked fluviodeltaic cycles in the Upper Proterozoic Godkeila Member, Varanger Peninsula, northern Norway. *Norwegian Journal of Geology* 75, 229–242.

Røe, S.-L. 2003: Neoproterozoic peripheral-basin deposits in eastern Finnmark, N. Norway: stratigraphic revision and palaeotectonic implications. *Norwegian Journal of Geology* 83, 259–374.

Røe, S.-L. & Hermansen, M. 1993. Processes and products of large, Late Precambrian sandy rivers in northern Norway. In Marzo, M. & Puigdefabregas, C. (eds.): *Alluvial sedimentation*. Blackwell Oxford, pp. 151–166.

Røe, S.-L. & Hermansen, M. 2006: New aspects of deformed cross-strata in fluvial sandstones: examples from Neoproterozoic formations in northern Norway. *Sedimentary Geology* 186, 283–293.

<https://doi.org/10.1016/j.sedgeo.2005.11.023>

Siedlecka, A. 1985: Development of the upper Proterozoic sedimentary basins of the Varanger Peninsula, East Finnmark, North Norway. *Geological Survey of Finland Bulletin* 331, 175–185.

Siedlecka, A. 1991: Nesseby, geology bedrock map 2335 2, scale 1:50 000. *Norges geologiske undersøkelse*.

Siedlecka, A. & Siedlecki, S. 1967: Some new aspects of the geology of Varanger Peninsula (Northern Norway). *Norges geologiske undersøkelse* 247, 288–306.

Siedlecka, A. & Edwards, M.B. 1980: Lithostratigraphy and sedimentation of the Riphean Båsnæringen Formation, Varanger Peninsula, north Norway. *Norges geologiske undersøkelse* 355, 27–47.

Siedlecka, A. & Roberts, D. 1996: Finnmark Fylke. Bedrock geology map M, scale 1:500,000, *Norges geologiske undersøkelse*.

Siedlecka, A., Pickering, K.T. & Edwards, M.B. 1989: Upper Proterozoic passive margin deltaic complex, Finnmark, N Norway. In Whateley, M.K.G. & Pickering, K.T. (eds.): *Deltas: Sites and traps for fossil fuels*. Geological Society, London, Special Publications 41, pp. 205–219.

<https://doi.org/10.1144/GSL.SP.1989.041.01.15>

Siedlecka, A., Lyubtsov V.V. & Negrutsa, V.Z. 1995: Correlation between Upper Proterozoic successions in the Tanafjorden-Varangerfjorden Region of Varanger Peninsula, northern Norway, and on Sredni Peninsula and Kildin Island in the northern coastal area of Kola Peninsula in Russia. *Norwegian Geological Survey Special Publication* 7, 217–232

Siedlecka, A., Roberts, D. & Olsen, L. 1998: Geologi på Varangerhalvøya - En oversikt med ekskursjonsforslag. *Gråsteinen* 3. Norges geologiske undersøkelse, 122 pp.

Siedlecka, A., Roberts, D., Nystuen, J.P. & Olovyanishnikov, V.G. 2004: Northeastern and north-western margins of Baltica in Neoproterozoic time: evidence from the Timanian and Caledonian orogens. In Gee, D.G. & Pease, V. (eds.): *The Neoproterozoic Timanide orogen of eastern Baltica*. Geological Society, London, Memoirs 30, 169–190. <https://doi.org/10.1144/GSL.MEM.2004.030.01.15>

Soares, D.M., Alves, T.M. & Terrinha, P. 2012: The breakup sequence and associated lithospheric breakup surface: their significance in the context of rifted continental margins (West Iberia and Newfoundland margins, North Atlantic). *Earth and Planetary Science Letters* 355, 311–326.

<https://doi.org/10.1016/j.epsl.2012.08.036>

Sturt, B. A., Pringle, I.R. & Roberts, D. 1975: Caledonian nappe sequence of Finnmark, northern Norway, and the timing of orogenic deformation and metamorphism. *Geological Society of America Bulletin* 86, 710–718. [https://doi.org/10.1130/0016-7606\(1975\)86<710:CNSOFN>2.0.CO;2](https://doi.org/10.1130/0016-7606(1975)86<710:CNSOFN>2.0.CO;2)

Swift, D.J.P. 1985. Response of the shelf floor to flow. In: Tillman, R.W., Swift, D.J.P. & Walker, R.G. (eds.): *Shelf Sands and Sandstone Reservoir*. Society of Sedimentary Geology Short Course Notes 13, pp.135–241. <https://doi.org/10.2110/scn.85.13.0135>

Tirsgaard, H. & Øxnevad, I.E.I. 1998: Preservation of pre-vegetational mixed fluvio–aeolian deposits in a humid climatic setting: an example from the Middle Proterozoic Eriksfjord Formation, Southwest Greenland. *Sedimentary Geology* 120, 295–317. [https://doi.org/10.1016/S0037-0738\(98\)00037-2](https://doi.org/10.1016/S0037-0738(98)00037-2)

Wetzel, A., Allenbach, A. & Allia, V. 2003: Reactivated basement structures affecting the sedimentary facies in a tectonically “quiescent” epicontinental basin: An example from NW Switzerland. *Sedimentary Geology* 157, 153–172. [https://doi.org/10.1016/S0037-0738\(02\)00230-0](https://doi.org/10.1016/S0037-0738(02)00230-0)

Wheatley, D.F. & Chan, M.A. 2018: Clastic pipes and soft-sediment deformation of the Jurassic Carmel Formation, Southern Utah, USA: implications for pipe formation mechanisms and host-rock controls. *Journal of Sedimentary Research* 88, 1076–1095. <https://doi.org/10.2110/jsr.2018.45>

Williams R.T., Goodwin L.B., Sharp W.D. & Mozley P.S. 2017: Reading a 400,000-year record of earthquake frequency for an intraplate fault. *The Proceedings of the National Academy of Sciences* 114, 4893–4898. <https://doi.org/10.1073/pnas.1617945114>

Yokokawa, M. 1995: Combined-flow ripples: genetic experiments and applications for geologic records. *Kyushu University Memoirs of the Faculty of Science, Series D, Earth and Planetary Sciences* 29, 1–38. <https://doi.org/10.5109/1543655>

Zhang, W., Roberts, D. & Pease, V. 2015: Provenance characteristics and regional implications of Neoproterozoic, Timanian-margin successions and a basal Caledonian nappe in Northern Norway. *Precambrian Research* 268, 153–167. <https://doi.org/10.1016/j.precamres.2015.07.006>

Zhang, W., Roberts, D. & Pease, V. 2016: Provenance of sandstones from Caledonian nappes in Finnmark, Norway: Implications for Neoproterozoic–Cambrian palaeogeography. *Tectonophysics* 691, 198–205. <https://doi.org/10.1016/j.tecto.2015.09.001>